Journal of Vertebrate Paleontology

ISSN: (Print) (Online) Journal homepage: https://www.tandfonline.com/loi/ujvp20

Tusked walruses (Carnivora: Odobenidae) from the Miocene–Pliocene Purisima Formation of Santa Cruz, California (U.S.A.): a new species of the toothless walrus *Valenictus* and the oldest records of Odobeninae and Odobenini

Robert W. Boessenecker, Ashley W. Poust, Sarah J. Boessenecker & Morgan Churchill

To cite this article: Robert W. Boessenecker, Ashley W. Poust, Sarah J. Boessenecker & Morgan Churchill (29 Jan 2024): Tusked walruses (Carnivora: Odobenidae) from the Miocene–Pliocene Purisima Formation of Santa Cruz, California (U.S.A.): a new species of the toothless walrus *Valenictus* and the oldest records of Odobeninae and Odobenini, Journal of Vertebrate Paleontology, DOI: 10.1080/02724634.2023.2296567

To link to this article: https://doi.org/10.1080/02724634.2023.2296567

Journal of Vertebrate Paleontology e2296567 (33 pages)

DOI: 10.1080/02724634.2023.2296567

ARTICLE

TUSKED WALRUSES (CARNIVORA: ODOBENIDAE) FROM THE MIOCENE–PLIOCENE PURISIMA FORMATION OF SANTA CRUZ, CALIFORNIA (U.S.A.): A NEW SPECIES OF THE TOOTHLESS WALRUS *VALENICTUS* AND THE OLDEST RECORDS OF ODOBENINAE AND ODOBENINI

ROBERT W. BOESSENECKER,*[,1,2] ASHLEY W. POUST,[3,4] SARAH J. BOESSENECKER,[1] and MORGAN CHURCHILL[5]
[1]Charleston Center for Paleontology, Charleston, South Carolina, U.S.A., bobby@charlestoncenterforpaleo.org, sarah@charlestoncenterforpaleo.org;
[2]University of California Museum of Paleontology, University of California, Berkeley, California, 94720, U.S.A.;
[3]Department of Paleontology, San Diego Natural History Museum, San Diego, California, 92112-1390, U.S.A., apoust@sdnhm.org;
[4]University of Nebraska State Museum, University of Nebraska, Lincoln, Nebraska, 68588-0338, U.S.A.;
[5]Department of Biology, University of Wisconsin Oshkosh, Oshkosh, Wisconsin, 54901, U.S.A., churchim@uwosh.edu

ABSTRACT—Currently limited to cold climates near the Arctic circle, living walruses are the sole survivors of a previously much more diverse clade that occupied coastal waters throughout the northern hemisphere during the Mio–Pliocene. Though pinniped faunas have the highest diversity of walruses in the Miocene, the Purisima Formation of California records a moderately diverse assemblage of four walrus species. We report new specimens of tusked walruses (Odobeninae) including the oldest known members of Odobeninae, and Odobenini, and fossils of the specialized toothless odobenine walrus *Valenictus* Mitchell, 1961. Among these is the new species *Valenictus sheperdi* sp. nov., represented by a complete skull and referred post-crania from lower Pliocene strata within the Purisima Formation (5.33–4.89 Ma). Additionally, we report a geochronologically younger skull of *Valenictus chulavistensis* Deméré, 1994 from further up section (4.89–3.59 Ma). Expanded phylogenetic analysis recovers Odobeninae including *Ontocetus* Leidy, 1859 as the earliest diverging lineage in the Odobenini, and places a monophyletic *Valenictus* as the sister taxon to *Pliopedia*, Kellogg, 1921 which is included in a phylogeny for the first time; *Odobenus* is sister to the *Valenictus* + *Pliopedia* clade. Discovery of an isolated metacarpal near the base of the formation provides the oldest known well-dated evidence of odobenines. A diverse assemblage of molluskivores characterized the Neogene eastern North Pacific and their extinction around the Pliocene–Pleistocene boundary coincided with tectonically driven paleogeographic changes on the Pacific coast. The loss of temperate walruses may have provided opportunities for both new molluskivores and the otariid and phocid pinnipeds that make up present North Pacific pinniped communities.

SUPPLEMENTARY FILE(S)—Supplementary file(s) are available for this article for free at www.tandfonline.com/UJVP

http://zoobank.org/urn:lsid:zoobank.org:pub:C41482D3-7D4D-4FEF-8028-4FFD98DFAC0A

Citation for this article: Boessenecker, R. W., Poust, A. W., Boessenecker, S. J., & Churchill, M. (2024) Tusked walruses (Carnivora: Odobenidae) from the Miocene–Pliocene Purisima Formation of Santa Cruz, California (U.S.A.): a new species of the toothless walrus *Valenictus* and the oldest records of Odobeninae and Odobenini. *Journal of Vertebrate Paleontology*. https://doi.org/10.1080/02724634.2023.2296567

Submitted: November 27, 2022
Revisions received: November 9, 2023
Accepted: November 15, 2023

INTRODUCTION

The extant walrus *Odobenus rosmarus* Brisson, 1762 is an iconic pinniped uniquely bearing elongated canine tusks, and is the third largest pinniped after the elephant seals (*Mirounga* spp. Gray, 1827), weighing 800–1200 kg (females and males, respectively; Fay, 1982). Unlike most pinnipeds belonging to the Otariidae (eared seals) and Phocidae (true seals) families, *Odobenus* feeds predominantly on mollusks and has no other close living relatives (Boessenecker & Churchill, 2021). While the specialized *Odobenus* famously inhabits Arctic environments, the Bering Sea, and the higher latitudes of the North Atlantic, the Odobenidae were formerly more diverse in terms of feeding morphology (Deméré, 1994b; Boessenecker & Churchill, 2013), body size (Boessenecker & Churchill, 2018; Velez-Juarbe & Salinas-Marquez, 2018), and distribution (Repenning & Tedford, 1977; Deméré, 1994b; Geraads, 1997; Deméré et al., 2003; Kohno & Ray, 2008; Boessenecker & Churchill, 2021). Certain later diverging “imagotariines” (e.g., *Pontolis* True, 1905, *Osodobenus* Biewer et al., 2020) evolved enlarged ever-growing tusk-like canines large in diameter but short (Biewer et al., 2020); somewhat larger and short upper and lower tusks are present in the Dusignathinae (Barnes & Raschke, 1991; Deméré, 1994b). Long tusks (defined here as

---

*Corresponding author.

Color versions of one or more of the figures in the article can be found online at www.tandfonline.com/ujvp.

having an erupted length greater than 75% of bizygomatic skull width) characterize most Odobeninae (*Odobenus*, *Ontocetus*, *Valenictus*) though the earliest diverging odobenines either lacked tusks completely (*Aivukus* Repenning & Tedford, 1977) or possessed short tusks with massive, ever-growing roots and globular dentine (*Protodobenus* Horikawa, 1995; however, the holotype is a juvenile, and adult tusk length is unclear; Horikawa, 1995).

Long-tusked walruses (Odobenini) evolved during the Early Pliocene (Kohno et al., 1995b), and inhabited subtropical through cold temperate settings prior to the onset of Pleistocene glaciations (Repenning & Tedford, 1977; Deméré, 1994B; Kohno & Ray, 2008; Boessenecker et al., 2018). Fossils of *Ontocetus* (formerly *Alachtherium* Du Bus, 1867 and *Prorosmarus* Berry & Gregory, 1906; Deméré, 1994a) are known from Pliocene strata in Europe and from the Early Pliocene through Early Pleistocene of the east coast of North America (Kohno & Ray, 2008; Boessenecker et al., 2018), as well as from Japan (Kohno et al., 1998), suggesting trans-Arctic dispersal. The oldest fossils of *Odobenus* are known from uppermost Pliocene sediments of Japan (maximum age of 2.7 Ma; Miyazaki et al., 1992; Kohno et al., 1995b), followed by late Middle Pleistocene fossil occurrences in the North Atlantic (maximum of 240,000 years; Boessenecker et al., 2018, and references therein), suggesting a Pliocene western North Pacific origin of *Odobenus* followed by a Middle Pleistocene dispersal to the North Atlantic through the Arctic (Kohno et al., 1995b; Kohno & Ray, 2008; Boessenecker et al., 2018; Boessenecker & Churchill, 2021).

Pliocene rocks of the eastern North Pacific, however, have revealed a different walrus fauna than that present in the western North Pacific or North Atlantic. The North Pacific seems to be the cradle of early walrus diversity given that all early diverging walruses have been recovered from this region, supporting it as the center of origin for most walrus lineages (Deméré, 1994a; Kohno et al., 1995a; Miyazaki et al., 1995; Deméré et al., 2003). During the Late Miocene and Pliocene, "imagotariine" walruses, a paraphyletic grade of early diverging walruses, were replaced in the eastern North Pacific by more derived forms within the Neodobenia, including the dusignathine double-tusked walruses (e.g., *Dusignathus* Kellogg, 1927, *Gomphotaria* Barnes & Raschke, 1991) and non-tusked (*Aivukus*) and long-tusked odobenine walruses (*Pliopedia*, *Valenictus*; Barnes & Raschke, 1991; Biewer et al., 2020; Boessenecker & Churchill, 2018; Deméré, 1994a, 1994b; Parham et al., 2022; Repenning & Tedford, 1977). During the Middle and Late Miocene in Japan, pinniped faunas dominated by large desmatophocid seals and "imagotariines" were replaced in the Late Miocene and Pliocene by odobenine walruses including a ?tuskless (or short-tusked) form (*Protodobenus*), long-tusked forms (*Ontocetus*, and eventually *Odobenus*), and early sea lions (Kohno et al., 1995b, 1998; Miyazaki et al., 1992, 1995). The only pinnipeds common to both regions during the Pliocene were the fur seals *Thalassoleon* Repenning and Tedford, 1977 and *Callorhinus* Gray, 1859, which may have had circum-North Pacific distributions (Berta & Deméré, 1986; Boessenecker, 2011; Deméré & Berta, 2005; Kohno, 1992; Kohno & Yanagisawa, 1997).

The Late Neogene is a critical time in marine mammal evolution. Pliocene faunas are well known and starkly different from today in terms of taxonomy and ecological diversity (Boessenecker, 2013a; Deméré et al., 2003; Miyazaki et al., 1995; Whitmore & Kaltenbach, 2008), but the intervening time—the Pleistocene—is poorly recorded in terms of fossils with most specimens being Late Pleistocene in age and not described in detail. A large shift in the taxonomic composition of faunas is evident, but the timing and pace of that turnover have been obscured by limited marine vertebrate fossils of Early and Middle Pleistocene age (and incomplete material in general), especially when approaches at the faunal scale have required examination at the epoch level (Pimiento et al., 2017). Within the eastern North Pacific, Pliocene pinniped assemblages are generally composed of several walrus taxa and a single otariid fur seal, with an absence of phocid seals (but see Velez-Juarbe & Valenzuela-Toro, 2019). This contrasts strongly with the modern fauna, which includes two phocids (northern elephant seal *Mirounga angustirostris* Gill, 1866, harbor seal *Phoca vitulina* Linneaus 1758), several otariids (northern fur seal *Callorhinus ursinus* Linnaeus, 1758, Townsend's fur seal *Arctocephalus townsendi* Merriam 1897, California sea lion *Zalophus californianus* Lesson, 1828, Steller's sea lion *Eumetopias jubatus* Schreber, 1776) and no odobenids. Multispecies otariid assemblages seem to have been in place by at least the Middle Pleistocene, perhaps following immigration from the western North Pacific (Poust & Boessenecker, 2017). The timing of arrival of phocids remains poorly constrained, but no later than Middle Pleistocene (Boessenecker, 2013a). Extant Pacific walrus rarely range south of the Aleutian Peninsula, though some fossils of *Odobenus* have been reported in Late Pleistocene deposits in British Columbia (Harington & Beard, 1992) and as far south as northern California (Harington, 1984), but these occurrences lack robust paleoclimatic context (e.g., glacial vs. interglacial, paleotemperature). This contrast in faunal composition indicates a near total replacement of the eastern North Pacific pinniped fauna with an extinction of walruses sometime in the Late Pliocene–Early Pleistocene and subsequent dispersal of otariid and phocid pinnipeds into this region.

The Purisima Formation of northern California (Fig. 1) has produced several diverse and stratigraphically separated marine vertebrate fossil assemblages dating to the latest Miocene through Late Pliocene. While collections from the Purisima Formation are numerically modest compared with the expansive collections from Pliocene rocks of southern California (e.g., Capistrano, San Mateo, and San Diego formations), assemblages from this formation are emerging as the most thoroughly studied from the Pacific coast of North America (e.g., Boessenecker, 2013a, 2017; Boessenecker et al., 2015; Repenning & Tedford, 1977). The Purisima Formation preserves sharks, bony fishes, birds, a sea turtle, pinnipeds, dolphins, baleen whales, and a sea cow (e.g., Boessenecker et al., 2014: table 1).

A moderately diverse pinniped assemblage has been reported from the Purisima Formation, with otariids (*Thalassoleon* sp. cf. *T. macnallyae*, *Callorhinus gilmorei* Berta & Deméré, 1986, *Pithanotaria* sp. Kellogg, 1925) and odobenids well represented (*Dusignathus* spp., cf. *Osodobenus* sp., *Gomphotaria* sp. nov., and *Valenictus* sp.; Kellogg, 1927; Repenning & Tedford, 1977; Boessenecker, 2013a, 2017). This pinniped assemblage is an aggregate one, and most published specimens are known from the base of the formation (e.g., *Thalassoleon* sp., cf. *T. macnallyae*, *Dusignathus santacruzensis*; Kellogg, 1927; Mitchell, 1962; Repenning & Tedford, 1977); Pliocene pinnipeds include *Callorhinus gilmorei*, *Dusignathus* sp., cf. *D. seftoni*, *Valenictus* sp., and new material of *Valenictus* reported in this study. This matches the approximate numerical diversity of the modern pinniped fauna (2 phocids, 3 otariids), but is somewhat lower in diversity than early Late Miocene assemblages (1 otariid, 1 desmatophocid, 5–6 + walruses; e.g., Biewer et al., 2020; Boessenecker & Churchill, 2018; Powell et al., 2019).

Valenictus was originally reported to be an aberrant walrus based upon an isolated, nearly complete pachyostotic humerus with highly derived proportions from the Early Pliocene Deguynos Formation of inland southern California, deposited within the proto-gulf of California (Mitchell, 1961). Subsequently a similar (but fragmentary) humerus was discovered in the San Joaquin Formation in the Kettleman Hills of central California (Repenning & Tedford, 1977), and a wealth of skeletons, skulls, tusks, and postcrania were later discovered and reported by Deméré (1994b) from the Pliocene San Diego Formation of

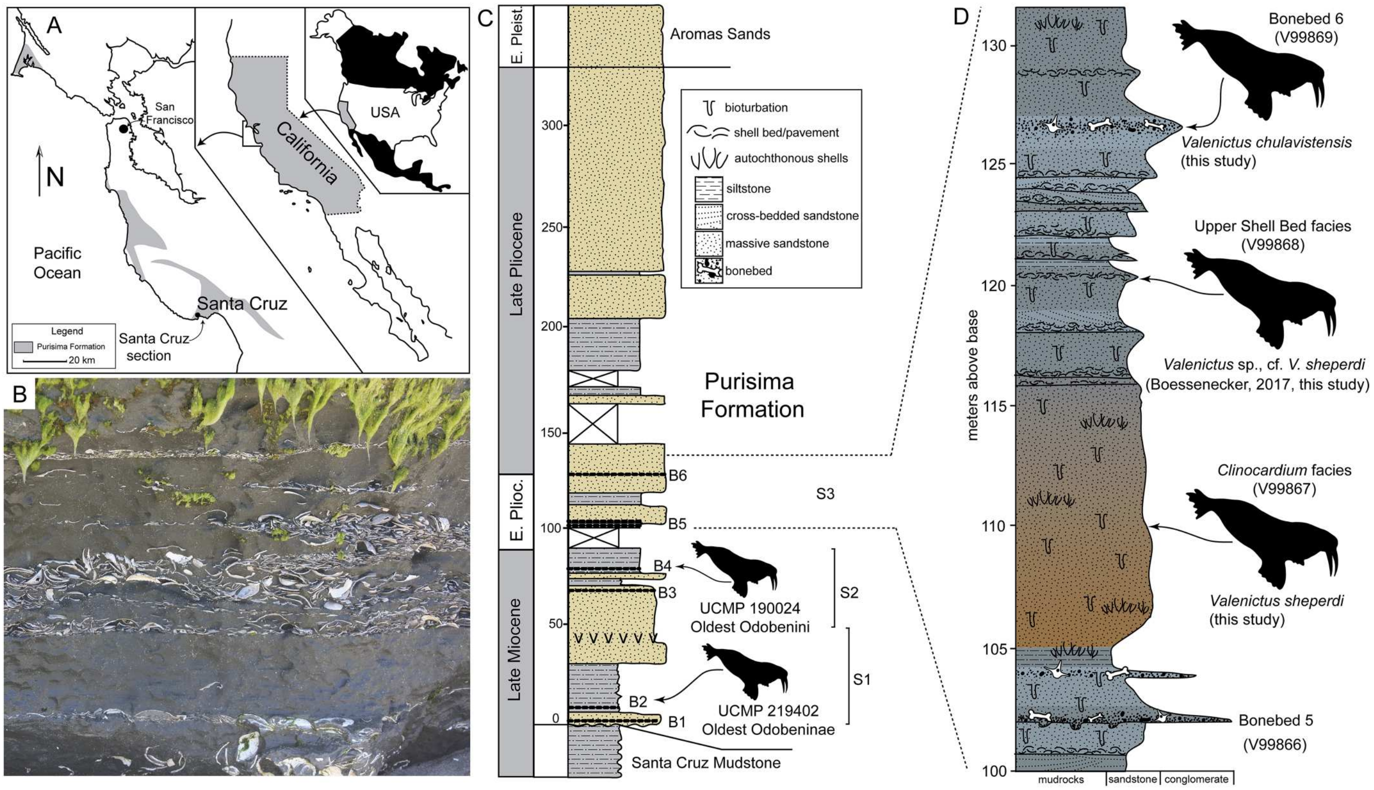

FIGURE 1. Geologic context of odobenine fossils reported in this study. **A**, geologic map of the Purisima Formation, Santa Cruz, California; **B**, exposure of *Valenictus*-bearing mollusk-rich sandstone ~120 m above the base of the Purisima Formation; **C**, generalized stratigraphic column of the Santa Cruz section of the Purisima Formation (modified from Powell et al., 2007:fig. 1); **D**, detailed stratigraphic column of the upper middle part of the Santa Cruz section of the Purisima Formation (modified from Boessenecker, 2017). **Abbreviations**: **B**#, bonebed numbers corresponding to Boessenecker et al. (2014). **S**#, subsection numbers corresponding to Boessenecker et al. (2014).

southern California. Well-preserved fossils of this new species *Valenictus chulavistensis* revealed that *Valenictus* was a long-tusked odobenine walrus lacking all teeth except for C^1 and exhibiting thickened and highly dense bone (pachyosteosclerosis) throughout its appendicular skeleton. Since then, undescribed postcrania of *Valenictus* have been reported from the Salada Formation of Baja California Sur (Barnes, 1998), and a well-preserved astragalus has been reported from the Purisima Formation (Boessenecker, 2017). Phylogenetic analysis indicated that *Valenictus* was closely related to the extant walrus, *Odobenus* (Deméré, 1994b). The surprising subtropical to warm temperate climatic conditions and highly specialized, autapomorphic skeleton of *Valenictus* (Deméré, 1994b) typify the strangeness of Pliocene marine vertebrates from the North Pacific (Boessenecker, 2013a).

This study reports newly discovered fossils of *Valenictus* from the Purisima Formation of northern California including skulls and a partial femur, supplementing the single isolated postcranial bone already reported. Among these is a complete skull representing the newly named species *Valenictus sheperdi*, and an incomplete skull referable to *Valenictus chulavistensis.* This study also reports other diagnostic but isolated remains of long-tusked walruses, representing the oldest known well-dated records of Odobenini and Odobeninae from the eastern North Pacific.

GEOLOGIC BACKGROUND

The Purisima Formation consists of a series of shelf deposits exposed in Santa Cruz, San Mateo, and Marin counties and consisting of shallow marine sandstone, siltstones, and claystones deposited in one or more basins controlled by wrench tectonics and subsequently separated by strike-slip faulting into several tectonic blocks (Capitola, La Honda subblocks of Santa Cruz structural block and the Point Reyes structural block; Powell et al., 2007, and references therein; Fig. 1).

The Santa Cruz section of the Purisima Formation is richly fossiliferous and exposed chiefly in coastal cliffs from Point Santa Cruz east to Aptos in Santa Cruz County. The Purisima Formation records initial rapid deepening of the basin and several shallowing upward parasequences indicative of an overall shoaling trend punctuated by minor transgressive adjustments (Boessenecker et al., 2014; Norris, 1986). The Santa Cruz section of the Purisima Formation was designated as an alternate reference section by Powell et al. (2007) since the original type section in the coastal cliffs near the mouth of Purisima Creek in Halfmoon Bay is now inaccessible by foot (Boessenecker, pers. obs. 2006). The Santa Cruz section of the Purisima Formation is divisible into three subsections (divided by erosional gaps between outcrops), numbered 1, 2, and 3 by Boessenecker et al. (2014). Subsection 1 (= the lower part of the Santa Cruz section, Fig. 1C) represents the basal 50 meters of the Purisima Formation and initial shallowing of the basin from offshore (= outer shelf) diatomites to massively bedded sparsely fossiliferous transition zone (= middle shelf) siltstones and sandstones deposited below (or near) storm weather wave base (Boessenecker et al., 2014). Subsection 2 (= the lower middle part of the Santa Cruz section, Fig. 1C) consists of massively bedded sandstones and siltstones deposited at transition zone and proximal offshore depths (Boessenecker et al., 2014); additionally, the Miocene–Pliocene boundary is present near the top of this subsection (Powell et al., 2007). Subsection 3 (= the upper middle part of the Santa Cruz section, Fig. 1D) records the final shallowing of the Purisima Formation and grades into thick coquinas and cross-bedded sandstones deposited above fair-weather wave base (Norris, 1986; Boessenecker et al., 2014).

An isolated odobenine metacarpal (UCMP 219402) was collected from Bonebed 2 approximately 3–4 meters above the base of the Purisima Formation near the base of Subsection 1 (Fig. 1C), which was deposited in the distal transition zone or proximal offshore depths (Boessenecker et al., 2014). This stratum is younger than the basal glauconite that produced a K/Ar date of 6.9 ± 0.5 Ma and below an ash bed recently dated to 6.3 Ma (J. Vasquez & S. Burgess, pers. comm., 2022); this specimen was collected from magnetozone R1 or N1 of Madrid et al. (1986) which correspond to chrons C3Ar and C3An.2n (respectively) and offer an alternate minimum age of 6.43 Ma (updated from Powell et al., 2007:fig. 1; Gradstein et al., 2012) for UCMP 219402. Geological context for each odobenine-bearing horizon is provided below.

An isolated tusk fragment (UCMP 190024) was collected from Bonebed 4 approximately 82–83 meters above the base of the Purisima Formation near the top of Subsection 2 (Fig. 1C); this bonebed, also known as the Crab Marker Bed (Madrid et al., 1986), is a pervasively bioturbated fine sandstone overlying and underlying finely laminated and bioturbated siltstone indicating deposition at offshore depths. Fossils recovered from this stratum include crustacean elements, bivalves, phosphatic molds, isolated, fragmentary, and articulated vertebrates. Large, lightly indurated phosphate nodules containing articulated crustacean exoskeletons, mollusk shells, marine mammal skulls, and even articulated skeletons indicate reworking at transition zone or offshore depths (Boessenecker et al., 2014). This bed approximates the Miocene–Pliocene boundary (Madrid et al., 1986; Powell et al., 2007) and marks the base of Chron C3r (updated from Powell et al., 2007:fig. 1) and therefore this specimen dates to approximately 6.03–5.23 Ma (Gradstein et al., 2012).

A nearly complete cranium of *Valenictus sheperdi* (UCMP 219061) was collected in a large (~40 kg) concretion found loose on the beach, but found in the vicinity of and matching the lithology of the "*Clinocardium* facies" of Perry (1988), which consists of lightly indurated medium grained, massively bedded, bluish gray, weathering to brown/reddish brown sandstone with sparsely packed shells of the bivalve *Clinocardium meekianum* Gabb, 1866 and the gastropod *Nassarius grammatus* Dall, 1917; dark grains of volcanic origin are common. Concretions typically envelop vertebrate and invertebrate fossils, including large clusters of the cockle *Clinocardium meekianum*; common fossils from this interval include the ark clam *Anadara trilineata* Gray, 1847, gastropods (*Neverita lewisii* Gould, 1847, *Nassarius grammatus*, *Crepidula princeps* Conrad, 1855), sand dollars (*Dendraster gibbsi* Rémond, 1863), and rare barnacles (*Balanus* sp. De La Costa, 1778, typically encrusting gastropods). Mollusks from the "*Clinocardium* facies" are the largest in absolute size from anywhere in subsection 3 (sensu Boessenecker et al., 2014). According to Norris (1986) and Boessenecker et al. (2014), the "*Clinocardium* facies" was deposited below fair-weather wave base but above storm-weather wave base, and therefore within the 'middle shelf' or Transition Zone, perhaps in 10–40 m water depth. UCMP locality V99867 is approximately 23–24 m above the Miocene–Pliocene boundary as recognized by Powell et al. (2007; 76–77 m above the base of the Purisima Formation, within subsection 3 of Boessenecker et al., 2014).

The *Clinocardium* facies is overlain by the "Upper Shell Bed Facies" of Perry (1988), which yielded a partial femur of *Valenictus* (SCMNH 21366). The "Upper Shell Bed Facies" consists of cross-bedded siltstone and fine sandstone with many shell beds concentrated both by storms (concave up bivalve shells) and by seafloor currents (concave down bivalves); shell beds are from 1–20 cm thick, and associated with hummocky cross-stratification and low-angle cross-stratification. Invertebrate diversity is highest within this section (Perry, 1988). This section was interpreted as representing deposition in the lower shoreface, perhaps from 5–20 m water depth (Boessenecker et al., 2014; Norris, 1986; Perry, 1988). The "Upper Shell Bed Facies" of Perry (1988) is in turn overlain by the "Concretionary Bed" of Perry (1988), also referred to as Bonebed 6 by Boessenecker et al. (2014; =UCMP locality V99869; Fig. 1D), which is a phosphatic hardground formed during a depositional hiatus corresponding to Gilbert Chrons C2Ar through C3n.3n, or 4.89–3.59 Ma (Gradstein et al., 2012; Madrid et al., 1986). Therefore, an age of 5.33–4.89 (Early Zanclean) can be assigned to fossils from the "*Clinocardium* Facies" and "Upper Shell Bed Facies," and an age range of 4.89–3.59 Ma can be assigned to specimens from the "Concretionary Bed" (Bonebed 6). One skull (UCMP 137426) appears to have been derived *ex situ* from this thin stratum.

A second nearly complete cranium referable to *Valenictus chulavistensis* (UCMP 137426) was collected in an isolated concretion from a separate locality, in the geographic vicinity of locality UCMP V6875, but assigned a unique locality owing to stark difference in lithology. The lithology of the enveloping concretion consists of strongly cemented fine grained sandstone with phosphate pebbles, which according to Barnes and Perry (1989) matches the lithology of the "Concretionary Bed" described above. Though exposed 1–1.5 km to the northeast, this concretion most likely was eroded out of older cliffs sometime during the Pleistocene. Many concretions of this lithology can be observed exposed at the base of the Upper Pleistocene terrace deposits directly overlying the Purisima Formation, indicating erosion from geochronologically younger Purisima strata. Based on this lithologic correlation, this specimen of *Valenictus chulavistensis* therefore corresponds to an age of 4.89–3.59 Ma.

MATERIALS AND METHODS

UCMP 219091 was preserved within a 40 kg concretion; initial preparation was undertaken by RWB at MOR from 2010–2011 using a pneumatic chisel scaler and a hammer and chisel, followed by finer mechanical preparation using pneumatic air scribes. Preparation continued at CCNHM from July 2017 to September 2018. To preserve the integrity of the skull, matrix was left within the left temporal fossa (e.g., Barnes, 1989) of UCMP 219091. Bathing in 16 liters of 10% acetic slowly removed most remaining matrix. Intermittent acid baths approximately 1–2 weeks in duration were separated by overnight rinsing, drying, and consolidation of exposed bone prior to the next bath. Preparation was halted after it began to hollow out the interorbital region of the frontal. UCMP 137426 was prepared mechanically at LACM, leaving only a thin rind of concretionary matrix on bone surfaces. Preparation was likely completed using a bath of dilute formic acid preparation (J. Velez-Juarbe, pers. comm. 2022). All specimens were photographed with a Canon Eos Rebel T5 using an 18–55 mm zoom lens and a Nikon D610 and 60 mm macro lens. Anatomical terminology generally follows Deméré (1994b), Deméré and Berta (2002), and Evans and Lahunta (2013). Cranial suture age was calculated using the method from Sivertsen (1954). Epicontinental seaway area was estimated using paleogeographic maps from Hall (2002) and the program ImageJ (Schneider et al., 2012).

To determine the evolutionary relationships of *Valenictus sheperdi*, we performed a phylogenetic analysis of the family Odobenidae. Twenty-nine species of extinct walrus were included, alongside the extant *Odobenus*, representing every described species of walrus, as well as *Ontocetus* sp. from Japan (SFMCV-0001; Kohno et al., 1998). Seven outgroup taxa were also selected, representing a full range of pinniped diversity, including two early diverging "enaliarctines" (*Enaliarctos emlongi* Berta, 1991 and *Pteronarctos goedertae* Barnes, 1989), one otariid (*Callorhinus ursinus*), two extinct desmatophocids (*Desmatophoca oregonensis* Condon, 1906 and *Allodesmus kernensis* Kellogg, 1922) and two extant phocids (*Erignathus barbatus* Erxleben, 1777 and *Monachus Monachus* Herman, 1779). We also coded UCMP 137426 as a separate OTU in order to test the hypothesis that this specimen represents *Valenictus chulavistensis.* We coded *Pliopedia pacifica* Kellogg, 1921 for the first time, combining the holotype and USNM 187328 into a composite OTU. Two separate analyses were completed; the first analysis included all taxa, however in the second analysis we excluded several fossil taxa known only from very incomplete material. The same search method parameters were used in both analyses. Taxa excluded in this second analysis were *Kamtschatarctos sinelnikovae* Dubrovo, 1981, *Pelagiarctos* sp. Barnes, 1988, *Nanodobenus arandai* Velez-Juarbe and Salinas-Marquez 2018, and *Valenictus imperialensis.*

The character matrix (Supplementary Files S1, S2) created for this study (using Mesquite 3.81; Maddison & Maddison, 2023) consisted of 35 OTUs and 143 characters, drawn from Boessenecker and Churchill (2013), with modifications from Tanaka and Kohno (2015), Biewer et al. (2020), and this study. These include 76 cranial, 14 mandibular, 40 dental, 12 postcranial and 1 body size character(s) (Supplementary Information; Supplementary Files S1, S2). Character coding was based largely on personal examination of specimens and casts (Supplementary File S2), supplemented with information from the literature (Tanaka & Kohno, 2015; Magallanes et al., 2018; Velez-Juarbe & Salinas-Marquez, 2018; Biewer et al., 2020). Some characters used by Boessenecker and Churchill (2013) used scaled polymorphic coding after Churchill et al. (2014), though character states were not ordered into a morphological continuum (Biewer et al., 2020). In some characters (n = 4), the states were simply reordered into a continuum; in other cases, some states needed to be removed and defined as separate characters (n = 2). All other characters that could form a morphological continuum were converted to ordered characters (n = 46). Overall, 59 characters (including polymorphic characters) were treated as ordered (characters 7–9, 12, 18, 22, 24–25, 27, 33, 34, 37, 40–43, 47, 49, 52, 55–56, 59–60, 62–63, 65, 67–69, 71–74, 81, 83, 91, 94, 97, 99–100, 105, 107, 111–118, 120–122, 127–128, 132, 135, 139, 143) and all remaining characters were treated as unordered. Ordered characters were treated as additive with a weight of 1 for each internal step. For a list of characters and descriptions, see Supplementary Information.

Phylogenetic analyses were carried out in TNT 1.6 using a new technology search with 10,000 random addition sequences and tree-fusing and sectorial options checked, and all other settings set to default options; memory options include 1000 mb RAM and space for 100,000 trees. *Enaliarctos emlongi* was assigned as the outgroup in all analyses. To assess nodal support, bootstrap values were calculated, using symmetrical resampling and 1000 replicates.

Institutional Abbreviations—**CCNHM**, Mace Brown Museum of Natural History, College of Charleston, Charleston, SC, U.S.A.; **LACM**, Natural History Museum of Los Angeles County, Los Angeles, CA, U.S.A.; **MOR**, Museum of the Rockies, Bozeman, MT, U.S.A.; **NMR**, Natural History Museum Rotterdam, Rotterdam, the Netherlands; **OCPC**, Orange County Paleontology Collection, Santa Ana, Orange County, CA, U.S.A.; **SDSNH**, San Diego Society of Natural History, which operates the San Diego Natural History Museum (**SDNHM**), San Diego, CA, U.S.A.; **UCMP**, University of California Museum of Paleontology, Berkeley, CA, U.S.A.; **USNM**, Smithsonian Institute, Washington D.C., U.S.A.

SYSTEMATIC PALEONTOLOGY

MAMMALIA Linnaeus, 1758
CARNIVORA Bowdich, 1821
PINNIPEDIA Illiger, 1811
ODOBENIDAE Allen, 1880
ODOBENINAE Mitchell, 1968
ODOBENINAE indeterminate
(Fig. 2A, B)

Referred Specimen—UCMP 219402, a left metacarpal 1 from UCMP locality V99877 (= Bonebed 2 of Boessenecker et al., 2014; Fig. 1C), approximately 3 meters above the base of the Purisima Formation, by R.W. Boessenecker December 23, 2007; Late Miocene, 6.9–6.43 Ma.

Description and Identification—UCMP 219402 is an unusually robust metacarpal (Fig. 2A, B) identifiable as an odobenine walrus owing to its lateral bowing and proximal inflation. The proximal half is massively inflated, and the transverse width is over 200% the width of the narrowest part of the diaphysis. A deeply excavated pit for the *m. extensor pollicis* is situated proximally on the lateral surface near the posterior border of the metacarpal. In cross section, the metacarpal is thickest posteriorly and tapers to a thin anterior crest, as in *Odobenus rosmarus* and *Valenictus chulavistensis* (SDSNH 83719). The proximal articular surface is nearly flat, like *Odobenus*, and differing from the saddle-like condition in imagotariines, dusignathines, *Pliopedia*, and *Aivukus* where the trochlea extends onto the lateral surface; the articular surface is also posteriorly canted relative to the diaphysis (similar to *Odobenus* and *Valenictus*), whereas it is perpendicular to the diaphysis in all dusignathine and imagotariine walruses, as well as *Aivukus*, *Pliopedia*, and other pinnipeds. The ventral side is flat and slightly concave. A prominent proximal tubercle is positioned posteriorly, adjacent to the articular surface. Unlike all other odobenids for which a metacarpal 1 is known, the diaphysis curves and is anteriorly bowed with a distal end facing posterodistally; this condition is shared with *Odobenus*, *Pliopedia*, *Valenictus*, and *Aivukus*. Fractures exposed during collection and preparation showed that UCMP 219402 is chiefly composed of cancellous bone (Boessenecker, pers. obs., 2007) and differs from the pachyosteosclerotic condition of *Valenictus chulavistensis* postcrania (though pachyosteosclerosis was not reported by Deméré, 1994B, in the astragalus of *V. chulavistensis*). Lastly, UCMP 219402 is unusually short (length = 370% of distal articular width), similar to *Valenictus* (370% in SDSNH 83719), but shorter relative to other odobenines such as *Odobenus* (400%), *Pliopedia* (490%), *Aivukus* (460%), and imagotariines (490% in *Imagotaria downsi* Mitchell, 1968, USNM 23859). UCMP 219402 is most similar to *Odobenus rosmarus* but the degree of inflation, anterior bowing, and the size of the anterior crest is clearly more derived. This morphology is unknown among all published odobenids, but compares well with OCPC 2159, a partial unpublished and incompletely prepared (non-*Valenictus*) odobenine skeleton from the Niguel Formation of Orange County, California. UCMP 219402 is proportionally one of the most massively inflated odobenine metacarpals yet discovered, precluding assignment to any existing odobenid species, and strongly suggests the existence of an as-yet unidentified odobenine close in morphology to *Odobenus* in the latest Miocene of the eastern North Pacific. Lastly, UCMP 219402 does not compare well with the metacarpal 1 of a forelimb (LACM 3011) referred to *Dusignathus santacruzensis* collected about 20 meters upsection in the Purisima Formation (Mitchell, 1962; Repenning &

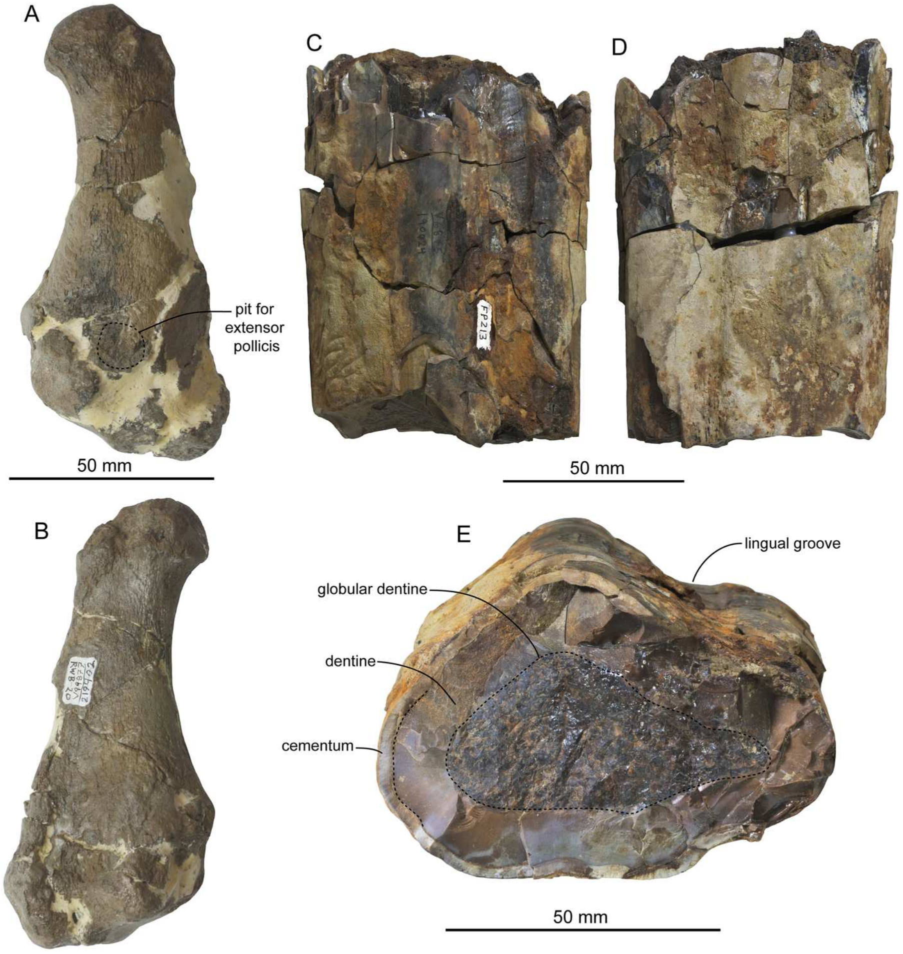

FIGURE 2. The oldest known records of Odobeninae and Odobenini. **A**, right metacarpal 1 of Odobeninae indet., UCMP 219504, dorsal view; **B**, same, ventral view; **C**, isolated C^1 tusk of Odobenini indet., UCMP 190024, in lingual view; **D**, same, labial view; **E**, same, cross section.

Tedford, 1977); UCMP 219402 differs in being much more proximally inflated with a posterolaterally canted proximal articulation and a diaphysis that is more laterally bent. In these features LACM 3011 compares favorably with *Imagotaria*, *Pontolis*, and *Titanotaria* Magallanes et al., 2018.

ODOBENINI Deméré, 1994b
ODOBENINI indeterminate
(Fig. 2C–E)

Referred Specimen—UCMP 190024, a partial tusk collected from the Crab Marker Bed (= Bonebed 4 of Boessenecker et al., 2014; V6875; Fig. 1C), approximately 77 meters above the base of the Purisima Formation, by F.A. Perry March 6, 1978; latest Miocene to earliest Pliocene, 6.03–5.23 Ma.

Description and Identification—UCMP 190024 is a segment of a large tusk near the alveolar margin (Fig. 2C, D). It has a subtriangular cross section, with a nearly flattened lingual surface and a strongly convex labial surface. Two narrow lingual furrows and a single broad, shallow labial furrow are present. A large core of globular dentine with a roughly triangular cross section is developed. The globular dentine is surrounded by a 12–15 mm thick layer of dentine; this is in turn surrounded by a 3–4 mm thick layer of cementum. UCMP 190024 is identifiable to Odobenini owing to the presence of a globular dentine core (Deméré, 1994a, Kohno et al., 1995b; Ray 1975). UCMP 190024 compares well with tusks of *Odobenus rosmarus*, *Ontocetus emmonsi* Leidy, 1859, and *Valenictus chulavistensis*, but owing to incompleteness, not identifiable further.

VALENICTUS Mitchell, 1961

Amended Diagnosis—Odobenin walruses possessing a humerus with a broad deltopectoral crest lacking a sharp crest, a greatly thickened greater tuberosity, greatly enlarged medial entepicondyle, proximal and distal ends massively enlarged, diaphysis relatively short, and narrow bicipital groove. Putative synapomorphies preserved in all species with a skull included toothlessness, numerous palatal foramina, and a pentagonal nasal.

VALENICTUS CHULAVISTENSIS Deméré, 1994
(Figs. 3, 4, 5, 6, and 7)

Odobeninae new species Barnes and Perry, 1989

Amended Diagnosis—A large species of *Valenictus* (maximum male CBL = 393 mm; maximum female CBL = 304 mm; see Table 1) differing from *Valenictus imperialensis* in possessing a humerus with larger overall size, more sigmoidal posterior profile, sharply keeled supinator ridge, more robust and rectangular entepicondyle, and more obtuse angle between the shaft and axis of the distal trochlea in anterior/posterior view. Differing from *Valenictus sheperdi* sp. nov. in: (1) smaller overall size (*V. sheperdi* female CBL = 390 mm), (2) broader space between canines (21–24% CBL v. 15% in *V. sheperdi*), (3) a short and transversely blunt maxillary crest between the canine and zygomatic arch, (4) anteroposteriorly broad and swollen paroccipital process, (5) smaller and scattered foramina

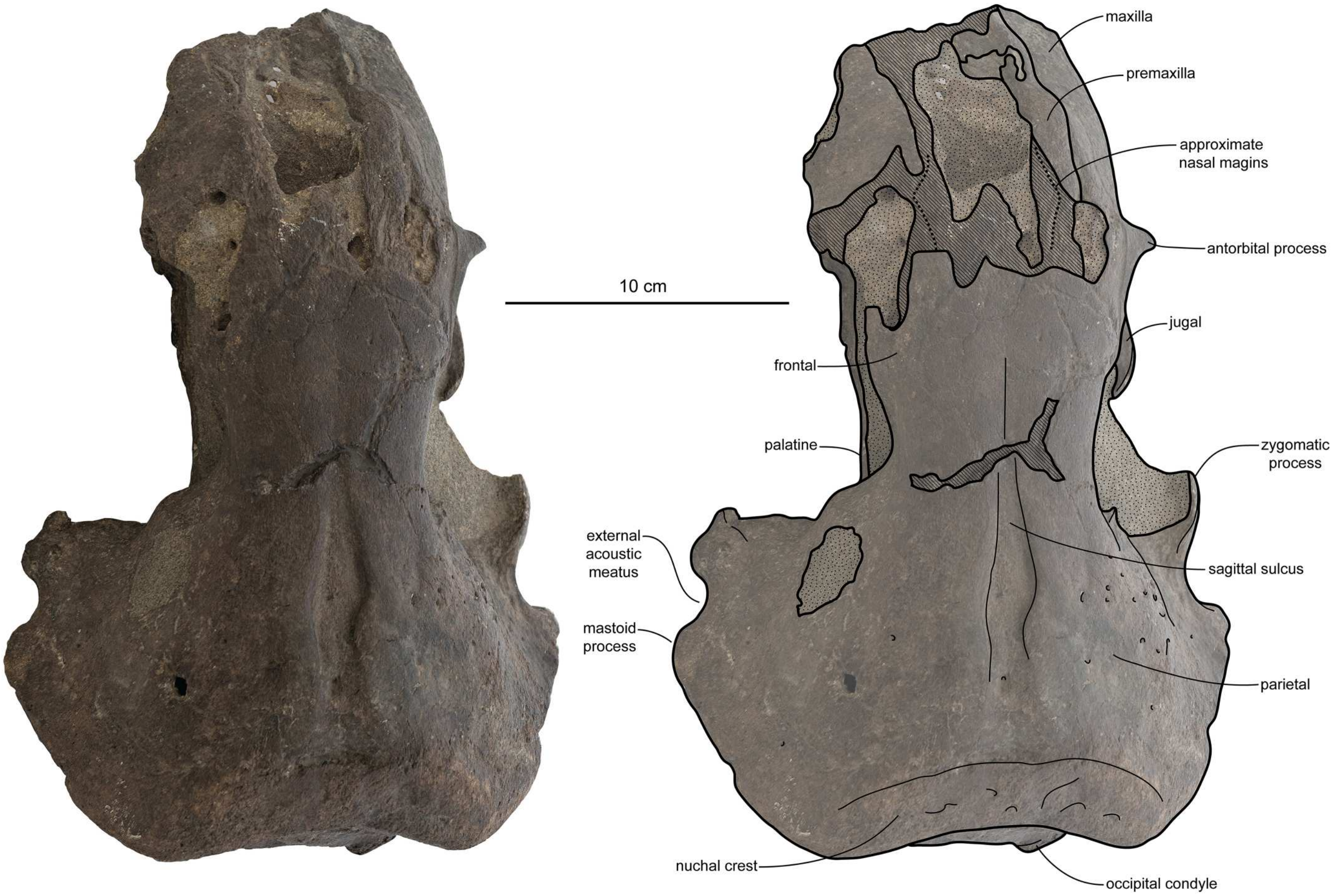

FIGURE 3. Referred cranium of *Valenictus chulavistensis* from the Purisima Formation, UCMP 137426, in dorsal view.

in palate lacking sulci, (6) continuously convex anterior margin of the nuchal crest (rectangular in *V. sheperdi*), and rectangular margin of the internal choanae (rounded in *V. sheperdi*). Also possessing the following synapomorphies of Odobeninae and Odobenini: enlarged, continuously growing upper canines with globular dentine cores, narrow, longitudinally and transversely arched palate, mastoid processes widely flaring and forming widest part of skull, foreshortened temporal fossae and zygomatic arches bearing dorsoventrally expanded postorbital process.

Referred Specimen—UCMP 137426, a nearly complete but slightly abraded cranium missing parts of the alveolar margin of the rostrum, zygomatic arches, and left mastoid process; collected *ex situ* on the beach by E. Burman in 1989 in the vicinity of UCMP locality V-6875, but stratigraphically originating from the Pebbly Marker Bed of Madrid et al. (1986; = Concretionary bed of Perry, 1988, and Bonebed 6 of Boessenecker et al., 2014; Fig. 1D), approximately 126 meters above the base of the formation; late Early to early Late Pliocene, 4.89–3.59 Ma. Detailed locality data on file at UCMP.

Identification—UCMP 137426 shares with *Valenictus chulavistensis*, to the exclusion of *Valenictus sheperdi*, a wide spacing between the canines (~21–24% CBL; 15% in *V. sheperdi*), a short maxillary crest lacking a sharp ventral edge; an anteroposteriorly thick paroccipital crest; a continuously convex anterior margin of the nuchal crest in dorsal view; elongate sulci absent from the palate.

Ontogenetic Age and Sex—Despite the surficial abrasion and incompleteness of UCMP 137426, all but one suture (median maxillary suture) can be scored for the Sivertsen (1954) method, providing a suture age of approximately 27–31 (Table 2); sutures I–VI are clearly suture score 4 (fully closed and obliterated) but suture VIII (basisphenoid-presphenoid) is possibly partially to fully closed (suture score 2–4) and owing to incompleteness the maxilla-premaxilla suture is best scored as open to nearly completely closed (suture score 1–3). These suture scores indicate that UCMP 137426 is an adult, and of similar ontogenetic age as the *Valenictus sheperdi* type specimen (UCMP 219091). UCMP 137426 has relatively low nuchal crests, canine alveoli that are both transversely narrow (width approximately 40% of alveolus length) and relatively small (alveolus length 12% of estimated condylobasal length), indicating that this specimen is a female.

Description

A brief description of UCMP 137426 is warranted, but the description will be limited to features not preserved in published *Valenictus chulavistensis* specimens from the San Diego Formation and where differences exist with *Valenictus sheperdi*. Unlike the broken holotype skull (SDSNH 36786) and the more complete but diagenetically distorted paratype skull (SDSNH 38227) of *Valenictus chulavistensis*, UCMP 137426 is undistorted and faithfully preserves the original proportions of the skull and rostrum. The rostrum of UCMP 137426 (Figs. 3–5) is somewhat elongate (34% of condylobasal length), intermediate in proportion between the relatively more elongated skulls of ancestral imagotariine walruses

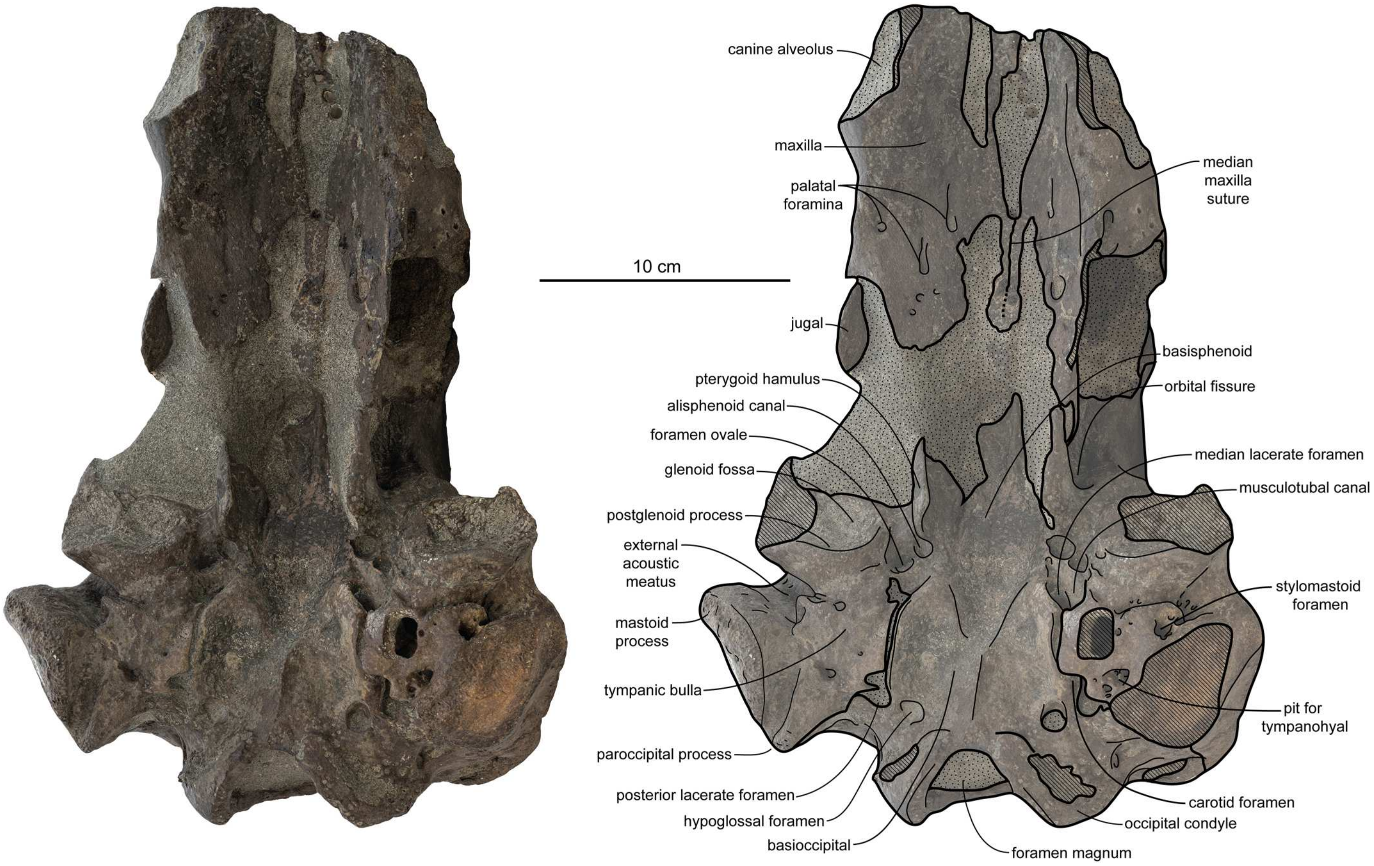

FIGURE 4. Referred cranium of *Valenictus chulavistensis* from the Purisima Formation, UCMP 137426, in ventral view.

(e.g., *Imagotaria*, *Neotherium* Kellogg, 1931) and *Odobenus*. This differs from the paratype of *V. chulavistensis*, which appears to be diagenetically foreshortened; undistorted crania discovered by SDNHM since publication of Deméré (1994b), such as SDSNH 63036, 83719, and 90497, confirm this. In this regard, undistorted specimens of *Valenictus chulavistensis* such as UCMP 137426 and *Valenictus sheperdi* resemble the rostrum:braincase proportions of at least one well-preserved *Ontocetus emmonsi* cranium (e.g., NMR 999100010019; Erdbrink & Van Bree, 1990:pl. 1). The rostrum of UCMP 137426 is more elongate than in the distorted paratype (SDSNH 38227), and also highlights a somewhat triangular and more elongate temporal fossa (Fig. 3)—roughly 25% of condylobasal length, as opposed to the nearly circular fossae (18%) preserved in SDSNH 38227.

The narial margin, while incomplete, was clearly concave in lateral view (Fig. 5) as in *Valenictus sheperdi*, and likely also had a prominent prenarial process. Unlike *Odobenus* and the distorted *Valenictus chulavistensis* paratype skull, the anterior margin of the maxilla, following the inclination of the underlying canine, slopes approximately 50° from the basal plane of the skull; this condition is confirmed by the undistorted holotype maxilla and referred rostrum fragment SDSNH 38228 (Deméré 1994b:fig. 2d).

The interorbital region and anterior dorsal braincase is not preserved in the holotype (Fig. 7) and was scraped away by construction equipment during the discovery of the paratype skull, but is well-preserved in UCMP 137426, if slightly worn. The right nasal appears to have a laterally convex suture with the premaxilla, similar to *Valenictus sheperdi*, perhaps giving the combined nasals a hexagonal shape in dorsal view (Fig. 3). The suture between the maxilla, nasals, and frontal appears to have been transverse as in *Odobenus*, but this region is quite fractured and waterworn. The dorsal margin of the skull was quite planar in lateral view (Fig. 5), like *Valenictus sheperdi* (UCMP 219091), and unlike the continuously convex profile in the diagenetically foreshortened *V. chulavistensis* paratype (SDSNH 38227). The dorsal surface of the braincase is transversely flat and tabular from the nuchal crest anteriorly to the level of the antorbital processes (Fig. 4). Posteriorly, paired sagittal sulci are present rather than a sagittal crest (Fig. 3), as in *Valenictus sheperdi* and *Pliopedia pacifica* (USNM 187328; Repenning & Tedford, 1977:pl. 24.6). Like the *V. chulavistensis* paratype, UCMP 137426 has a rounded rather than rectangular (as in *Ontocetus emmonsi*; Van Beneden 1877:pl. 1.1) dorsolateral margin of the braincase in posterior view. Similarly, the nuchal crest is convex (as in the *V. chulavistensis* paratype) rather than rectangular in dorsal view as in *V. sheperdi*.

While UCMP 137426 differs from *Valenictus sheperdi* in possessing a more inflated mastoid process, it is less extremely inflated than in the male holotype and paratype specimens. UCMP 137426 further differs in lacking the ventrally projecting mastoid process (Fig. 6) of these male specimens of *Valenictus chulavistensis*. In UCMP 137426 the mastoid projects below the postglenoid process roughly the depth of the zygomatic at the postglenoid, as opposed to 150% of that distance in the male holotype and paratype specimens of *Valenictus chulavistensis*. A similar condition, however, is seen in unpublished female skulls of *V. chulavistensis* (SDSNH 63036, 83719). The ventral crest of the mastoid process itself seems consistently more anterolateral than in specimens from the San Diego Formation, perhaps 32° from the sagittal plane versus 51° in the paratype and 55° in SDSNH 63026 and 47° in SDSNH 83719. This angle is approximately 46° in *Valenictus sheperdi*.

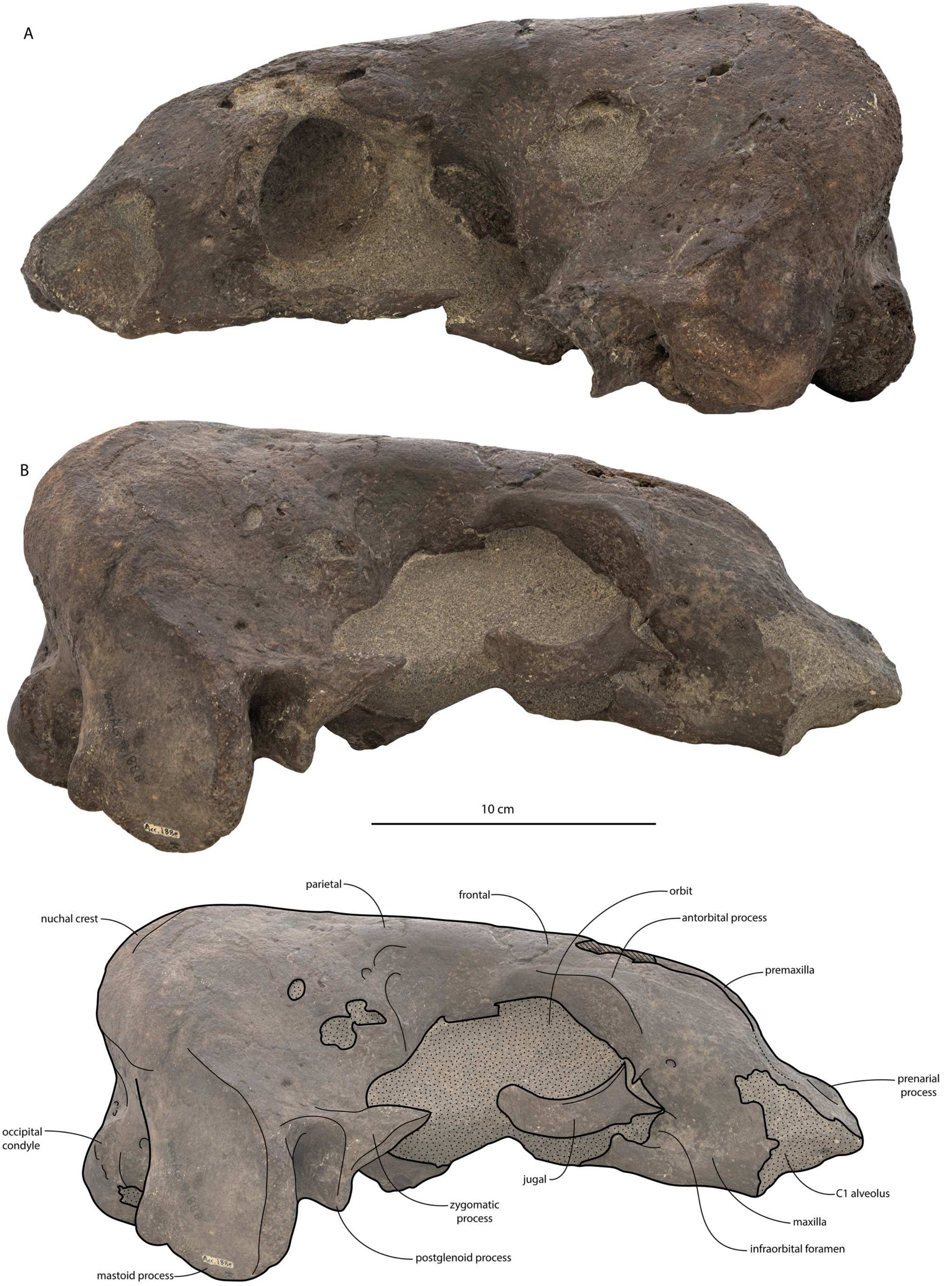

FIGURE 5. Referred cranium of *Valenictus chulavistensis* from the Purisima Formation, UCMP 137426. **A**, left lateral view; **B**, right lateral view.

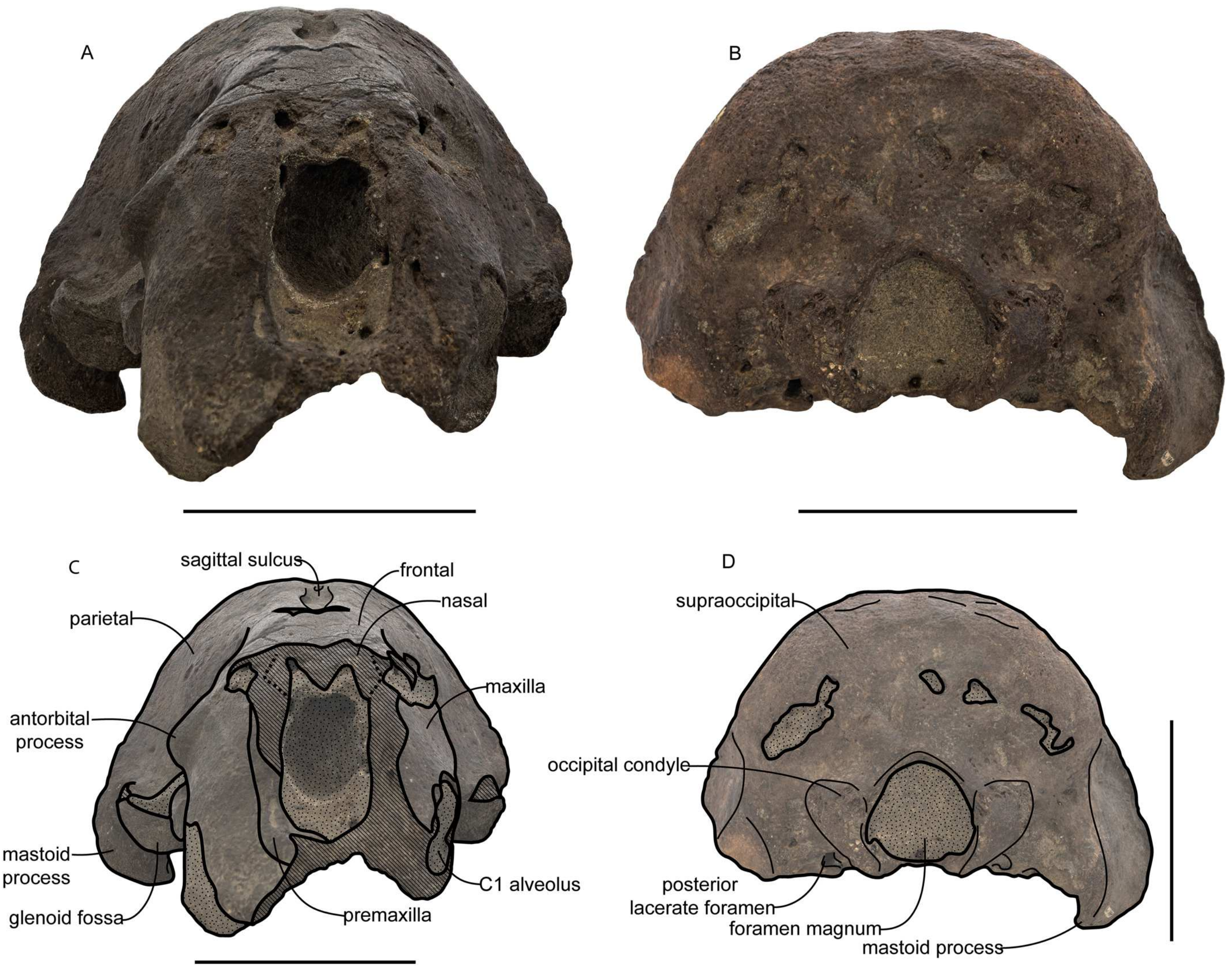

FIGURE 6. Referred cranium of *Valenictus chulavistensis* from the Purisima Formation, UCMP 137426. **A**, anterior view; **B**, posterior view.

Like the paratype and other specimens of *V. chulavistensis*, the bulla in UCMP 137426 is ventrally flattened (Fig. 4). UCMP 137426 differs from the paratype in lacking medial and anterior ventral tuberosities on the bulla. A broad, shallow hyoid fossa is present in the paratype and other San Diego Formation specimens, but in UCMP 137426 it is a more distinctly excavated trough extending posteriorly towards the paroccipital process. The hypoglossal foramina are somewhat crushed in the *V. chulavistensis* paratype, but in UCMP 219091 (*Valenictus sheperdi*) and 137426 (*Valenictus chulavistensis*) they are circular (6.7 mm diameter on right, 9.0 mm on left in UCMP 219091), and positioned just posteromedial to the posterior lacerate foramen (Fig. 4). Like the paratype, the posterior lacerate foramen and opening for the posterior carotid canal are stacked so that a nearly combined bilobate fissure is present (Fig. 4). The posterior carotid canal opens at about the level of the hypoglossal foramen in UCMP 137426 and the *V. chulavistensis* paratype, whereas in *V. sheperdi* the posterior carotid canal opens anterior to the hypoglossal foramen.

Fractures in the parietal during preparation revealed dense (osteosclerotic) bone with small pores, similar to the osteosclerotic condition visible in fractures of the *Valenictus chulavistensis* holotype, though not described by Deméré (1994b).

VALENICTUS SHEPERDI, sp. nov.
(Figs. 8, 9, 10, 11, 12, 13, 14, and 15)

Holotype—UCMP 219091, a nearly complete cranium, collected from UCMP locality V99867 by Forrest Sheperd, January 2011.

Etymology—*sheperdi*, named in honor of Mr. Forrest Sheperd, who found and donated the holotype specimen when he was a young fossil collector.

Type locality and horizon—Collected from a large calcareous sandstone concretion found loose on the beach in Santa Cruz County, California, with associated matrix and mollusks matching the "*Clinocardium* facies" of Perry (1988), and originally derived approximately 104–114 meters above the base of the Purisima Formation (Fig. 1D); earliest Pliocene, 5.33–4.89 Ma. Detailed locality data on file at UCMP.

Diagnosis—*Valenictus sheperdi* bears one synapomorphy of Odobeninae, dorsoventrally expanded postorbital process, and

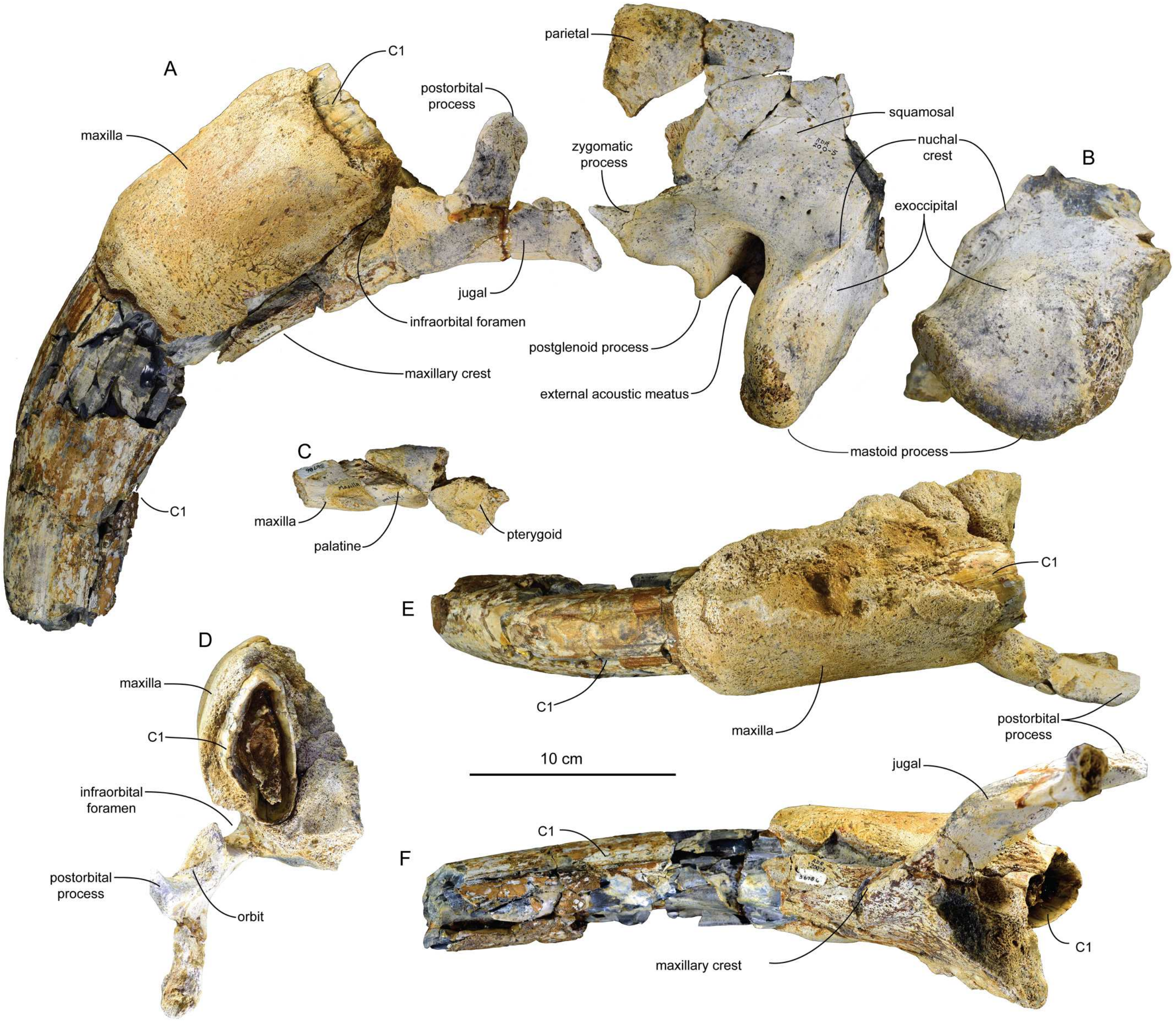

FIGURE 7. Holotype cranium of *Valenictus chulavistensis* from the San Diego Formation, SDSNH 56786. **A**, cranium in lateral view; **B**, exoccipital in posterior view; **C**, pterygoid strut in lateral view; **D**, maxilla and C^1 in proximal view; **E**, maxilla and C^1 in anterodorsal view; **F**, maxilla and C^1 in posteroventral view.

several synapomorphies of Odobenini, including enlarged canine alveoli and alveolar processes of the maxillae, enlarged and widely flaring paroccipital processes that form the widest part of the skull, a sagittal sulcus on the dorsal midline of the braincase, elongate/elliptical bony nares, anteroposteriorly expanded nuchal crest, and a posteriorly expanded palate with a foreshortened pterygoid strut. UCMP 219091 belongs to *Valenictus* in lacking incisors and upper postcanine teeth, possessing a less foreshortened skull than in *Odobenus.* UCMP 219091 is not referable to *Valenictus chulavistensis* and represents a new species of *Valenictus* based on the following features: (1) narrower space between canines (15% CBL versus 21–24% in *V. chulavistensis*); (2) a ventrally sharp and elongate maxillary crest between the canine and jugal (measuring 21% CBL v. 19–14% in *V. chulavistensis*); (3) anteroposteriorly narrow paroccipital process with a sharp ventral crest (anteroposteriorly thick and swollen in *V. chulavistensis*), (4) large foramina in palate with deeply entrenched sulci; (5) truncated (transversely flattened) anterior margin of the nuchal crest (continuously convex in *V. chulavistensis*); and (6) rounded rather than rectangular posterior margin of the internal choanae. *Valenictus sheperdi* cannot be readily compared with *Valenictus imperialensis* owing to a lack of overlapping parts.

Ontogenetic Age and Sex—UCMP 219091 appears to be a female owing to the relatively narrow rostrum (37% of CBL; 37% of CBL in SDSNH 83717, female *V. chulavistensis*) and small, narrow canine alveoli; in the confirmed male holotype of *V. chulavistensis* the anteroposterior width of the canine at the alveolar rim is 18% of CBL and the transverse width is 12% of CBL; in UCMP 219091 the length of the canine alveolus is 13% CBL and the width is only 6%, indicating that it is substantially smaller and narrower than known males of *Valenictus*

TABLE 1. Table of measurements (in mm) of *Valenictus* crania from the Purisima and San Diego formations.

	Valenictus sheperdi	*Valenictus chulavistensis*							
Specimen	UCMP 219091	SDSNH 36786 Holotype	SDSNH 38227	UCMP 137426	SDSNH 63022	SDSNH 83690	SDSNH 83715	SDSNH 83719	SDSNH 90497
Condylobasal length	360		251	316.2	345.5		293	304	392.5
Palate length (prenarial process to choanae)	198.6		145	>142.0	245.5		183	157	
Rostrum length: ant. premaxilla to post. nasal	140							82.7	127
A/P length of nasals	71				94.4				68
Temporal fossa length	81.5		73.8	114.8	97.3		82	83.3	97
Length of fossa anterior to pterygoid hamulus	105.7		75.3	119.16	83.7			92.87	
Intertemporal length (supraorbital process to ant. braincase margin)	86.5		53.5	50.5				38.4	37.5
Braincase length	138		132.2	141.5	170			136.7	135
Max. width of braincase	150–155		174	132.4	>158			162	
Length of zygomatic: tip of zyg. to post temporal fossa	23.9			22.6	34.4			36	27.5
Width of skull across canines	123.3		123.5	118.2	181.6		118	125.5	
Width of palate between canines	48.9		50.8	64.6	67.8		57.9	58.7	56
Max length of canine alveolus	48.4	80.5	58.8	50.8	65.5	28.8	41.7	41	76.6
Max width of canine alveolus	27.3	47.1	37.7	31	40.5	17.2	26.8	28.8	47.1
Max. width of palate	119		78.8	97.3	73.6		76	84.5	
Antorbital width	139.5		120	140 est	199			137.1	
Max. width nasals	46				72.6			54.5	45.6
Min. width nasals	36 (31.1 anteriorly)				42				33.9
Postorbital width of frontal	91.50 €			97.6	115.9			90	
Least intertemporal width	73		75.9	72.5	85.5			71.5	
Bizygomatic width	205.2		205		263.1		178	197.2	
Mastoid width	249.2		247	222	297			249.4	
Diagonal max. length of mastoid to paroccipital	75.7 left/68.8 right		76.8	74.1	85		75.8	61.9	109
Breadth across condyles	96.9		93	103.3	121.7		89.5	102.8	
Max width of basioccipital, at level of posterior lacerate foramen	75.5		61.7	83.1	85.3		78		
Min width of basioccipital (measure at anterior tip of bulla)	56.6		45.5	55.8	67		49.2		
Transverse width of glenoid fossa	56.7	59.9	33.1	57.2	67.6	53.7	51.7	46.8	66.5
Transverse width internal choanae	44.3		32.8	32.5	56		40.8		
Max diameter of infraorbital foramen	21.5	20.9	31.1	24.1	36.6	22	31.5	36.2	33.6
Max diameter orbit	50		34.9 /51.3	46.3	44.4			35.2	53.3
Height of jugal including postorbital process	46.7	33.2	25		18.5		20.1	20.2	33.1
Height of jugal below postorbital process	22	28.3	28		33.1		13.3	12.5	34.9
Length of jugal/zygomatic overlap	29.6	37.9	37.6		35.7		25.6	16.7	28.2
Occipital shield, foramen magnum to occipital apex	97.4		91.2	92.9	94.5			69.5	99
Max. length bulla	46	~41.9	51.3	49.5	54.1		53.3		
Max width of bulla	50.2	~44.1	44.2	50.5	60.4		46.1		
Palate width (20%)	50.3		44.8	56.2			61.3		55.8
Palate depth (20%)	30.5		42.6	34.5			49		>68.7
Palate width (40%)	75.1		59.2	76.6	72.4		68.9		
Palate depth (40%)	52.7		40.1	44.2	42.7		41		
Palate width (60%)	98.3		81.4	92.1	75.7		74.8		
Palate depth (60%)	50.8		36.8	34.4	31.4		19		
Palate width (80%)	78.8		72.8	81.3	65.1		61.3		
Palate depth (80%)	29.8		26.4	22.8	13.7		9.1		
Transverse width nares	40.7		30.4	41.8				39.1	52.6
length from ant. tip of skull to ant. margin of braincase	194		116.3	174	143.8			192	256
length of postorbital process to post. margin of temporal fossa	45		20.3		43.8			42.9	44.6

chulavistensis. The canine alveolus is proportionally narrow, with a width to length ratio of 46% (versus 60.5% SDSNH 36786), and also absolutely smaller (52/24 mm in UCMP 219091 v. 81/49 mm in the *V. chulavistensis* holotype). UCMP 219091 has a suture age (Sivertsen, 1954) of 28.5, indicating skeletal maturity (Table 2).

Description

UCMP 219091 consists of a complete cranium missing only some minor fragments of the canine alveolar rim, the anterior tip of the left nasal, and a fragment of the right palatine (Figs. 8–15). The skull is quite large (condylobasal length = 360 mm; see Table 1).

Rostrum—The rostrum is proportionally narrow for an odobenine and dominated by the alveolar process of the maxilla that surrounds the massive canine alveoli (Figs. 8–12). The lateral surface of the maxilla here is subcylindrical and laterally convex in cross section, accommodating the canine root. In dorsal view the lateral margins of the rostrum behind the canines are straight and parallel; anterior to the canine alveoli the rostral edge of the premaxilla is curved medially and runs anteromedially toward the prominent prenarial process. The prenarial process is visible in dorsal, ventral, and lateral view, and is positioned along the alveolar margin, unlike *Odobenus* where it is elevated.

The premaxilla-maxilla suture is nearly completely closed aside from the posterior 35 mm (Figs. 8, 12); proximally the premaxilla is tapered and overlaps the anterior nasals by 3 cm, terminating at the midpoint of the nasals. The premaxilla-maxilla suture diverges anterolaterally before fading into solid bone. The bony nares are slightly elliptical (60 × 45 mm) in anterior view and elevated only 1.6 mm above the alveolar margin, unlike *Odobenus* (Deméré, 1994a). However, the nares are 4 cm posterior to the prenarial process. The derived condition in *Odobenus* (e.g., Deméré, 1994a, character 1, state 2) may simply be a consequence of the reorientation of the anterior side of the rostrum into a vertical surface as opposed to the more anterodorsally facing surface in *Valenictus* and most other pinnipeds. A short triangular shelf is present between the nares and the prenarial process.

The nasals are uniquely shaped amongst odobenids. Rather than being rectangular or triangular as in most odobenids and otariids, each nasal is approximately pentagonal with a rectangular posterior half, and widening anterior to the midpoint and then narrowing anteriorly (Fig. 8). A similarly shaped nasal is present in SDSNH 90497 and 83719, suggesting this morphology is synapomorphic for *Valenictus*.

The rostrum is plesiomorphic in being more elongate than *Odobenus* with a sloping facial plane (Figs. 10, 11). This is correlated with the somewhat procumbent tusks (130° from horizontal) rather than the near vertical facial plane in *Odobenus* resulting from the tusks descending at nearly a right angle (100–105° from horizontal), similar to UCMP 137426 and other specimens of *Valenictus chulavistensis*. Each maxilla bears an alveolar process housing the enlarged C^1 alveolus that descends far below the prenarial process and ventral to the maxillary crest, as in *Odobenus* and *Ontocetus emmonsi* (a proposed synapomorphy of Odobenini). A broad, shallow trough anterior to the infraorbital foramen lies posteroventral to the swollen alveolar process of the maxilla. The alveolar processes of the maxilla are highly vascularized ventrally; there is 5–8 mm of bone around the tusk root, and the alveolar rim is thinnest medially, slightly thicker laterally, and thickest along the anterior and posterior margins (Figs. 9, 13).

TABLE 2. Suture closure scores of *Valenictus* crania from the Purisima Formation (after Sivertsen, 1954).

Suture	*Valenictus sheperdi* (UCMP 219091)	*Valenictus* sp., cf. *V. chulavistensis* (UCMP 137426)
I: occipital-parietal	4	4
II: squamosal-parietal	4	4
III: Median parietal	4	4
IV: median frontal	4	4
V: frontal-parietal	4 (left)/3 (right)	4
VI: basioccipital-basisphenoid	4	4
VII: median maxilla suture	2	?
VIII: basisphenoid-presphenoid	?	2–4?
IX: premaxilla-maxilla	3	1–3?
Minimum suture age:	28.5	27

Palate—The palate is deeply vaulted (60 mm deep and 80 mm wide at most; Figs. 9, 13), and near the canines the surface is vertical and even underhanging immediately between the canines (e.g., the palate widens dorsally). As in *Valenictus chulavistensis* (Deméré, 1994b), no alveoli of any incisors, premolars, or molars are present (Figs. 9, 13), nor are there any obvious remodeled alveoli filled with bone caused by tooth loss, or even transversely thickened alveolar bone wide enough to accommodate teeth. A pair of trough-like incisive foramina are present in the palate medial to the canines (Fig. 13); they are 45 mm long, 6–8 mm wide and separated by a 6–9 mm wide ridge which is in turn bisected by the anastomosing median premaxilla and maxilla suture.

The lateral half of the palate is strongly vascularized and includes the following types of vascularization (Fig. 13): (1) a small foramen 1 cm anteromedial to the C1 alveolus; (2) a posteriorly directed foramen 1 cm dorsal to the alveolar margin at the level of the posterior canine alveolus with a 4–5 cm long sulcus running posteriorly and parallel to the maxillary crest; (3) a row of dorsally opening foramina 2 cm above the alveolar margin and extending from the midpoint of the c1 to the anterior margin of the temporal fossa (11 on right, 14 on left). These foramina are contiguous with dorsally to posterodorsally oriented sulci (~2–3 mm wide) anteriorly; posteriorly the sulci are shorter and transversely to dorsally oriented. The foramina become smaller and more closely spaced posteriorly; (4) a cluster of ventrally opening foramina more medially positioned (~25 mm from midline) and some contiguous with the medial ends of the group 3 sulci (=reentrant foramina); (5) a few scattered, smaller (1–2 mm diameter) foramina on the posteriormost maxilla, about 1 cm anterolateral to the maxillopalatine suture with short (2–5 mm long) sulci; and (6) a bilateral pair of small, ventrally opening foramina on the palatine on the pterygoid strut.

The palate in general is narrowly hexagonal (Fig. 9); it is widest at the level of the anterior margin of the zygomatic root, and narrows slightly anteriorly and posteriorly from here. Within the anterior 2/3 the palate is trough-like. The palatal process of the maxilla is a small, subrectangular corner; the lateral edge of the maxilla here is blade-like and transversely thin. The maxillopalatine suture is nearly transverse and slightly anteriorly bowed; the suture is positioned at the level of the postorbital process. Despite breakage, the internal choanae have a rounded and continuously concave anterior margin rather than the rectangular margin in the *V. chulavistensis* paratype.

Orbit, Intertemporal Region, Temporal Fossa, and Zygomatic Arch—The orbit is approximately circular and formed as a well-defined, laterally directed cup-like fossa (Figs. 10–12, 14); the postorbital process is quite high and triangular, and the antorbital process extends far laterally. The orbit diameter is 13% of CBL. The maxillary root of the zygomatic arch bifurcates and surrounds the large infraorbital foramen, which is approximately circular and 20 mm in diameter. It is overhung by the inflated maxilla and thus obscured in dorsal view. A cluster of seven foramina are present within the right infraorbital foramen on its medial wall.

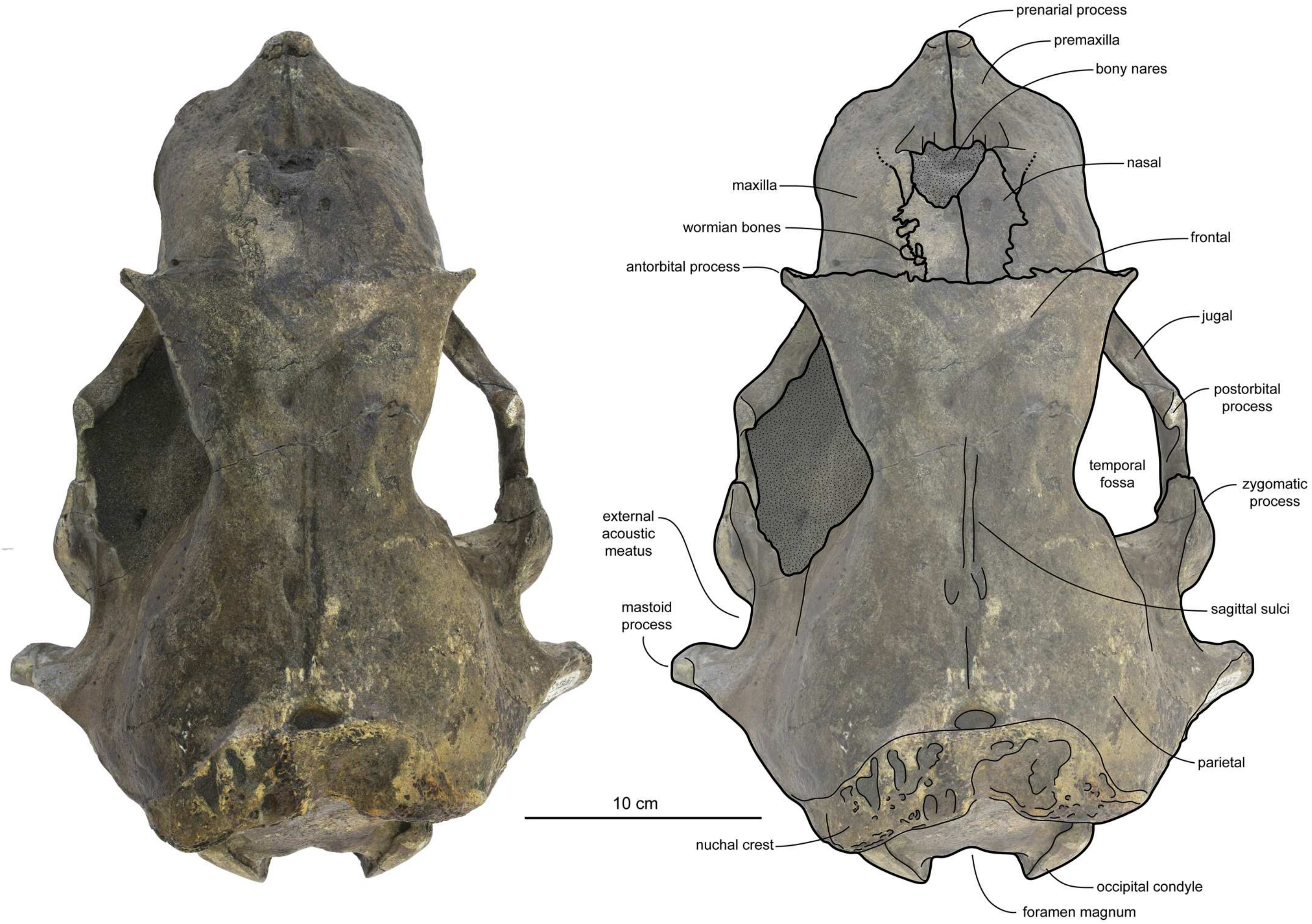

FIGURE 8. Holotype cranium of *Valenictus sheperdi* from the Purisima Formation, UCMP 219091, in dorsal view.

The maxilla-jugal suture is mostly closed on the right side but is clear on the left (Figs. 10, 11); it is roughly V-shaped with a posterior wedge of maxilla penetrating between splints of the jugal. The postorbital process is prominent and rises 35 mm above the ventral margin of the orbit, and bears a triangular base. The medial side of the jugal is a deeply concave fossa. Posteriorly the zygomatic process overlaps the jugal by 25 mm. The zygomatic arch is somewhat laterally bowed (Figs. 8, 9); the jugal is transversely narrower than in *Odobenus* and the zygomatic arch is similarly dorsoventrally expanded relative to earlier diverging odobenids (e.g., most "imagotariines"; *Neotherium*, *Imagotaria*, *Pontolis* spp.), though not as extremely so as in *Odobenus*.

The orbital wall is shallowly concave and dominated by a large orbital vacuity (Figs. 11, 14). The vacuity is certainly expanded by breakage but was likely at least 40 mm anteroposteriorly long and 30 mm dorsoventrally deep. Anteriorly the ventral margin of the vacuity is intact; the palatine forms most of the ventral and anteroventral edge of the vacuity, and the palatine/frontal contact excludes the maxilla from the vacuity. The maxillofrontal suture continues from the middle of the orbit anterodorsally to the dorsal edge of the antorbital process. The optic foramen is circular (4 mm diameter) and positioned within the orbitosphenoid, and dorsomedially in the orbital fissure (Fig. 14). Dorsolateral to the foramen is a deep pit here identified as the origin of m. levator palpebrae. The anterior opening of the alisphenoid canal is probably located within the fissure, but situated deeply within and not visible. A shallow vertical trough is developed dorsal to the orbital fissure, and may be the origin of a belly of m. temporalis medialis.

The antorbital process is acutely triangular in dorsal (Fig. 8) and lateral view (Figs. 10, 11) and bears an anteroposteriorly flattened flange at its ventrolateral apex that projects laterally in front of the orbit. The antorbital process is composed of both maxilla and frontal; the process is distinguished from the rest of the maxilla by a vertical trough anteriorly. The antorbital process is at the same dorsoventral level as the postorbital process. The composite frontomaxillary and frontonasal suture is straight and transverse with a slight posterior V-shape and thus nearly identical to the condition in *Odobenus* rather than the posteriorly V-shaped suture in *Ontocetus* sp. (SMFCV-0001) and the dusignathines (*Gomphotaria*, *Dusignathus seftoni*). The intertemporal region is hourglass-shaped and like *Odobenus* has a shallowly V-shaped notch in its lateral margin at the narrowest part; this differs from the approximately straight sides of the intertemporal region in *Ontocetus*. The intertemporal region is narrowest at the level of the anterior tip of the zygomatic arch (Fig. 8).

The palatine has a posterodorsal tongue-like process that extends into the orbital fissure (Figs. 11, 14); the orbitosphenoid lies dorsal to this, forming the dorsomedial walls of the fissure. The lateral and dorsolateral walls of the fissure are formed by the frontal and alisphenoid, and the suture between these two elements is completely closed. The fissure is at least 40 mm deep (anteroposteriorly) and funnel shaped (as in *Odobenus*), and 15 mm wide (transversely) by 30 mm high (dorsoventrally).

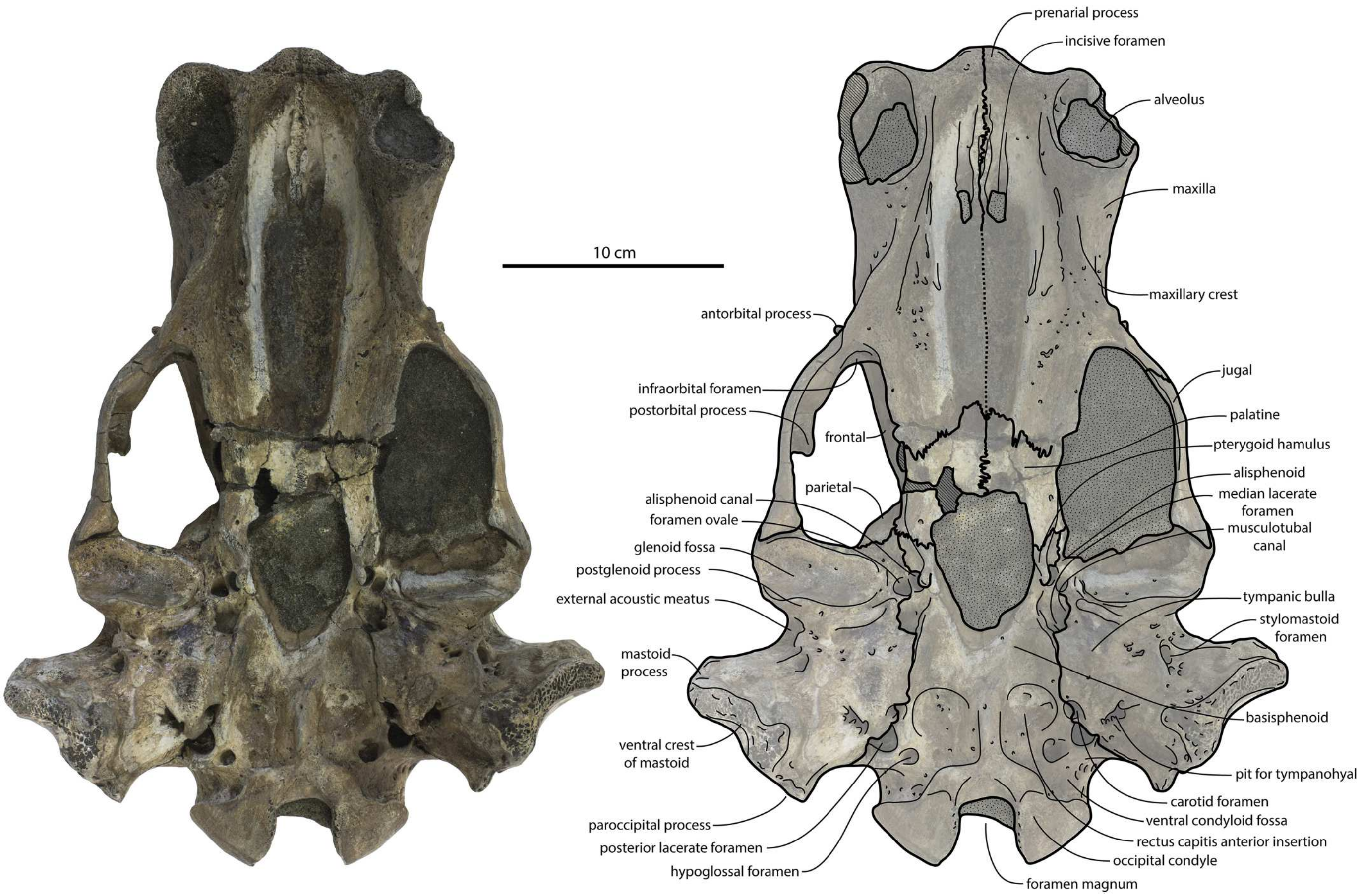

FIGURE 9. Holotype cranium of *Valenictus sheperdi* from the Purisima Formation, UCMP 219091, in ventral view.

Braincase—Aside from the paroccipital process, the braincase is approximately circular in dorsal view (Fig. 8) with smoothly convex lateral margins. Rather than bearing a sagittal crest as in dusignathines and "imagotariines," the roof of the braincase is flat like other Odobenini and bears a sagittal sulcus. Anteriorly this sulcus bifurcates and a pair of shallow sulci are present (Fig. 8); this is similar to the condition in *Pliopedia pacifica* (Repenning & Tedford, 1977) and *Valenictus chulavistensis* but differs from the single sulcus in *Odobenus*. Posteriorly the sulcus terminates in a deep transversely oriented pit immediately anterior to the broad nuchal crest.

The nuchal crest is developed as an anteriorly thrusted, anteroposteriorly expanded and flattened surface (Figs. 8, 15) for the superficial muscles of the neck used in extension and rotation of the neck (m. splenius, m. rhomboideus anticus, m. capitis semispinalis, and m. biventer cervicis; Howell, 1929). Unlike in *V. chulavistensis*, *Odobenus*, or *Ontocetus*, the expanded nuchal crest in UCMP 219091 bears a straight, transverse anterior margin rather than a smoothly convex edge and forms a trapezoidal shape in dorsal view. Several anteroposteriorly oriented irregular ridges and furrows are present on the nuchal crest. Laterally the low nuchal crest continues anteroventrally to form the dorsal edge of the enlarged paroccipital process; this ridge is not elevated. The occipital shield is vertical and bears several vertical to subvertical and slightly radially oriented ridges and troughs for the deeper muscles of the neck (m. rectus capitis posterior major and minor, and m. obliquus capitis superior; Howell, 1929), also involved in rotation and extension of the head and neck. A low external occipital crest is present (Fig. 15). The condyles are teardrop shaped and become wider dorsally (Fig. 15); deep dorsal condyloid fossae are present immediately dorsal to each condyle.

Basicranium—The occipital condyles are set out on a distinct neck and defined by trough-like ventral condyloid fossae (Figs. 8–11, 15). A rectangular anterior extension of each condyle surface extends anteromedially at the level of the hypoglossal foramen. This is unique to UCMP 219091, and only developed to a lesser degree in *Valenictus chulavistensis* and *Odobenus*. The foramen magnum is nearly circular with vertical, straight sides and a concave dorsal margin.

The combined basioccipital-basisphenoid is approximately rectangular (Fig. 9). The basioccipital bears a prominent median blunt ridge separating the fossae for the left and right *m. rectus capitis* and *m. longus capitis* insertions. The *m. rectus capitis ventralis* insertion is a smooth concave fossa medial to the posterior lacerate foramen, whereas the m. longus capitis is a smaller, less concave, and roughened facet medial to the basioccipital-bullar fissure.

The mastoid process is enormous and ventrolaterally extended to form the widest part of the skull (Figs. 8, 9, 15); it is anteromedially compressed with a sharp ventral crest that is posteriorly concave. The medial part of this crest is expanded into a large knob. A smaller tubercle is present posteromedial to the knob; it is unclear which, or if both, are the paroccipital process. The postglenoid process is low and blunt; the glenoid fossa is shallowly concave in the anteroposterior plane, approximately rectangular, and transversely oriented. A preglenoid process is not developed.

The external acoustic meatus is funnel shaped, circular, and approximately 20 mm in diameter (Figs. 10, 11). A rugose bony tubercle extends from the squamosal into the ventral part of the meatus. A large (8 mm diameter) and circular stylomastoid

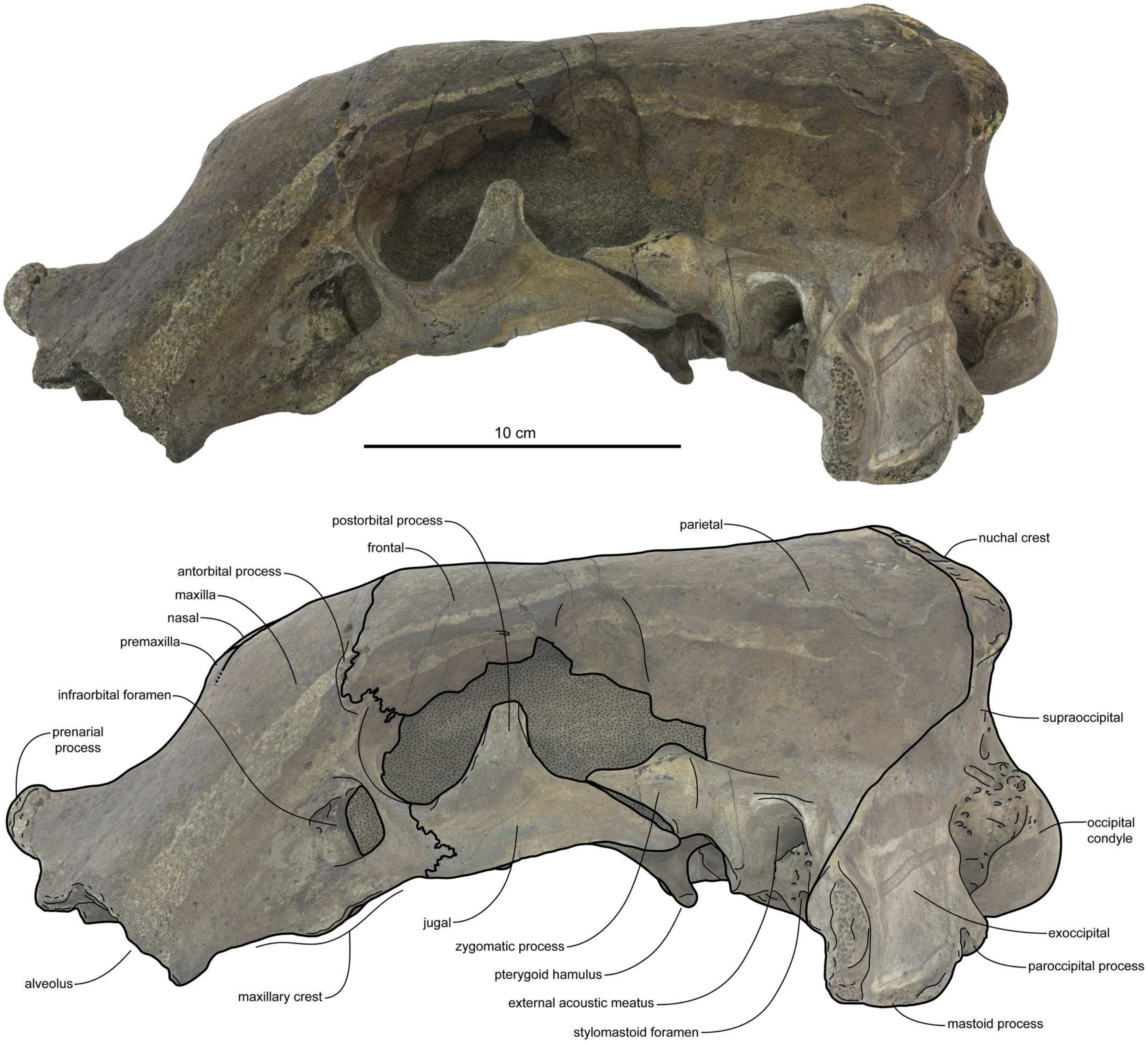

FIGURE 10. Holotype cranium of *Valenictus sheperdi* from the Purisima Formation, UCMP 219091, in left lateral view.

foramen is positioned far lateral on the bulla and immediately ventral to the external acoustic meatus; it opens on the anterior surface of the mastoid process. The bulla is ventrally flattened (Fig. 9); it is slightly concave laterally and near the stylomastoid foramen bears several minute foramina. Medially the bulla is slightly convex and bears a low centrally positioned tubercle. Overall, the bulla is shaped like a medially widening trapezoid. A large, deep hyoid fossa is present: it is lenticular and fissure-like with a raised lip on the bulla anteromedially, and several fine parallel sulci (20 mm long) emanate laterally onto the medial side of the mastoid process. The bulla bears a large, rounded tubercle posterior to the hyoid fossa; it divides the hyoid fossa from the posterior lacerate foramen and carotid canal. The hypoglossal foramen is large and opens anteroventrolaterally; it is situated between the condyle and the posterior lacerate foramen. The left hypoglossal foramen is 10 mm in diameter whereas the left is only 7 mm. A small tubercle lies lateral to the right foramen but not the left one.

The posterior lacerate foramen is large (12 × 9 mm) and D-shaped; it is anterolaterally flattened owing to the aforementioned tubercle on the bulla (Fig. 9). The foramen is separated from the round posterior opening of the carotid canal by a narrow septum on the left; a continuous fissure separates the bulla from the basioccipital on the right side. The medial edge of the bulla is slightly concave and wavy, forming a sharp horizontal crest separated from the basioccipital by a narrow fissure (Fig. 9).

The anterior composite fissure (= petrotympanic fissure + eustachian canal + medial lacerate foramen) is large, and septa dividing these foramina are recessed deeply within the composite fissure (Fig. 9). It measures 13 mm wide by 10 mm deep, and is approximately circular. The bulla bears a triangular prong anteriorly, just lateral to the fissure. The bulla is separated from the glenoid fossa by a shallow groove, followed by two parallel grooves and ridges which terminate anteromedially at the anterior prong of the bulla.

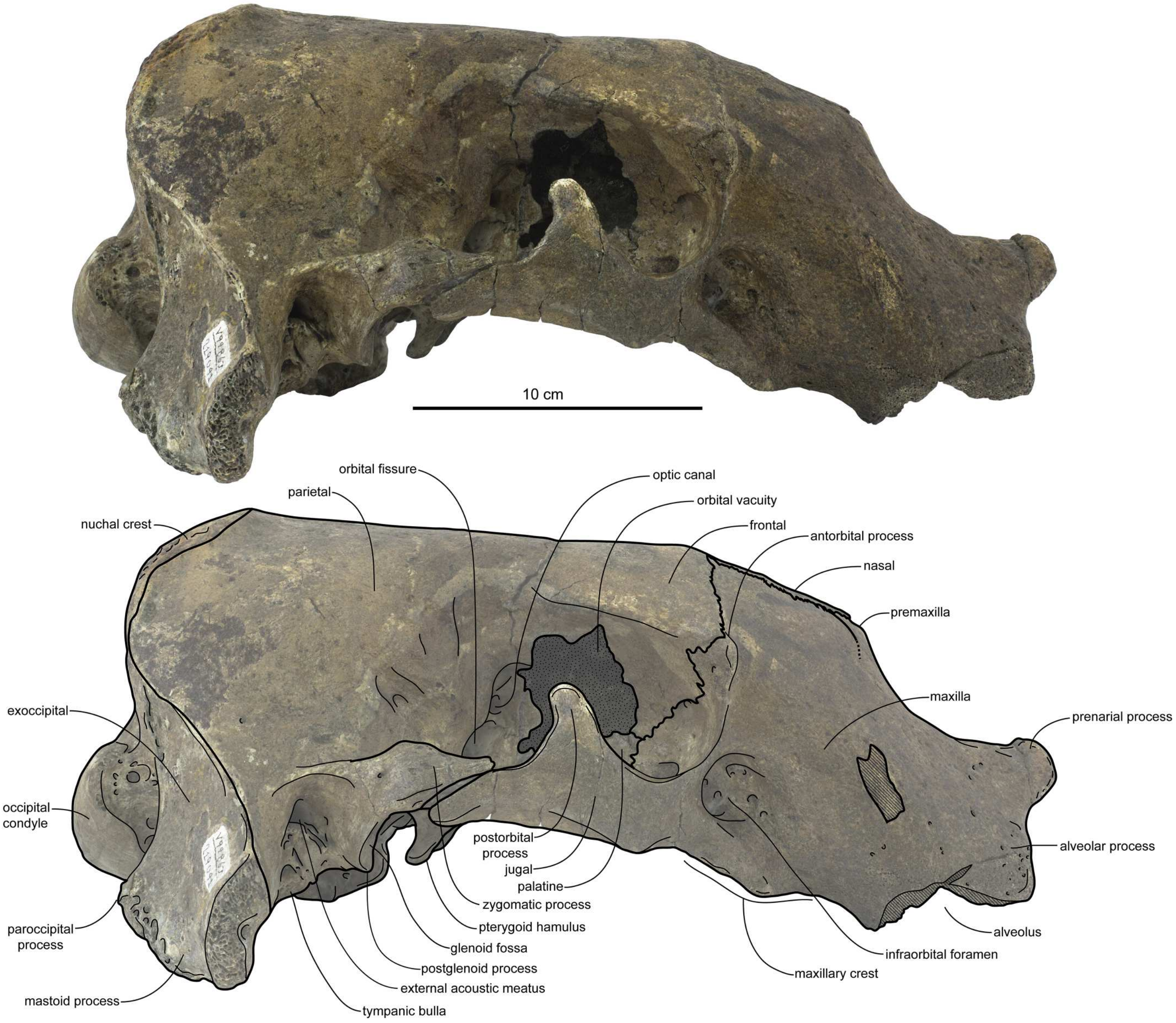

FIGURE 11. Holotype cranium of *Valenictus sheperdi* from the Purisima Formation, UCMP 219091, in right lateral view.

The posterior opening of the alisphenoid canal is vertical, circular, and large (9 mm diameter; Fig. 9). It is positioned directly posterior to the pterygoid hamulus and immediately posterolaterally adjacent to the slightly smaller foramen ovale. It is separated from the foramen ovale by a thin (1.5 mm) crest. The pterygoid has a blocky base with a quadrate exposure in lateral view; anteriorly the pterygoid is overlapped by a dorsoventrally thin and triangular sheet of the palatine. Dorsal to the hamulus, the pterygoid shares a suture with the alisphenoid. The palatine-alisphenoid suture is incompletely closed, mortised, and transversely oriented; it extends dorsolaterally into the orbital fissure. The alisphenoid-squamosal suture is completely closed. The pterygoid hamulus is long, narrow, finger-like, and transversely narrow. It projects posteroventrally and curves slightly laterally at its apex.

Comparisons

Valenictus sheperdi differs from early diverging odobenines *Aivukus* and *Protodobenus* in its larger size and possession of greatly enlarged canine tusks. *Valenictus* shares with *Pliopedia* paired bilateral sulci on the dorsal surface of the braincase rather than a single sulcus as in *Odobenus* and *Ontocetus*. *Ontocetus* differs from *Valenictus sheperdi* in retaining incisors and postcanines, having a much wider palate, a rectangular outline of the braincase in posterior view (but see *Ontocetus emmonsi* specimen figured by Erdbrink & Van Bree, 1990:pl. 1a), and a more massively inflated mastoid process. *Valenictus sheperdi* differs from *Valenictus chulavistensis* chiefly by exhibiting a truncated, rectangular nuchal crest apex, a narrower oral opening, a more sharply defined and elongate maxillary crest, an anteroposteriorly flattened mastoid process with a sharper ventral edge, and a more strongly vascularized palate. *Valenictus sheperdi* differs from *Odobenus rosmarus* in possessing more procumbent canine tusks, loss of the upper incisors and premolars, more ventrally positioned bony nares, a less inflated rostrum, and a rectangular outline of the nuchal crest in posterodorsal view (all but the last also shared with *Valenictus chulavistensis*). *Valenictus sheperdi* cannot be directly compared with

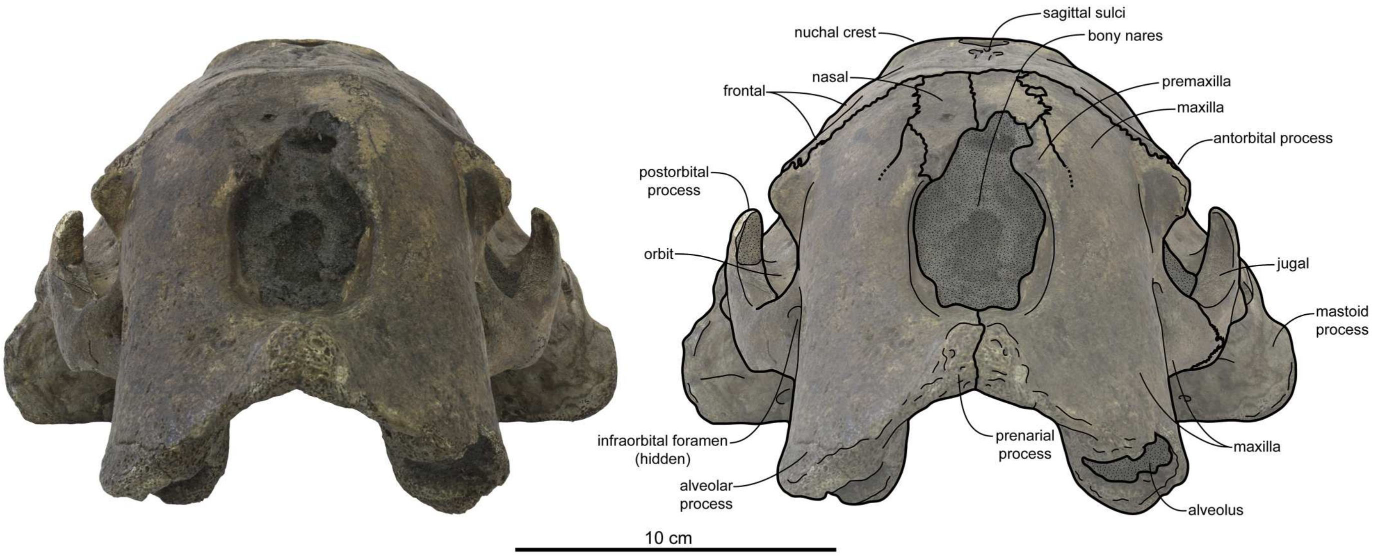

FIGURE 12. Holotype cranium of *Valenictus sheperdi* from the Purisima Formation, UCMP 219091, in anterior view.

Valenictus imperialensis, since the former is known only from a cranium and the latter from a humerus (Mitchell, 1961). However, because individual skeletons of *Valenictus chulavistensis* preserve humeri and crania, the humerus size of *Valenictus sheperdi* can be predicted as well as the cranial size of *Valenictus imperialensis*. The male holotype of *Valenictus chulavistensis* possesses an estimated 410 mm long skull and 310 mm long humerus (Deméré, 1994b:tables 2, 5). Applying this ratio to *Valenictus sheperdi* results in a predicted humeral length of 272 mm, as compared with the 242 mm long humerus of *Valenictus imperialensis*. Likewise, *Valenictus imperialensis* has a predicted skull length of 322 mm; these suggest a slightly smaller predicted size for *Valenictus imperialensis* than *Valenictus sheperdi*. If the proportionally robust *Valenictus imperialensis* holotype is a male, this would suggest larger body size in *Valenictus sheperdi*.

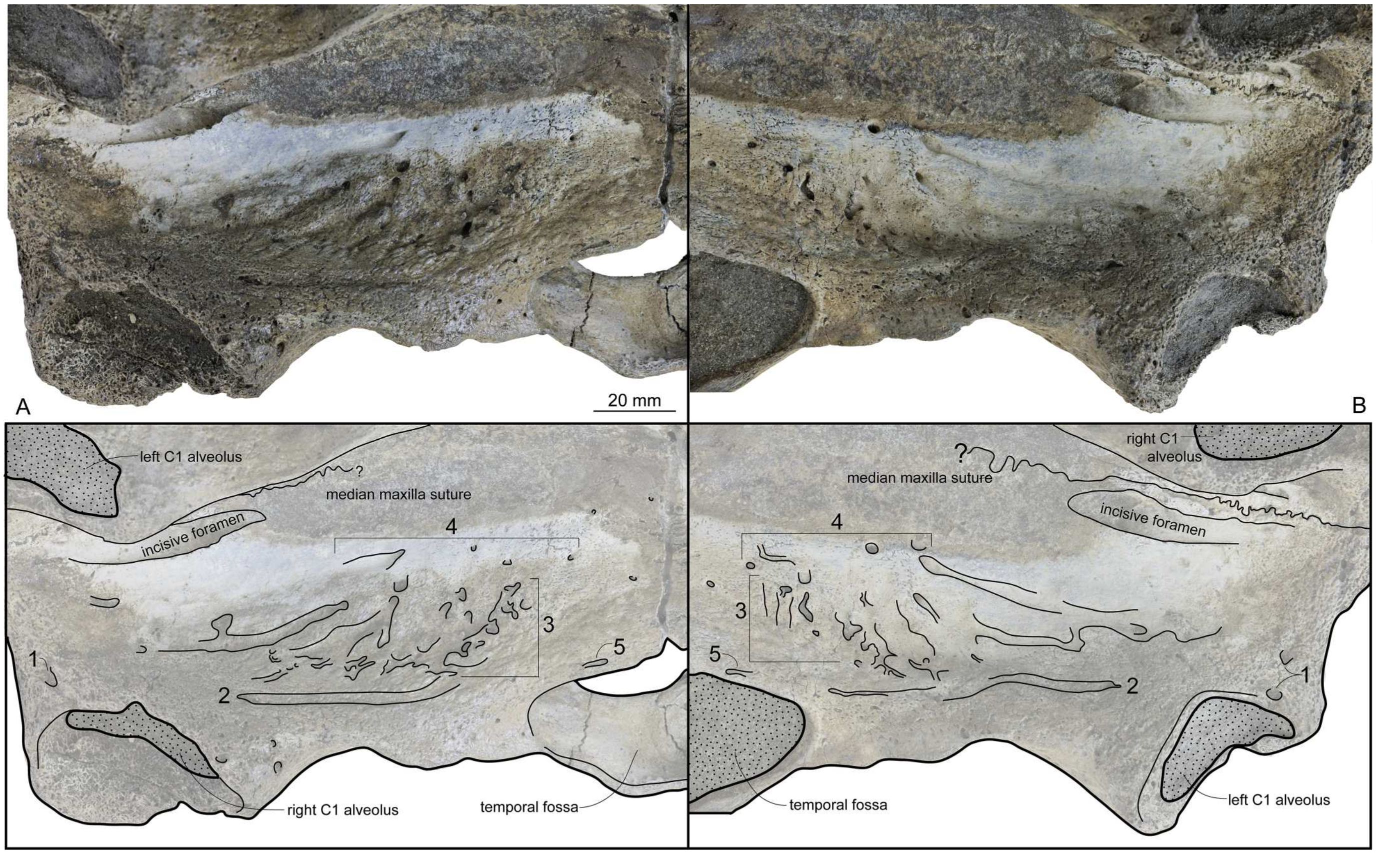

FIGURE 13. Holotype palate of *Valenictus sheperdi* from the Purisima Formation, UCMP 219091. **A**, right side of palate in ventromedial view; **B**, left side of palate in ventromedial view. Numbered foramina correspond to the description.

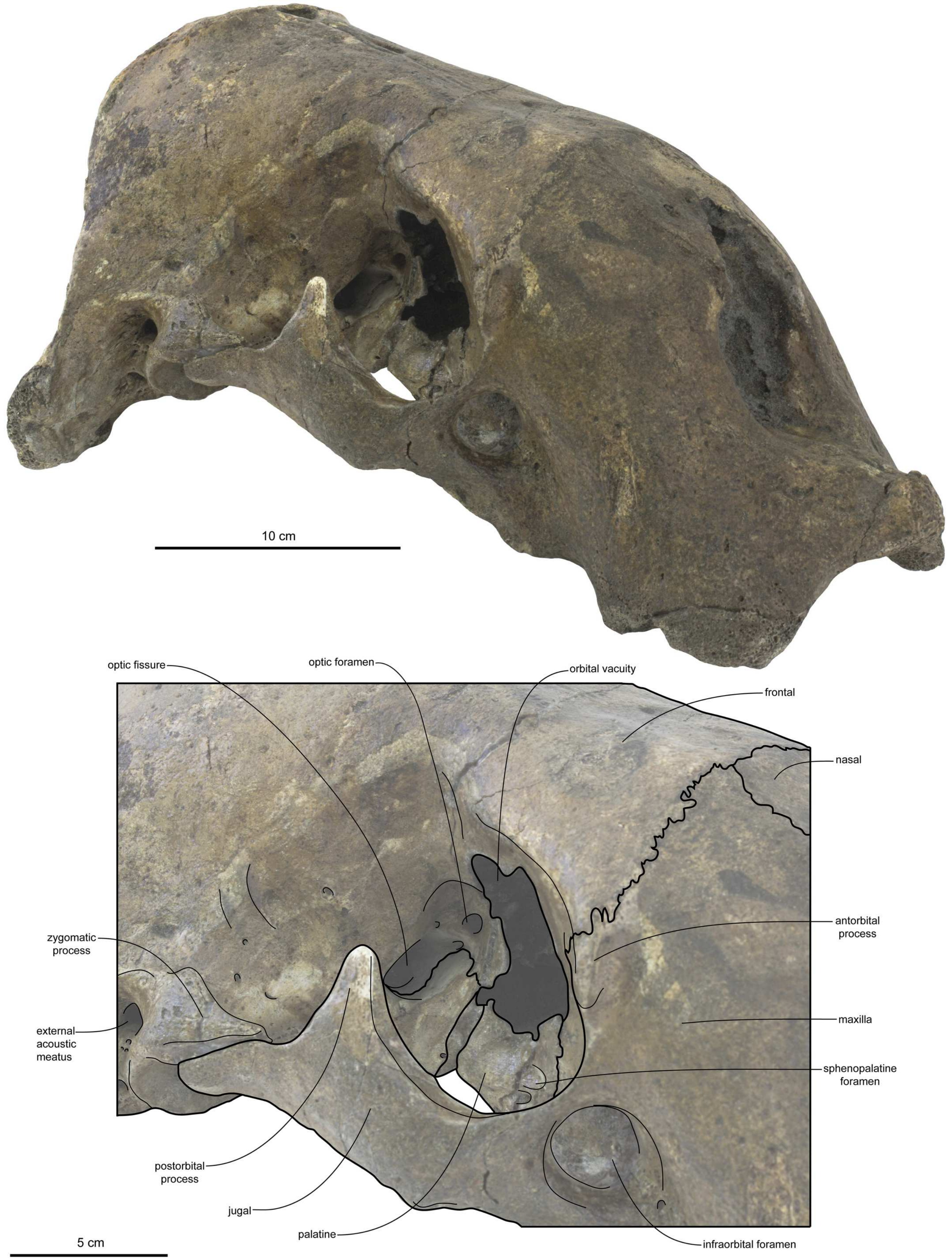

FIGURE 14. Holotype cranium of *Valenictus sheperdi* from the Purisima Formation, UCMP 219091, in oblique anterolateral view, and detail of orbit.

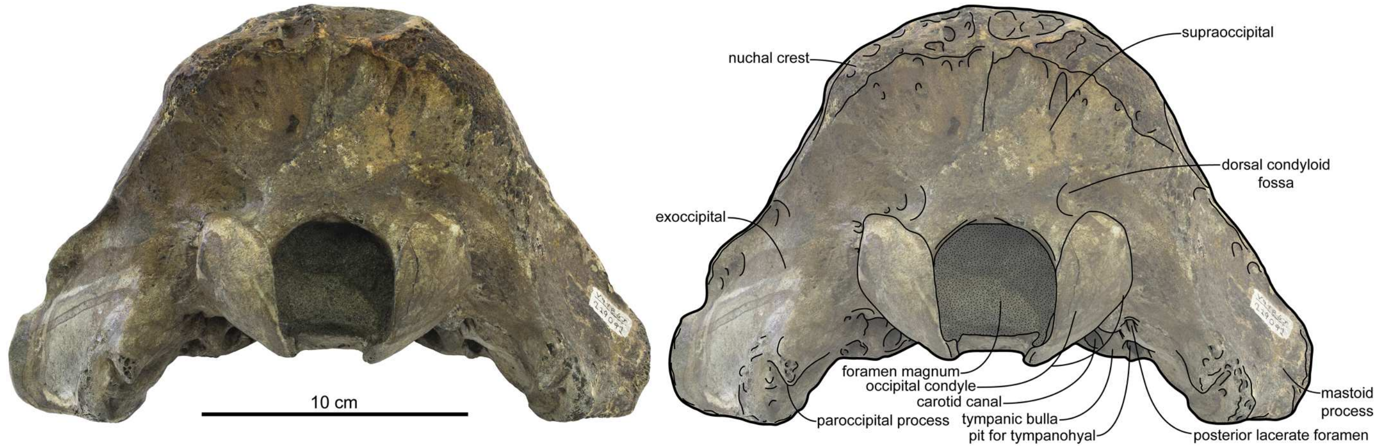

FIGURE 15. Holotype cranium of *Valenictus sheperdi* from the Purisima Formation, UCMP 219091, in posterior view.

VALENICTUS sp., cf. *V. SHEPERDI* (Fig. 16)

Valenictus sp. Boessenecker, 2017

Referred Material—SCMNH 21366, partial right femur, collected from SCMNH locality 1 on April 1, 2001 by David Landes; UCMP 269337, complete astragalus collected from UCMP locality V-99868 by Wayne Thompson December 14, 2014; both specimens derived from the "Upper Shell Bed facies" of Perry (1988); Early Pliocene, 5.33–4.89 Ma.

Description and Identification—Partial right femur SCMNH 21366 (Fig. 16A) is referrable to *Valenictus* owing to its pachyosteosclerotic condition (visible in the broken cross section), its large size, and transversely expanded distal end (e.g., SDSNH 83719). The proximal end is missing but the distal two-thirds of the femur is preserved in a sandstone concretion; only the anterior side is exposed. The diaphysis gradually widens and the distal third of the femur is nearly rectangular, as the diaphysis is medially and laterally swollen, and approximately as wide as the lateral and medial entepicondyles. The patellar fossa is transversely broad and subrectangular. Distal expansion of the femur appears to be unique to *Valenictus*, as it is not present in *Odobenus rosmarus*, *Ontocetus emmonsi*, or dusignathinae (*Dusignathus seftoni*, SDSNH 77891; *Gomphotaria pugnax*, LACM 121508). Instead, other odobenids have an abrupt widening of the distal diaphysis towards the entepicondyles. Several femora of *Valenictus chulavistensis* (e.g., SDSNH 83719) match the morphology of SCMNH 21366, but are smaller.

UCMP 269337 is a large astragalus with a wide capitulum, wide neck, and J-shaped ectal facet, lacking a distinct lateral tuberosity and lacking a groove separating the navicular and sustentacular facets (Fig. 16B, C). These features are shared only with *Valenictus chulavistensis*. However, UCMP 269337 differs from astragali of *V. chulavistensis* in possessing a much deeper intertrochlear pit and a medial plantar tuberosity that is less distinctly separated from the ectal facet. See Boessenecker (2017) for a longer description of the astragalus.

These postcrania are tentatively referred to *Valenictus sheperdi* owing to their origination from a slightly higher stratigraphic horizon with identical age control (5.33–4.89 Ma); these specimens are perhaps 1 Ma older than UCMP 137426, the Purisima

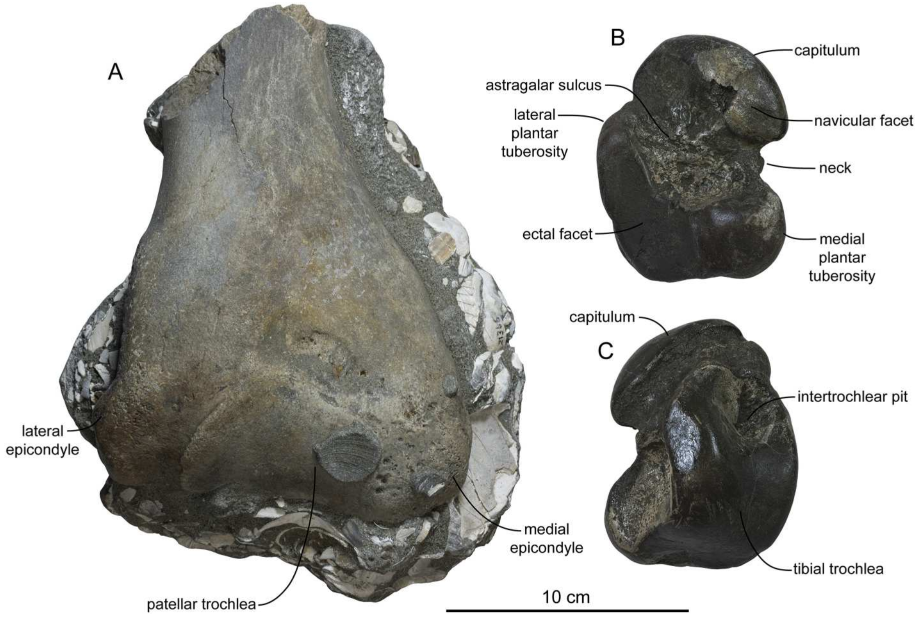

FIGURE 16. Referred postcrania of *Valenictus* sp., cf. *V. sheperdi* from the Purisima Formation. **A**, right femur SCMNH 21366, in anterior view; **B**, right astragalus, UCMP 269337 in ventral (plantar) view; **C**, same, in dorsal (tibial) view.

Formation specimen of *Valenictus chulavistensis.* As noted by Boessenecker (2017), the astragalus UCMP 269337 exhibits several features (e.g., wide capitulum, wide neck, J-shaped ectal facet) unique to *Valenictus chulavistensis* noted by Deméré (1994b), but differs in a few minor features (see below), interpreted by Boessenecker (2017) as precluding assignment to *V. chulavistensis*, and identified UCMP 269337 as *Valenictus* sp. The femur SCMNH 21366 differs from the femur of *Valenictus chulavistensis* female SDSNH 83719 in somewhat larger size (35% larger), but otherwise this specimen does not differ in morphology from *V. chulavistensis.* Owing to larger size and older age than specimens of *Valenictus chulavistensis* from the San Diego and Purisima formations, and identical age with *Valenictus sheperdi*, these specimens are provisionally referred as *Valenictus* sp., cf. *V. sheperdi*.

Phylogenetic Results

Phylogenetic analyses in this study are broadly concordant with prior studies (Biewer et al., 2020; Boessenecker & Churchill, 2013; Deméré, 1994a; Kohno, 2006; Magallanes et al., 2018; Tanaka & Kohno, 2015), but provide new insights into the relationships of Odobeninae and Neodobenia. When all walrus taxa are included in the phylogenetic analysis, 65 most parsimonious trees were recovered with a best tree score of 596 (Figs. 17, S1; Supplementary File S3). When the four incomplete walrus taxa (*Kamtschatarctos sinelnikovae*, *Pelagiarctos* sp., *Nanodobenus arandai*, and *Valenictus imperialensis*) are excluded from the analysis, only six trees are recovered, with a best score of 589 (Fig. S2; Supplementary File S4). Both the strict consensus from the more inclusive analysis and the majority rule tree from the more exclusive analysis had similarities in topology and support, the major difference being the much lower resolution in the more inclusive analysis, with most early diverging “imagotariines” (*Proneotherium* Kohno et al., 1995a, *Kamtschatarctos*, *Pelagiarctos*, *Nanodobenus*, *Pseudotaria* Kohno, 2006, *Neotherium*, *Archaeodobenus* Tanaka & Kohno, 2015) occurring in an unresolved polytomy alongside the outgroup taxa. In both analyses, there was no resolution within the genus *Valenictus*, although the genus was recovered as monophyletic with moderate support. For the purpose of describing results, we will focus on the strict consensus tree from the more exclusive analysis (Fig. 17, S1) and on relationships within Odobeninae. For a more comprehensive reporting of phylogenetic results for non-odobenine Odobenidae, see Supplementary Information.

Odobeninae is recovered as monophyletic (Fig. 17) with strong support (BS = 96), with *Aivukus* as the earliest diverging taxon. Characters that support odobenine monophyly include possession of a broad intertemporal region (5:1), an upper tooth row that terminates anterior to the temporal fossa (18:0), broad and square nasals that extend to the frontal-maxilla suture (23:2), loss of a sagittal crest (59:3), loss of the M^2 (107:2), enlarged medial entepicocondyle that is greater than half of the width of the distal trochlea (135:1), and a rugose surface for the insertion of the pollicle extensor on metacarpal 1 (137:2). *Protodobenus* is recovered as the next diverging taxon and sister to all other odobenine walruses, with moderate support (BS = 66). Characters that support this relationship include possession of a rostrum which is wider posterior to the canine (10:0), transversely and longitudinally arched palate (25:3), large and broad hamular processes of the pterygoid (29:1), absence of the squamosal fossa (55:2), a mandibular condyle significantly elevated above the toothrow (88:1), possession of globular orthodentine in the C^1 (98:1), and loss of the M_1 (122:3). Other characters that may support this relationship, or may support monophyly of Odobeninae overall, include possession of short nasals (22:222:2), a straight margin to the posterior edge of the palate (26:1), overlap of the palatine by the alisphenoid (28:1), and premolariform lower canines (99:1).

Odobenini, with *Ontocetus* as the earliest diverging lineage (Fig. 17), is recovered with strong support (BS = 86). Characters that support this relationship include possession of an infraorbital foramen that is visible only in lateral view (20:1), a funnel-shaped optic foramen (45:1), a greatly enlarged mastoid process (52:3), anterodorsally or laterally oriented nuchal crests (57:1), possession of only one incisor (91:3), greatly enlarged canines forming true tusks (96:1 and 97:1), loss of postcanine enamel (105:2), posteromedial displacement of the P^1 (111:1). More ambiguous characters include possession of an antorbital width 55% or greater than the bizygomatic width (3:1).

Ontocetus itself is recovered as paraphyletic, although with only weak support, with *O. emmonsi* the sister taxon to a clade comprising *Odobenus*, *Pliopedia*, and *Valenictus.* This clade is united by the presence of nuchal crests that form a broad arc (58:4), the presence of a single longitudinal sulcus (62:1), a swollen and blunt paraoccipital process (64:1), and loss of the M1 (107:3). A more ambiguous character that may diagnose this clade is a pterygoid strut overridden by the palate (32:4).

The next diverging taxon within Odobenini includes the extant walrus *Odobenus* (Fig. 17), which is recovered with moderate support (BS = 72). Characters that support this placement include possession of a posteriorly positioned orbital vacuity (43:2), greatly enlarged canines (97:2), loss of the M^1 (107:5), and the presence of a deltoid tuberosity on the humerus separate from the pectoral crest (132:2). A more ambiguous character supporting this clade is the presence of only a single I^1 (91:3).

Pliopedia and *Valenictus* are recovered with moderate support (BS = 66) as forming a clade, although relationships within this clade are unresolved (Fig. 17). Two characters support this topology, including the presence of paired sulci on the dorsal surface of the skull (62:2) and a wide and prominent lesser tuberosity of humerus (134:1). *Valenictus* is also recovered as monophyletic, although with poor support. Characters that support monophyly of *Valenictus* include the presence of a prominent maxillary crest (17:1) and the loss of both upper incisors (91:4) and postcanines (107:6) and increased bone density (131:1). Within *Valenictus*, *V. sheperdi* is found to be the sister taxon to a clade formed by *V. chulavistensis* and UCMP 137426, although again with poor support.

DISCUSSION

Oldest Records of Odobeninae and Odobenini

Prior to this study, the oldest known record of the odobenines was the Upper Miocene walrus *Aivukus cedrosensis* from the Almejas Formation of Isla Cedros, Baja California, Mexico (Repenning & Tedford, 1977). However, the absolute age of most specimens from this geologic unit is unclear, which Barnes (1998) estimated to be 8–6 Ma. Radiometric dates are not available on Isla Cedros, but on the mainland (Vizcaino Peninsula), minimum ages for the Almejas Formation are derived from overlying basalts yielding dates of 6.48 and 5.7 Ma (Sawlan & Smith, 1984). Though *Aivukus* is possibly older (to be confirmed with further dating from Isla Cedros), precise paleomagnetic or radioisotopic dates for the section at Isla Cedros are not available. However, the occurrence of finely serrated teeth identified as *Carcharodon* sp., cf. *C. carcharias* Linnaeus, 1758 (Barnes, 2008; possibly representing transitional species *Carcharodon hubbelli* Ehret et al., 2012) suggests a maximum age of 6.03 Ma, given that the oldest well-dated occurrence of serrated *Carcharodon* teeth from the eastern North Pacific occur approximately 75 m above the base of the Purisima Formation that corresponds to the base of Chron C3r (Madrid

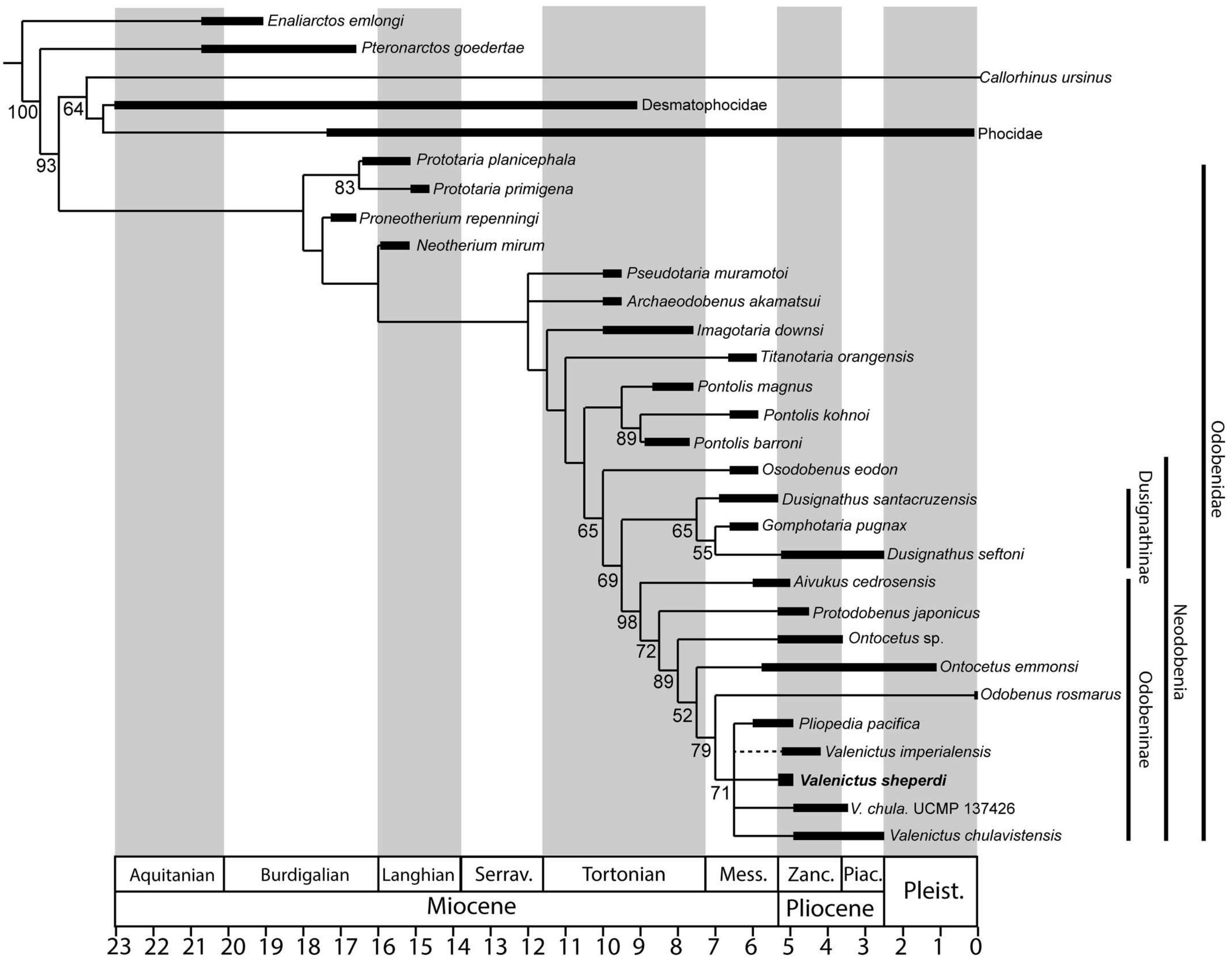

FIGURE 17. Time calibrated reduced strict consensus cladogram of odobenid relationships based on the strict consensus tree (n = 6; best tree score 589) recovered under equal weighting excluding fragmentary taxa (*Pelagiarctos*, *Kamtschatarctos*, *Nanodobenus*, *Valenictus imperialensis*). Stratigraphic ranges from Boessenecker (2013), Magallanes et al. (2018), Biewer et al. (2020), with updates to the Almejas and San Diego Formation ranges (see above; Buzcek et al., 2021). Position of *Valenictus imperialensis* included a posteriori based on more inclusive analysis; *Desmatophoca* and *Allodesmus* combined as Desmatophocidae, and *Erignathus* and *Monachus* combined as Phocidae.

et al., 1986; Powell et al., 2007; Stewart & Perry, 2002), with an age control of 6.03–5.23 Ma (Gradstein et al., 2012). An age of approximately 6–5.7 Ma, or slightly younger, can be summarized for the Almejas Formation. Therefore, at present, the oldest known well-dated odobenine specimen is the isolated first metacarpal (UCMP 219402) reported herein, found in the same layer as teeth of the non-serrated ancestral great white shark *Carcharodon hastalis* Agassiz, 1843 (Fig. 1C), dated to 6.9–6.03 Ma, which is slightly older than *Aivukus cedrosensis*. All other records of odobenines from the western North Pacific and North Atlantic are Early Pliocene at the oldest (Boessenecker et al., 2018; Kohno & Ray, 2008; Kohno et al., 1995b). It is noteworthy that UCMP 219402 is more derived than the metacarpal 1 of *Aivukus* and may represent an odobenin rather than an odobenine. From this we predict the discovery of older Odobenini and Odobeninae in early Messinian or even late Tortonian age rocks in the North Pacific. Accordingly, the oldest dusignathines including specimens of *Dusignathus santacruzensis* from the basal Purisima Formation (maximum age 6.9 Ma; see above) and *Gomphotaria pugnax* from the Capistrano Formation (maximum age 6.6 Ma; Barboza et al., 2017) further attest to an earliest Messinian or Tortonian origin for Neodobenia.

Several records of long-tusked walruses (Odobenini) date to the Early Pliocene (Zanclean) including *Valenictus* (Boessenecker, 2017; this study), *Ontocetus emmonsi* (Boessenecker et al., 2018), and isolated odobenin tusks from Japan (Kohno et al., 1995b). The fragmentary odobenine *Pliopedia pacifica* was assigned to the Odobenini by Deméré (1994a), and this assignment was confirmed in our cladistic analysis (Fig. 17; see below). *Pliopedia* was originally reported from the Paso Robles Formation, potentially latest Miocene in age, and from the Pliocene Etchegoin Formation (Repenning & Tedford, 1977). However, more recently reported ash dates from the Paso Robles Formation indicate it is no older than 5.0 Ma (Powell et al., 2007), and the record of *Pliopedia pacifica* from the Etchegoin Formation has a maximum age of 4.8 Ma (Bowersox, 2005; see also Magallanes et al., 2018). Several tusks with globular dentine that are undoubtedly assignable to the Odobenini (possibly representing partial tusks of *Ontocetus*) have been reported from the Lower Pliocene Horokaoshirarika Formation of Japan, and dated to 5.2–3.8 Ma (Kohno et al., 1995b), representing some of the oldest well-dated records of Odobenini worldwide. This age range was curtailed somewhat by Tanaka and Ichishima (2016), who summarized the age as 4.5–3.5 Ma. At present, the oldest known Atlantic walrus record is *Ontocetus emmonsi* from the Palmetto local fauna in the Bone Valley Formation of Florida, dating to 5.6–4.6 Ma (see Boessenecker et al., 2018:appendix 1).

UCMP 190024, a massive tusk with globular dentine, was collected from the Crab Marker Bed of the Purisima Formation (Fig. 1C). This stratum is the first appearance datum of the diatom *Thalassiosira praeoestrupii* Dumont et al., 1986 (Dumont et al., 1986; Madrid et al., 1986), which corresponds to the Miocene–Pliocene boundary, and indicates an age of about 5.33 Ma for UCMP 190024 (Dumont et al., 1986; Powell et al., 2007). Because UCMP 190024 was collected from strata corresponding to Chron C3R (= R3 of Madrid et al., 1986), an age of 6.033–5.235 Ma can be assigned, straddling the Miocene–Pliocene boundary. Given current understanding of the age of the Horokaoshirarika Formation (Tanaka & Ichishima, 2016) and an entirely Pliocene age for *Pliopedia pacifica* (Bowersox, 2005; Powell et al., 2007), UCMP 190024 appears to be, at present, the oldest known record of the Odobenini—suggesting a latest Miocene origin of the clade. We expect future discoveries to corroborate this, and perhaps future discoveries from Southern California, Baja California, and Japan will reveal an earlier origin of long-tusked walruses (Odobenini).

The Origin of Long-Tusked Walruses in the Eastern North Pacific

Long-tusked walruses (Odobeninae, and more specifically, Odobenini) clearly have a North Pacific center of origin along with the family Odobenidae and the double-tusked walruses, Dusignathinae (Biewer et al., 2020; Boessenecker & Churchill, 2021; Deméré, 1994a; Kohno et al., 1995a, b; Repenning & Tedford, 1977). The presence of plesiomorphic odobenines in both Japan and Baja California has led to suggestions of an origin in the western (Horikawa, 1995) and eastern North Pacific (Repenning & Tedford, 1977), though fossils from California and Baja California are older (see above) and a higher number of endemic lineages within Neodobenia might further suggest an eastern North Pacific origin for odobenines during the Late Miocene (e.g., Velez-Juarbe & Salinas-Marquez, 2018: fig. 4). The origin of the first molluskivorous walruses such as *Gomphotaria* (Barnes & Raschke, 1991) has been tied to the diversification and proliferation of kelp species during the Late Miocene (Vermeij, 2012). Rather than being reliant on primary productivity driven by upwelling, productivity in this region is apparently driven by voluminous kelp forests (Vermeij, 2012). Many herbivorous marine invertebrates feed upon drift kelp, and the unusually high productivity in this region has driven the evolution of giant (sensu Vermeij, 2012) molluskan herbivores such as the world's largest abalone (*Haliotis rufescens* Swainson, 1822), chiton (*Cryptochiton stelleri* von Middendorf, 1847), and keyhole limpets (*Megathura* Soweby, 1825), as well as giant molluskivorous invertebrate predators including the world's largest moon snail (*Neverita lewisii*), the largest sea star (*Pycnopodia helianthoides* Brandt, 1835), and largest octopus (*Enteroctopus dofleini* Wülker, 1910), in addition to the largest cancrid crab (*Cancer productus* Randall, 1839) and largest bivalve-wrenching sea star (*Pisaster ochraceus* Brandt, 1835; Vermeij, 2012). Furthermore, many trophically important extant species in the region underwent diversification during the Late Miocene and are linked to the expansion of kelp forests (Jacobs et al., 2004). Many unusually large mussels, oysters, scallops, and slipper shells inhabited now-lost Late Miocene–Pliocene embayments along the California coast (Vermeij, 2012), which would have provided ample prey for molluskivorous walruses. Kelp-driven gigantism in marine invertebrates in the eastern North Pacific likely led to the repeated evolution of molluskivorous mammals, beginning with the 'beach bear' *Kolponomos* Stirton, 1960 around the Oligocene–Miocene boundary, odobenine walruses in the Late Miocene, and true sea otters (*Enhydra* Linnaeus, 1758) during the Pleistocene (Vermeij, 2012).

Functional Morphology and Feeding Behavior of *Valenictus sheperdi*

Extant *Odobenus rosmarus* has the unique ability amongst carnivorans to protrude the eyeball laterally out of the orbit, likely an adaptation for short-distance binocular vision used during foraging on the seafloor (Kastelein et al., 1993). Protrusion of the eyeball is accomplished by contraction of the cone-shaped muscular envelope sheathing the extrinsic muscles of the eye and the eye itself; these are the m. levator palpebrae superioris, m. depressor palpebrae inferioris, and the m. orbitalis (Kastelein et al., 1993). These muscles originate from the large orbital fissure, which is also the origin of the m. retractor bulbi, which retracts the eye in *Odobenus* (Kastelein et al., 1993). This deep pit anterodorsal to the orbital fissure is not present in other pinnipeds or non-odobenine walruses, and suggests that these features are bony correlates of the specialized eye musculature of *Odobenus.* The *Valenictus sheperdi* holotype shares these unique bony features (Fig. 14), and suggests that *Valenictus* had the musculature and ability to protrude and retract its eyes. Though some matrix remains and bone fracturing obscures certain details, SDSNH 63026 suggests a similar morphology was present in *Valenictus chulavistensis.* Just like *Odobenus*, this is likely an adaptation for seeing around the massively inflated rostrum (Kastelein et al., 1993; Fig. 15). Whether or not this orbital morphology is present in other odobenines such as *Ontocetus*, *Protodobenus*, and *Aivukus* is unclear owing to typical poor preservation and difficult preparation of this region.

Anteroposterior expansion and rugosity of the nuchal crest is shared with *Valenictus chulavistensis*, *Odobenus*, *Pliopedia*, and *Ontocetus* (Fig. 15); most of these walruses, except for *Pliopedia*, are confirmed to have possessed elongate upper tusks. The condition in the tuskless early odobenine *Aivukus* is difficult to assess owing to incompleteness (Deméré, 1994a); however, we note that the nuchal crest is incipiently expanded but possesses a triangular median apex resembling many Otariidae; we consider *Aivukus* unlikely to have possessed an expanded nuchal crest like members of Odobenini. Frustratingly, the other tuskless early odobenine, *Protodobenus*, also has a damaged braincase but the nuchal crest is not expanded as in *Odobenus*; however, the holotype is immature and perhaps the nuchal crest expanded later in growth (Horikawa, 1995). This crest is likely an insertion for the splenius (Deméré, 1994a), which extends the neck and head (Evans & Lahunta, 2013). We propose the expansion and greater importance of this muscle in Odobenini to be a result of the additional mass of the tusks and osteosclerotic bone of the skull and perhaps steadying of the head during benthic feeding. In this case, expansion of the nuchal crest is proposed as a possible indicator of benthic feeding behavior.

Valenictus sheperdi and some specimens of *Valenictus chulavistensis* (SDSNH 38228, 87315, 83719) possess palatal vascularization consisting of large palatal foramina and some sulci (Figs. 9, 13). We speculate that the palatal vasculature in *Valenictus* is homologous with the alveolar arteries branching off the superior alveolar canal, perhaps attesting to a recent loss of teeth;

however, CT scanning is necessary as some, or all, of these may also connect to the greater palatine canal.

Though the canines are not preserved, the large, deep alveoli and alveolar processes of *Valenictus sheperdi* (Figs. 9–12) indicate that it possessed ever-growing tusks as in *Valenictus chulavistensis* and other Odobenini. These alveolar processes deviate about 50° from horizontal in the anterior direction in the *V. sheperdi* holotype, indicating that the tusks were somewhat procumbent like in *Valenictus chulavistensis* and *Ontocetus*. Like *Valenictus chulavistensis*, *V. sheperdi* does not possess any alveoli for teeth aside from the tusks. Species of *Valenictus* also possess a palate that is deeply transversely and longitudinally vaulted, as well as a palate that is extended further posteriorly relative to earlier diverging "imagotariine" walruses (e.g., *Neotherium*, *Proneotherium*, *Imagotaria*). Extant *Odobenus* possesses teeth including one incisor (but up to three in juveniles; McLaughlin et al., 2022) and 3–4 premolars and molars (Fay, 1982), but the teeth are not used in feeding. Feeding experiments and analysis of gut contents indicate that mollusks are held in place by the lips and that the shell does not enter the oral cavity, nor is ingested as might be expected if shells were masticated; likewise, non-mollusk prey recovered as gut contents lack tooth marks (Fay, 1982). Soft tissues of mollusks are removed from the shell by suction; negative pressure is generated by the ventral retraction of the tongue from the vaulted palate (Fay, 1982; Kastelein et al., 1997). Toothlessness has convergently evolved in suction-feeding marine mammals including early odontocetes (*Inermorostrum* Boessenecker et al., 2017, *Dolgopolis* Viglino et al., 2021), beaked whales, a eurhinodelphinid dolphin (*Vanbreenia* Bianucci & Landini, 2002), some delphinids (*Australodelphis* Fordyce, 2002), and partially in sperm whales (*Kogia* Gray, 1846, *Physeter* Linnaeus, 1758) and Risso's dolphin (*Grampus* Gray, 1828) which still possess mandibular teeth (Boessenecker et al., 2017; Fordyce et al., 2002; Viglino et al., 2020; Werth, 2000, 2006). Toothlessness has purportedly evolved in the archaic chaeomysticete *Maiabalaena* Peredo et al., 2018 (Peredo et al., 2018; but see Ekdale & Deméré, 2022; Gatesy et al., 2022), and within toothless Chaeomysticeti (Berta et al., 2016). Pinnipeds seem to be more dentally conservative than cetaceans, and among pinnipeds only *Valenictus* has evolved a degree of toothlessness paralleling ziphiids. The reduction of teeth is presumed to enhance flow through the oral cavity (Werth, 2006). Suction-feeding odontocetes capture soft-bodied prey using suction, typically squid and fish (Werth, 2000). In this context, *Valenictus chulavistensis* was interpreted as a more derived suction feeder than *Odobenus rosmarus* (Deméré, 1994b). *Odobenus rosmarus* appears to be affected by selection towards tooth reduction as it has already lost several tooth positions (I2, P4, M1) relative to other Odobeninae (e.g., *Aivukus*, *Ontocetus*; Deméré, 1994a) and the dental formula is highly variable (McLaughlin et al., 2022). *Valenictus sheperdi* possesses the same suite of adaptations as *Valenictus chulavistensis*, indicating that benthic suction-feeding specializations evolved surprisingly early within this lineage, within one million years of the earliest known fossil occurrences of Odobenini (see above).

Trace evidence of walrus predation or foraging activity reported from the fossil record includes feeding pits attributed to Pleistocene *Odobenus rosmarus* (Gingras et al., 2007) and bitten margins of large bivalves from Pliocene–Pleistocene strata of the North Sea, attributed to *Ontocetus emmonsi* (Moerdijk & Post, 2021). Feeding pits have not yet been observed in mollusk-rich (Fig. 1B) shallow marine sandstones of the Purisima Formation or other Pliocene strata in California, but we suggest that future field studies attempt to search for such traces in Purisima Formation strata where sedimentary structures are well-preserved, including the Año Nuevo section, and section 3 and overlying strata of the Purisima Formation east of Santa Cruz. Careful searching in the San Diego Formation (San Diego County) and the Etchegoin and San Joaquin formations in the Kettleman Hills (Kings County) may also prove fruitful. We do not predict that bitten mollusks as attributed to *Ontocetus emmonsi* by Moerdijk and Post (2021) would be expected given that *Valenictus* is toothless and lacks incisors, but other tooth-bearing odobenine walruses (perhaps possessing incisors), albeit rare, do occur in the California Pliocene in addition to dusignathines (Boessenecker, 2013a; Deméré, 1994a; Repenning & Tedford, 1977), and such evidence may be found among extensive mollusk collections from the Purisima, Etchegoin, San Joaquin, or San Diego formations.

According to Fay (1982), *Odobenus rosmarus* feeds predominantly on large shallow-burrowing (< 20 cm deep burrows) bivalves, including *Astarte* Sowerby, 1816 (shallow burrower), *Hiatella* Bosc, 1801 (deep burrower) *Mya* Linnaeus, 1758 (deep burrower), *Clinocardium* Keen, 1936 (shallow burrower), *Macoma* Leach, 1819 (deep burrower), *Serripes* Gould, 1841 (shallow burrower), and *Tellina* Linnaeus, 1758 (shallow burrower), as well as epibenthic mollusks such as the snail *Buccinum* Linnaeus, 1758 and octopus. *Astarte*, *Hiatella*, *Mya*, and *Serripes* are most common in *O. rosmarus* stomach contents (Fay, 1982). Walruses do not dig with their tusks but use hydraulic jetting to excavate burrowing mollusks; owing to the depth of feeding pits, they apparently do not excavate clams deeper than 20 cm (Fay, 1982). Deep burrowing clams such as *Mya* are only represented by torn siphons in stomach contents and walruses suck and sever the siphon leaving the rest of the clam in the sediment, as it is buried below the depth at which walruses excavate (Fay, 1982). Several large mollusks commonly preserved in the Purisima Formation (Perry, 1988; Powell, 1998) would have offered plentiful food for walruses such as *Valenictus*. These include deep burrowers (>20 cm burrowing depth; *Panopea abrupta* Conrad, 1849, *Tresus pajaroanus* Conrad, 1837), shallow burrowers (<20 cm burrowing depth; *Anadara trilineata* Gray, 1847, *Macoma* spp., *Protothaca staleyi* Gabb, 1866, *Spisula* spp. Gray, 1837) and some epifaunal bivalves (*Modiolus rectus* Conrad, 1837) and gastropods (*Crepidula princeps*, *Neverita lewisii*), all of which are common in the Purisima Formation. Extant *Odobenus rosmarus* feeds on extant species in these genera that inhabit the Arctic seafloor (e.g., *Clinocardium nuttallii* Conrad, 1837, *Macoma calcarean* Gmelin, 1791, *Spisula polynyma* Stimpson, 1860; Fay, 1982).

Phylogeny of the Odobenidae and Relationships of *Valenictus*

The overall tree topology produced in our study (Fig. 17) is consistent with the results of prior recent phylogenetic analyses of walruses, when differences in taxon sampling are taken into account (Biewer et al., 2020; Boessenecker & Churchill, 2013; Tanaka & Kohno, 2015; Velez-Juarbe & Salinas-Márquez, 2018). When present, these differences in topology are usually correlated with portions of the tree with relatively poor support. The largest and most consistent difference in our phylogeny versus prior studies is the monophyly and resolution of Dusignathinae. This clade is recovered as monophyletic in our analysis (Fig. 17), with *Gomphotaria* the sister taxon to *D. seftoni*. However, there is only weak support for monophyly of this clade and relationships within it. Prior studies either recovered a monophyletic Dusignathinae with the relationships of taxa within unresolved (Boessenecker & Churchill, 2013; Biewer et al., 2020), or were unable to recover monophyly for this clade at all, placing them in an unresolved polytomy with a monophyletic Odobeninae (Tanaka & Kohno, 2015; Velez-Juarbe & Salinas-Márquez, 2018). Furthermore, in Tanaka and Kohno (2015), Odobeninae also largely consists of an unresolved polytomy, although a sister taxon relationship between *V. chulavistensis* and *Odobenus* is recovered with strong support.

Our study further disagrees with the placement of some later-diverging "imagotariine" walruses. Biewer et al. (2020) places *T. orangenensis* as diverging earlier than *Imagotaria downsi*. They also recover *P. magnus* as the sister taxon to *P. kohnoi*, within a monophyletic *Pontolis*. None of these clades are recovered with strong support. In contrast, we recover *Imagotaria* as diverging prior to a clade containing *Titanotaria* and *Pontolis*, and within the latter genus, *P. kohnoi* and *P. barroni* are recovered with strong support as sister taxa (Fig. 17). Minor differences between our study and prior studies can also be seen in the monophyly of *Prototaria* (Fig. 17), which forms a polytomy with later diverging walruses in Tanaka and Kohno (2015), and the placement of *Archaeodobenus*, which exists in an unresolved polytomy with *Pseudotaria* and later diverging walruses in Velez-Juarbe and Salinas-Márquez (2018), but resolved identically in Magallanes et al. (2018) and Biewer et al. (2020).

Other fossils of Odobenini warrant further study. Chief among these are fossils of *Ontocetus* and *Odobenus*. A well-preserved skull of *Ontocetus* from the Early Pliocene of Japan introduced by Kohno et al. (1998) awaits formal naming. Though all Pliocene walruses from the North Atlantic have been referred to *Ontocetus emmonsi* (Kohno & Ray, 2008), skulls assigned to *Ontocetus* from the Pliocene of Belgium (Hasse, 1909) and the Netherlands (Erdbrink & Van Bree, 1990) have been noted to possess differing counts of incisors and postcanines (Deméré, 1994a). We further note that the skull reported by Erdbrink and Van Bree (1990) lacks the distinctive rectangular outline of the occipital shield in posterior view, considered by Deméré (1994a) as an autapomorphy of *Ontocetus* (=*Alachtherium* in Deméré, 1994a) and present in partial skulls reported by Van Beneden (1877) and Hasse (1909). Despite recent attention to western North Atlantic *Ontocetus* material (Kohno & Ray, 2008), most well-preserved crania referred to *Ontocetus* are from the margins of the North Sea and await careful taxonomic revision. Further work is additionally needed on fossil specimens of *Odobenus* from the Western North Pacific. A distinctive mandible fragment from the Middle Pleistocene of Japan was named *Odobenus mandanoensis* Tomida, 1989 by Tomida (1989), suggesting a temperate North Pacific endemic species of *Odobenus*. Older remains include a well-preserved skull of *Odobenus* trawled from the seafloor and associated with Pliocene–Pleistocene foraminifera (Miyazaki et al., 1992). This skull is the oldest known occurrence of *Odobenus* and almost certainly represents an unnamed species, as it possesses some peculiarities of the basicranium that led Miyazaki et al. (1992) to identify the specimen as *Odobenus* sp. These include a lower and more elongate cranium, possession of an I2 (lost in *O. rosmarus*), smaller mastoid process, wider basioccipital, and a more curved canine tusk (Miyazaki et al., 1992). To this list we add the following novel observations: labial furrow on canine, more medially positioned toothrows, narrower intertemporal constriction and posteriorly constricted palate, and narrower opening of internal choanae. Further study of this specimen and a reevaluation of Pliocene through Middle Pleistocene specimens of *Odobenus* is clearly warranted (Boessenecker & Churchill, 2021).

Our phylogenetic analysis supports *Valenictus* monophyly and critically is the first to include *Valenictus imperialensis* (Fig. 17), known only from the holotype humerus (LACM 3926). Owing to the incompleteness of *Valenictus imperialensis*, however, *Valenictus* forms a polytomy in our more inclusive analysis. Regardless, this result still supports inclusion of *V. chulavistensis* and *V. imperialensis* in the same genus. In the more exclusive analysis, *Valenictus sheperdi* is recovered as the sister taxon to a clade formed by *Valenictus chulavistensis* and UCMP 137426. This latter relationship supports the assignment of UCMP 137426 to *Valenictus chulavistensis* rather than to *Valenictus sheperdi*, despite both being recovered from the Purisima Formation. However, *Valenictus sheperdi* and UCMP 137426 are stratigraphically separated, with the former occurring in Purisima Formation strata dating to the earliest Pliocene, 5.23–4.89 Ma, and UCMP 137426 occurring in a stratum dating to 4.89–3.59 Ma. UCMP 137426 therefore overlaps in age with fossils of *Valenictus chulavistensis* from the San Diego Formation (Buczek et al., 2021; Deméré, 1994b; Vendrasco et al., 2012; Wagner et al., 2001); critically, *Valenictus sheperdi* is older than the oldest age determinations for the base of the San Diego Formation (4.2 Ma, Vendrasco et al., 2012; 4.9 Ma, Buczek et al., 2021). Our phylogenetic results, when combined with the chronostratigraphic framework for Purisima Formation specimens of *Valenictus*, indicate *in situ* evolution of toothless walruses along the eastern North Pacific coastline and identify *Valenictus sheperdi* as a potential ancestor of *Valenictus chulavistensis* (and possibly *Valenictus imperialensis*).

Phylogenetic Relationships of *Pliopedia pacifica*

Pliopedia pacifica was named by Kellogg (1921) from the Paso Robles Formation of central California and based on USNM 13627, a fragmentary forelimb (including distal humerus, radius and ulna fragments, metacarpals, and a phalanx). Subsequently, Repenning and Tedford (1977) referred USNM 187328, a partial skeleton (consisting of a partial braincase, humerus, radius, and ulna) from the coeval Etchegoin Formation to *Pliopedia pacifica*. Although originally tentatively considered an otariid by Kellogg (1921), certain features unquestionably indicate odobenid affinities of the holotype including a wide medial lip of the distal trochlea of the humerus and a metacarpal with a rugosity for the m. extensor pollicis (Deméré, 1994a; Repenning & Tedford, 1977). Repenning and Tedford (1977) considered *Pliopedia* to be a dusignathine. Barnes and Raschke (1991:13) limited *Pliopedia pacifica* to the holotype and indicated that USNM 187328 was perhaps a different species, noting that "homologous bones of the two species are sufficiently different to indicate that they are not synonymous and are probably not even very closely related" without citing any particular morphological features. Deméré (1994a), however, agreed with Repenning and Tedford (1977), provided an updated diagnosis of *Pliopedia*, and considered it to be a member of the Odobenini based upon possession of several synapomorphies of the clade including the inflated braincase lacking a sagittal crest and anteroposteriorly expanded nuchal crest, and a distinct deltoid tubercle on the humerus.

Until now, *Pliopedia* has not been included within a phylogenetic analysis, owing to its fragmentary nature. We defined several new characters and character states that could help clarify the position of *Pliopedia* within Odobenidae, and coded a composite OTU with both the holotype (USNM 13627) and referred specimen USNM 187328, in agreement with Repenning and Tedford's (1977) concept of the species (but see Barnes & Raschke, 1991). *Pliopedia* is consistently recovered in our analysis with 58% bootstrap support as the sister taxon to *Valenictus* (Fig. 17). The *Pliopedia* + *Valenictus* clade is diagnosed by two synapomorphies, including paired sagittal sulci on the braincase (a single sulcus is present in *Ontocetus* and *Odobenus*) and a lesser tuberosity of the humerus that is medially prominent and transversely wider than the greater tuberosity. Our analysis confirms the hypothesis of Deméré (1994a) that *Pliopedia* is a member of the Odobenini and highlights diversification of the clade within the eastern North Pacific.

Even if the opinion of Barnes and Raschke (1991) is taken at face value that USNM 187328 is not assignable to *Pliopedia*, most codings in the OTU in our matrix based on the holotype are synapomorphies of the Odobenidae, Odobeninae, and Odobenini, and the codings that indicate a more specific placement by linking *Pliopedia* and *Valenictus* as sister taxa are preserved in USNM 187328 (e.g., paired parasagittal sulci) and a more robust and medially prominent lesser tuberosity. Because USNM 187328 is clearly not referable to *Valenictus* based on humeral features, it indicates the presence of at least two genera within the Odobenini in the eastern North Pacific during the Pliocene. Such observations are supported by a set of postcanine teeth with associated short tusks bearing globular dentine (LACM 28432) from the San Diego Formation, best identified as Odobenini indet. for now, likewise indicating at least two genera of Odobenini in the San Diego Formation as well (Boessenecker, 2013a). Further discoveries of more completely preserved specimens of *Pliopedia* are needed.

Paleogeographic Distribution of *Valenictus*

Though species of *Valenictus* date only to the Pliocene, this walrus inhabited a coastline and ecosystem very different from that of the modern California coastline (Fig. 18). Uplift of the coast ranges did not begin until the latest Miocene and Early Pliocene (Loomis, 1990; Bartow, 1991) and several large shallow marine embayments remained (Jacobs et al., 2004). Numerous shallow marine embayments with rich mollusk faunas are recorded in the Pliocene (Fig. 18A, B), including the Eel River Basin of northern California, the San Joaquin and Pismo basins of central California, and the Ventura, Los Angeles, and San Diego basins of southern California (Hall, 2002). The San Joaquin embayment and other shallow marine embayments disappeared during the Pliocene–Pleistocene transition (Fig. 18). From 8–5 Ma, the California coastline had approximately 33,587 km^2 of continental shelf space in addition to the modern shelf (27,471 km^2; measured from Chase et al., 1992a, b, and Grim et al., 1992, continental shelf under 60 meters depth), for a total of perhaps 61,000 km^2; from 5–2 Ma, this additional shelf space decreased to 20,970 km^2 for a possible total of 48,000 km^2 (measured from Hall, 2002). For comparison, the entire coastline from Washington to northern Baja California today only has 56,000 km^2 of shelf space under 75 m deep (= south-east Pacific region in Pyenson & Lindberg, 2011). This indicates that during the Late Miocene and Pliocene, available continental shelf space was perhaps twice as great than at present. One caveat is that paleodepth data are not available from maps published by Hall (2002). This regional tectonically mediated loss of shallow marine embayments and continental shelf space along the temperate eastern North Pacific coastline occurred in tandem with substantial eustatic sea level fluctuations and overall sea level fall across the Pliocene–Pleistocene boundary driven by growth of the northern hemisphere ice cap; changes in sea level have been implicated in mollusk and marine vertebrate extinctions (Bowersox, 2005; Hall, 2002; Pimiento et al., 2017). Over the course of the past 3 million years, the coastline has transitioned from one dominated by large, highly productive shallow marine embayments to more abundant rocky shore habitats. This change was largely driven by the uplift of the coast ranges (Bartow, 1991; Jacobs et al., 2004; Loomis, 1990).

Mollusk assemblages suggest that the Purisima Formation was deposited at temperatures similar to or slightly cooler than present in Monterey Bay (Hall, 2002; Powell, 1998). Other fossil occurrences of *Valenictus* (Barnes, 2005; Deméré, 1994b; Mitchell, 1961; Repenning & Tedford, 1977) are known from lower latitudes from the warm temperate to subtropical San Diego Formation (Hall, 2002; Vendrasco et al., 2012), the warm temperate San Joaquin Formation (Bowersox, 2005; Hall, 2002), the subtropical to tropical Imperial Group (Hall, 2002; Powell, 2008), and Pliocene Salada Formation of Baja California Sur (Barnes, 1994, 1998, 2005). Available evidence at present indicates that *Valenictus* inhabited at least subtropical through temperate waters, and possibly tropical through cold temperate conditions. *Valenictus chulavistensis* in particular is now known to have inhabited approximately 700 km of coastline from San Diego (32–33°N paleolatitude; Deméré, 1994B) to Santa Cruz (36–38°N paleolatitude; this study), as well as the San Joaquin embayment (35–36°N paleolatitude Deméré, 1994a; Repenning & Tedford, 1977; paleolatitudes from Hall, 2002). This wide latitudinal range (both for *Valenictus chulavistensis* and the genus *Valenictus* in general) contrasts with the restriction of extant *Odobenus* to high latitudes and cold temperate to polar waters, but parallels the wide latitudinal range of *Ontocetus* in the North Atlantic which ranged from the North Sea to Morocco and Florida (Kohno & Ray, 2008).

The Extinction of *Valenictus* and other Temperate Walruses

The extinct walrus *Valenictus* is not only noteworthy for its bizarre, highly derived toothless feeding morphology and extensive postcranial pachyosteosclerosis, but also for its temperate to subtropical latitudinal distribution, young geologic age, and close relationship with the extant walrus, *Odobenus rosmarus* (Barnes, 2005; Boessenecker, 2017; Deméré, 1994b; Mitchell, 1961). The extinction of *Valenictus*, along with other highly derived Pliocene marine mammals differing from modern counterparts in the region (e.g., *Herpetocetus* Van Beneden, 1872, *Semirostrum* Racicot et al., 2014, *Parapontoporia* Barnes, 1984, *Dusignathus*), implies considerable faunal change along the Pacific coast during the Pliocene–Pleistocene transition. When precisely did *Valenictus* go extinct? Specimens from the Purisima Formation reported herein, and the *Valenictus imperialensis* holotype specimen (Mitchell, 1961) are far from the youngest known specimens, the former bearing a minimum age of 3.59 Ma (Madrid et al., 1986) and the latter dating to 5.2–4.2 Ma (Dorsey et al., 2011). Fossils of *Valenictus* from the San Diego Formation within SDSNH collections are recorded as being derived from subunits 1–5 (Wagner et al., 2001) of the San Diego Formation. Wagner et al. (2001) correlated subunit 4 with cycle TB3.7 (corresponding to an age of 3.1–2.6 Ma) of Haq et al. (1987), and subunit 5–7 with cycle TB3.8 (corresponding to an age of 2.6–1.7 Ma). A partial humerus of *Valenictus chulavistensis* reported by Repenning and Tedford (1977) from the *Neverita* zone of the San Joaquin Formation can be assigned an age of 4.0–3.1 Ma (Bowersox, 2005), somewhat older than subunits 4 and 5 of the San Diego Formation. Pending further study of *Valenictus* from the San Diego Formation, an extinction date between 2 and 3 Ma is conservatively estimated. This seems consistent with the disappearance of many Pliocene marine mammal taxa sometime around the Pliocene–Pleistocene boundary or during the Early Pleistocene (Boessenecker, 2013a, b).

What led to the extinction of *Valenictus*? Other walruses, including the close relative *Pliopedia* and the more distant dusignathine walruses, also went extinct around the end of the Pliocene (Boessenecker, 2013a; Deméré, 1994b; Repenning & Tedford, 1977). Pliocene extinctions of mollusks driven by oceanic cooling (Stanley, 1986) evidently had little effect on the extinct Atlantic walrus *Ontocetus emmonsi*, which survived into the Early Pleistocene (Boessenecker et al. 2018). Pliocene–Pleistocene mollusk extinctions in the North Pacific, driven by cooling, were generally mild compared with the North Atlantic (Stanley, 1986), but nevertheless resulted in changes in diversity and ecology (Bonuso et al., 2021). The Pliocene mollusk fauna of the eastern North Pacific was quite different from the Quaternary as evidenced by a much higher diversity of pectinid scallops (Smith & Roy, 2006) and oysters (Bonuso et al., 2021), a number of unusually large bivalves (Vermeij, 2012), and was perhaps fostered by warmer water conditions (Bonuso et al., 2021; C.L. Powell, pers. comm., 2022). With the onset of northern hemisphere glaciation, climatic cooling and eustatic sea level fluctuations on the Pacific coast reduced available shelf space and led to intermittent changes in salinity in the largest

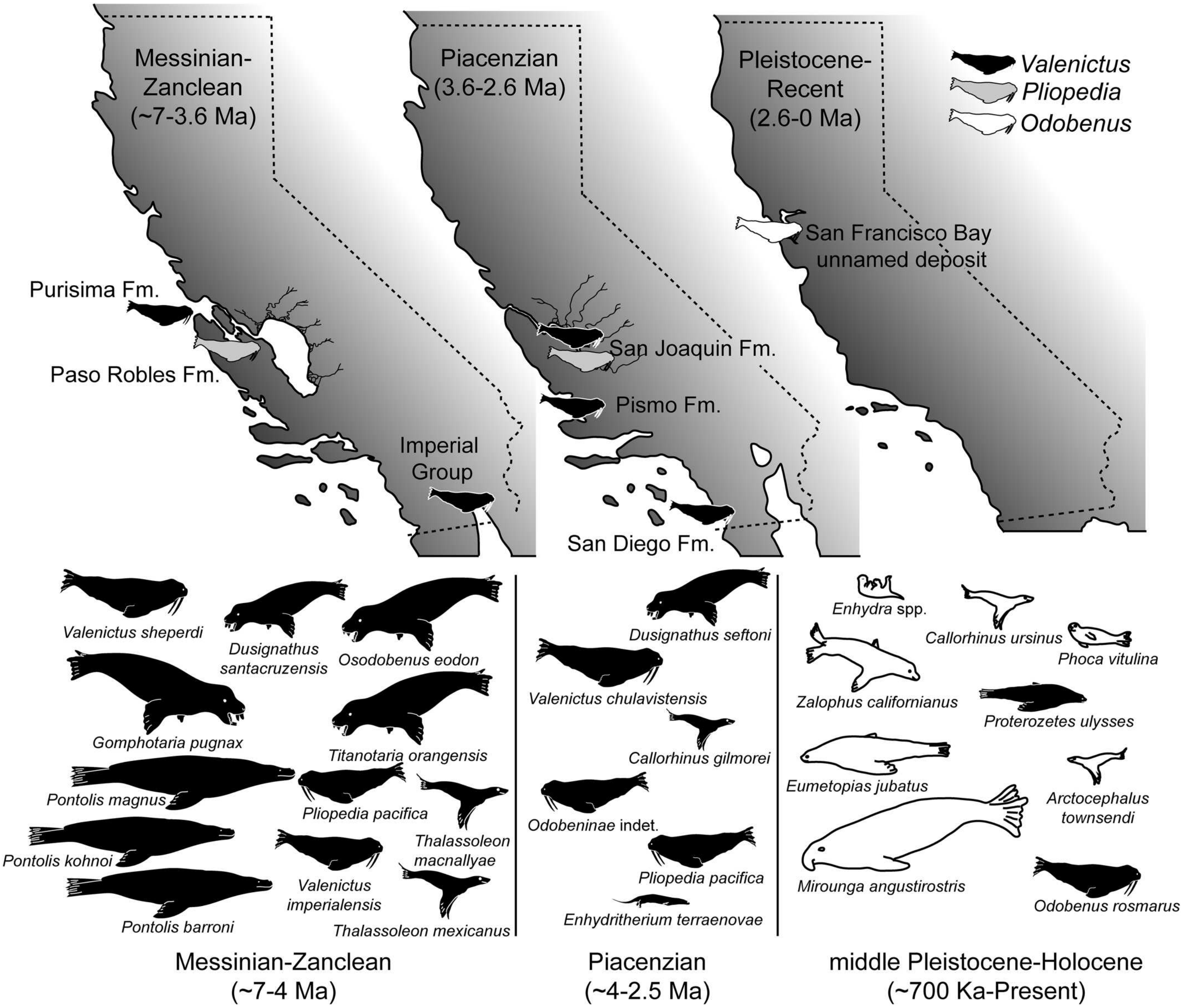

FIGURE 18. Paleogeographic and faunal context of *Valenictus*. **A**, paleogeographic maps of the California coastline during the latest Miocene and Early Pliocene, Late Pliocene, and Pleistocene (based on Hall, 2002; Boessenecker, 2013a; Boessenecker and Poust, 2015); **B**, aggregate marine carnivore faunas from the latest Miocene–Early Pliocene, Late Pliocene, and Middle Pleistocene–Holocene (based on Deméré et al., 2003; Boessenecker, 2013a; Magallanes et al., 2018; Biewer et al., 2020; this study), with extinct (or regionally extirpated) taxa in black and extant taxa in white, body sizes approximated.

Californian coastal embayment, the San Joaquin embayment (Bowersox, 2005). The shallowing and eventual draining of the San Joaquin embayment (Fig. 18) was driven chiefly by the uplift of the California coast ranges, shearing of the marine inlet ('Priest Valley strait') to this embayment, and the rapid uplift of the Sierra Nevada mountains which shed sediment into the basin, filling up remaining accommodation space (Bartow, 1991; Bowersox 2005; Jacobs et al., 2004; Loomis, 1990). Many other shallow marine embayments (e.g., Wilson Grove embayment, La Honda and Santa Cruz embayments, Pismo basin, Santa Maria basin, Ventura basin, Los Angeles basin, San Diego basin) were lost elsewhere along the west coast, largely due to tectonic uplift (e.g., uplift of the California coast ranges) rather than eustatic changes in sea level (Bartow, 1991). The loss of such embayments, along with the uplift of the California coast ranges, fundamentally changed the coastline from a lowland embayment-dominated shoreline to a rocky shoreline from the Pliocene to the Pleistocene (Jacobs et al., 2004). The extinction of giant molluskivores in the eastern North Pacific may have been driven by this tectonic and paleogeographic change along the Pacific coast, as the loss of shallow marine habitat has already been proposed to have driven other extinctions of Pliocene benthic feeding marine mammals such as *Herpetocetus* and *Semirostrum* and shallow marine/coastal odontocetes such as *Parapontoporia* (Boessenecker, 2013a, b; Boessenecker & Poust, 2015). The molluskivore niche was apparently filled by a number of survivors and immigrants including sea otters (*Enhydra lutris* Linnaeus, 1758; Kenyon, 1969), the extinct flightless duck *Chendytes* Miller, 1925 (Jones et al., 2021), and sea ducks (Mergini; but see

Vermeij, 2012, for comments on the ecology of molluskivorous sea birds). A number of molluskivorous fish may have also filled the niche including the wolf eel (*Anarrhichthys occelatus* Ayres, 1855), California sheepshead wrasse (*Semicossyphus pulcher* Ayres, 1854), bat rays (*Myliobatis californica* Gill, 1865), and California horn sharks (*Heterodontus francisci* Girard, 1855), all of which have broad eastern North Pacific coastal distributions in warm through cold temperate waters (Eschmeyer et al., 1983). Regardless of the causes of the extinction, the loss of the walrus fauna in the eastern North Pacific likely opened niche space for the arrival of new pinnipeds including sea lions (*Eumetopias*, *Proterozetes* Barnes et al., 2006, *Zalophus*), harbor seals (*Phoca*), and elephant seals (*Mirounga*) during the Early–Middle Pleistocene (Boessenecker, 2011, 2013a; Poust & Boessenecker, 2017). Critically, none of these immigrants have a fossil record geochronologically overlapping with temperate odobenines in the eastern North Pacific, suggesting physical drivers of their extinction rather than competition with newcomers. Further study of Pliocene ecology and Pliocene–Pleistocene faunal changes is needed to evaluate these hypotheses.

CONCLUSION

New fossil specimens of long-tusked walruses (Odobeninae) are reported from the Late Miocene–Pliocene Purisima Formation near Santa Cruz, California. Fragmentary specimens represent the oldest well-dated record of Odobeninae (first metacarpal, 6.9–6.03 Ma) and Odobenini (tusk fragment, 6.03–5.23 Ma). Two new crania from the Pliocene part of the Purisima Formation represent two species of the toothless walrus *Valenictus*, and include the northernmost record of *Valenictus chulavistensis* and the new species *Valenictus sheperdi*. *Valenictus sheperdi* is geochronologically older and larger than *Valenictus chulavistensis*, possesses a narrower and more highly vascularized palate flanked by a sharper maxillary crest, an anteroposteriorly flattened paroccipital process, rectangular nuchal crest, and rounded internal choanae. A greater degree of palatal vascularization may suggest a more recent loss of upper postcanine dentition in *Valenictus sheperdi*, consistent with its older geochronologic age. Phylogenetic analysis supports monophyly of *Valenictus* within the Odobenini and a newly reported sister taxon relationship with the poorly known odobenine *Pliopedia pacifica*. *Valenictus* was an obligate suction feeding nearly edentulous molluskivore only retaining upper canines. New fossils suggest that *Valenictus* was able to protrude its eyeballs like modern *Odobenus*, an adaptation for benthic foraging. The oldest records of Odobeninae, Odobenini, and *Valenictus* from the Purisima Formation indicate that tusked walruses, including the toothed ancestor of *Valenictus*, evolved alongside large herbivorous marine invertebrates driven by kelp-mediated high primary productivity. The gradual loss of productive shallow marine embayments resulting from basin infilling, uplift of the California coast ranges, and eustatic sea level fluctuations led to the extinction of the overspecialized walrus *Valenictus* (and all other temperate water walruses) around the end of the Pliocene, leaving only extant *Odobenus rosmarus* at high latitudes. This late Neogene walrus-dominated marine carnivoran assemblage was replaced in the Pleistocene by the modern sea lion, true seal, and sea otter dominated fauna along the Pacific coast of North America.

ACKNOWLEDGMENTS

First and foremost, we wish to thank F. Sheperd and family for discovering and donating the holotype of *Valenictus sheperdi*, along with the donors of other specimens reported in this study including E. Burman, D. Landes, and F.A. Perry. Thanks to J. Goedert for funding acid preparation at CCNHM. J. Velez-Juarbe graciously provided photographs of UCMP 137426 for this study. This study would not have been possible without extensive discussions on the Purisima Formation and mentorship from F.A. Perry and C.L. Powell, Jr. Thanks to C.L. Powell, Jr. for discussions on Pliocene mollusks. Discussions of walrus evolution and morphology with L.G. Barnes, A. Berta, T.A. Deméré, and N. Kohno helped us over the course of this study. We thank Gabriel Vogeli for photography at the SDNHM. We also thank the following curators and collections managers who facilitated access to specimens under their care: P.A. Holroyd (UCMP); L.G. Barnes, S. McLeod, and V. Rhue (LACM); T.A. Deméré, K. Randall (SDNHM); D.J. Bohaska, J. Ososki (USNM); F.A. Perry, K. Aston (SCMNH). Thanks to the editors (A. Friscia, P. Godoy) and two reviewers, T.A. Deméré and J. Velez-Juarbe, for comments that greatly improved the quality of this manuscript.

DISCLOSURE STATEMENT

No potential conflict of interest was reported by the author(s).

AUTHOR CONTRIBUTIONS

RWB designed the project and drafted the manuscript, all authors gathered the data, and RWB and MC analyzed the data. All authors edited the manuscript.

SUPPLEMENTARY FILE(S)

Supplementary File 1: Boessenecker et al. *Valenictus* matrix nexus.nex: cladistic matrix from this study, in nexus format.

Supplementary File 2: Boessenecker et al. *Valenictus* matrix TNT.tnt: cladistic matrix from this study, in tnt format.

Supplementary File 3: Trees all walruses no weighting 9_7.tre: tree file saved from search with all walrus OTUs.

Supplementary File 4: Trees no incomplete walruses no weighting 9_7.tre: tree file saved from more exclusive search.

Supplementary Information revised: phylogenetic character list from this study (Appendix S1), list of specimens examined from this study (Appendix S2), and additional reporting of phylogenetic analysis (Appendix S3).

LITERATURE CITED

Agassiz, L. J. R. (1843). *Recherches sur les poisons fossiles.* Volume 3. Imprimerie de Petitpierre, Neuchâtel.

Allen, J. A. (1880). History of North American pinnipeds: a monograph of the walruses, sea-lions, sea-bears and seals of North America. *United States Geological and Geographic Survey of the Territories Miscellaneous Publications*, *12*, 1–785.

Ayres, W. O. (1854). A number of short notices read before the Society at several meetings in 1854. *Proceedings of the California Academy of Sciences*, *1*, 3–22.

Ayres, W. O. (1855). A number of short notices read before the Society at several meetings in 1855. *Proceedings of the California Academy of Sciences*, *1*, 23–77.

Barboza, M.M., Parham, J. F., Santos, G-P., Kussman, B. N., Velez-Juarbe, J. (2017). The age of the Oso Member, Capistrano Formation, and a review of fossil crocodylians from California. *PaleoBios*, *34*, 1–16. https://doi.org/10.5070/P9341033797

Barnes, L. G. (1984). Fossil odontocetes (Mammalia: Cetacea) from the Almejas Formation, Isla Cedros, Mexico. *PaleoBios*, *42*, 1–46.

Barnes, L. G. (1988). A new fossil pinniped (Mammalia: Otariidae) from the middle Miocene Sharktooth Hill Bonebed, California. *Los Angeles County Museum Contributions in Science*, *403*, 1–26.

Barnes, L. G. (1989). A new enaliarctine pinniped from the Astoria Formation, Oregon, and a classification of the Otariidae (Mammalia: Carnivora). *Natural History Museum of Los Angeles County Contributions in Science*, *403*, 1–28.

Barnes, L. G. (1994). A Pliocene pinniped assemblage, including strange new walruses, from near Santa Rita, Baja California Sur, Mexico.

[Paper presentation]. *Journal of Vertebrate Paleontology*, *14*(supplement to number 3), 16A.

Barnes, L. G. (1998). The sequence of fossil marine mammal assemblages in Mexico. *Avances en Investigación: Paleontología de Vertebrados, Publicación Especial*, *1*, 26–79.

Barnes, L. G. (2005). *Dense-boned late Miocene and Pliocene fossil walruses of the Imperial Desert and Baja California: possible buoyancy-control mechanisms for feeding on benthic marine invertebrates in the Proto-Gulf of California* [Paper presentation]. Proceedings of the 2005 Desert Symposium, California State University, Fullerton, CA, USA.

Barnes, L. G. (2008). Miocene and Pliocene Albireonidae (Cetacea, Odontoceti), rare and unusual fossil dolphins from the eastern North Pacific Ocean. *Natural History Museum of Los Angeles County Science Series*, *41*, 99–152.

Barnes, L. G., and Perry, F. A. (1989): *A toothless walrus from the Purisima Formation in California, U.S.A*. [Paper presentation]. 8th Biennial Conference on the Biology of Marine Mammals, Pacific Grove, CA, U.S.A.

Barnes, L. G., and Raschke, R. E. (1991). *Gomphotaria pugnax*, a new genus and species of late Miocene dusignathine otariid pinniped (Mammalia: Carnivora) from California. *Natural History Museum of Los Angeles County Contributions in Science*, *426*, 1–27.

Barnes, L. G., Ray, C. E., and Koretsky, I. A. (2006). A new Pliocene sea lion, *Proterozetes ulysses* (Mammalia: Otariidae) from Oregon, U.S.A. In Z. Csiki (Ed.), *Mesozoic and Cenozoic Vertebrates and Paleoenvironments. Tributes to the career of Dan Grigorescu* (pp. 57–77). Editora Ars Docendi, Bucharest.

Bartow, J. A. (1991). The Cenozoic evolution of the San Joaquin Valley, California. U.S. *Geological Survey Professional Paper*, *1501*, 1–40.

Berry, E. W., and Gregory, W. K. (1906). *Prorosmarus alleni*, a new genus and species of Walrus from the Upper Miocene of Yorktown, Virginia. *American Journal of Science (1880–1910)*, 21(126), 444–450.

Berta, A., and Deméré, T. A. (1986). *Callorhinus gilmorei* sp. nov. (Carnivora: Otariidae) from the San Diego Formation (Blancan) and its implications for otariid phylogeny. *Transactions of the San Diego Society of Natural History*, *21*, 111–126.

Berta, A. (1991). New *Enaliarctos** (Pinnipedimorpha) from the Oligocene and Miocene of Oregon and the role of "Enaliarctids" in Pinniped phylogeny. *Smithsonian Contributions to Paleobiology*, *69*, 1–33.

Berta, A., Lanzetti, A., Ekdale, E. G., and Deméré, T. A. (2016). From teeth to baleen and raptorial to bulk filter feeding in mysticete cetaceans: the role of paleontological, genetic, and geochemical data in feeding evolution and ecology. *Integrative and Comparative Biology*, *56*(6), 1271–1284. https://doi.org/10.1093/icb/icw128

Bianucci, G., and Landini, W. (2002). A new short-rostrum odontocete (Mammalia: Cetacea) from the Middle Miocene of the eastern Netherlands. *Beaufortia*, *52*(11), 187–196.

Biewer, J. N., Velez-Juarbe, J., and Parham, J. F. (2020). Insights on the dental evolution of walruses based on new fossil specimens from California. *Journal of Vertebrate Paleontology*, *40*(5), e1833896. https://doi.org/10.1080/02724634.2020.1833896

Boessenecker, R. W. (2011). New records of the fur seal *Callorhinus* (Carnivora: Otariidae) from the Plio-Pleistocene Rio Dell Formation of Northern California and comments on otariid dental evolution. *Journal of Vertebrate Paleontology*, *31*(2), 454–467. https://doi.org/10.1080/02724634.2011.550362

Boessenecker, R. W. (2013a). A new marine vertebrate assemblage from the Late Neogene Purisima Formation in Central California, Part II: pinnipeds and cetaceans. *Geodiversitas*, *35*(4), 815–940. https://doi.org/10.5252/g2013n4a5

Boessenecker, R. W. (2013b). Pleistocene survival of an archaic dwarf baleen whale (Mysticeti: Cetotheriidae). *Naturwissenschaften*, *100*, 365–371. https://doi.org/10.1007/s00114-013-1037-2

Boessenecker, R. W. (2017). A new early Pliocene record of the toothless walrus *Valenictus* (Carnivora, Odobenidae) from the Purisima Formation of Northern California. *PaleoBios*, *34*, 1–6. https://doi.org/10.5070/P9341035289

Boessenecker, R. W., and Churchill, M. (2013). A reevaluation of the morphology, paleoecology, and phylogenetic relationships of the enigmatic walrus *Pelagiarctos*. *PLoS ONE*, *8*(1), e54311. https://doi.org/10.1371/journal.pone.0054311

Boessenecker, R. W., and Churchill, M. (2018). The last of the desmatophocid seals: a new species of *Allodesmus* from the upper Miocene of Washington, USA. *Zoological Journal of the Linnaean Society*, *184*(1), 211–235. https://doi.org/10.1093/zoolinnean/zlx098

Boessenecker, R. W., and Churchill, M. (2021). The surprising evolutionary heritage of the Atlantic walrus as chronicled by the fossil record. In Keighley, X., Jordan, P., Morten, T. O., and Desjardins, S. (Eds.). *The Atlantic Walrus* (pp. 9–37). Academic Press, London. https://doi.org/10.1016/B978-0-12-817430-2.00006-6

Boessenecker, S. J., Boessenecker, R. W., and Geisler, J. H. (2018). Youngest record of the extinct walrus Ontocetus emmonsi from the early Pleistocene of South Carolina and a review of North Atlantic walrus biochronology. *Acta Palaeontologica Polonica*, *63*(2), 279–286. https://doi.org/10.4202/app.00454.2018

Boessenecker, R. W., Ehret, D. J., Long, D. J., Churchill, M., Martin, E., and Boessenecker, S. J. (2019). The early Pliocene extinction of the mega-toothed shark *Otodus megalodon*: a view from the eastern North Pacific. *PeerJ*, *7*, e6088. https://doi.org/10.7717/peerj.6088

Boessenecker, R. W., Fraser, D., Churchill, M., and Geisler, J. H. (2017). A toothless dwarf dolphin (Odontoceti: Xenorophidae) points to explosive feeding diversification of modern whales (Neoceti). *Proceedings of the Royal Society B*, *284*(1861), 20170531. https://doi.org/10.1098/rspb.2017.0531

Boessenecker, R. W., F. A. Perry, and Schmitt, J. G. 2014. Comparative taphonomy, taphofacies, and bonebeds of the Mio–Pliocene Purisima Formation, Central California: strong physical control on marine vertebrate preservation in shallow marine settings. *PLoS ONE*, *9*(3), e91419. https://doi.org/10.1371/journal.pone.0091419

Boessenecker, R. W., and Poust, A. W. (2015). Freshwater occurrence of the extinct dolphin *Parapontoporia* (Cetacea: Lipotidae) from the upper Pliocene nonmarine Tulare Formation of California. *Palaeontology*, *58*(3), 489–496. https://doi.org/10.1111/pala.12153

Boessenecker, S. J., Boessenecker, R. W., and Geisler, J. H. (2018). Youngest record of the extinct walrus *Ontocetus emmonsi* from the early Pleistocene of South Carolina and a review of North Atlantic walrus biochronology. *Acta Palaeontologica Polonica*, *63* (2), 279–286. https://doi.org/10.4202/app.00454.2018

Bonuso, N., Zacherl, D. C., Vreeland, K., and Ditmar, J. (2021). Reconstructing oyster paleocommunity over the last 3.6 million years: a southern California case study. *PaleoBios*, *38*, 1–20. https://doi.org/10.5070/P938054472

Bosc, L.A.G., (1801). *Histoire naturelle des coquilles, Vol. 3.* De Imprimerie de Crapelet, Paris.

Bowdich, T. W. (1821). *An Analysis of the Natural Classification of Mammalia, for the Use of Students and Travelers*. J. Smith, Paris.

Bowersox, J. R. (2005). Reassessment of extinction patterns of Pliocene molluscs from California and environmental forcing of extinction in the San Joaquin Basin. *Palaeogeography, Palaeoclimatology, Palaeoecology*, *221*, 55–82. https://doi.org/10.1016/j.palaeo.2005.02.004

Brandt, J. F. (1835). *Prodromus Descriptionis Animalium ab H. Mertensio in orbis terrarum circumnavigatione observatorum*. Sumptibus Academiae, St. Petersburg.

Brisson, M. J. (1762). *Regnum Animale in Classes IX Distributum Sive Synopsis Methodica*. Jean-Baptiste Bauche, Paris.

Buczek, A. J., Hendy, A. J. W., Hopkins, M. J., and Sessa, J. A. (2021). On the reconciliation of biostratigraphy and strontium isotope stratigraphy of three southern Californian Plio–Pleistocene formations. *Geological Society of America Bulletin*, *133*(1–2), 100–114. https://doi.org/10.1130/B35488.1

Bus, Du. (1867). Sur quelques mammifères du Crag d'Anvers. *Bulletins de l'Académie royale des sciences, des lettres et des beaux-arts de Belgique (2)*, *24*, pp. 562–577.

Chase, T. E., Wilde, P., Normark, W. R., Evenden, G. I., Miller, C. P., Seekins, B. A., Young, J. D., Grim, M. S., and Lief, C. J. (1992a). Map showing bottom topography in the deep-sea basins of the Pacific continental margin, Cape Mendocino to Point Conception. U.S. *Geological Survey Miscellaneous Investigations Series Map*, *I-2090-C*.

Chase, T. E., Wilde, P., Normark, W. R., Evenden, G. I., Miller, C. P., Seekins, B. A., Young, J. D., Grim, M. S., and Lief, C. J. (1992b). Map showing bottom topography in the deep-sea basins of the Pacific Continental margin, Point Conception to Point Loma. *U.S. Geological Survey Miscellaneous Investigations Series Map*, *I-2089-C*.

Churchill, M., Boessenecker, R. W., and Clementz, M. T. (2014). Colonization of the Southern Hemisphere by fur seals and sea lions (Carnivora: Otariidae), revealed by combined evidence phylogenetic and Bayesian biogeographic analysis. *Zoological Journal of the Linnaean Society*, *172*(1), 200–225. https://doi.org/10.1111/zoj.12163

Condon, T. (1906). A new fossil pinniped (*Desmatophoca oregonensis*) from the Miocene of the Oregon coast. *University of Oregon Bulletin, 3*(3), 1–14.

Conrad, T. A. (1837). Description of new marine shells, from Upper California. Collected by Thomas Nuttall, Esq. *Journal of the Academy of Natural Sciences, Philadelphia*, *7*, 227–268.

Conrad, T. A. (1849). Fossils from northwestern America. In Dana, J. D., *U.S. Exploring Expedition, 1838–1842, under the command of Charles Wilkes.* C. Sherman, Philadelphia.

Conrad, T. A. (1855). Report on the fossil shells collected in California by W. P. Blake, geologist of the expedition under the command of Lieut. R. S. Williamson, U. S. Topographical Engineers, 1852. In Williamson, R.S. (Ed.), *Reports of explorations and surveys, to ascertain the most practicable and economical route for a railroad from the Mississippi River to the Pacific Ocean*. War Department, United States 33rd Congress, Washington, D.C.

Da Costa, E. M. (1778). *Historia Naturalis Testaceorum Britanniae, or the British Conchology*. Millan, B. White, Elmsley, and Robson, London.

Dall, W. H. (1917). Summary of the mollusks of the family Alectrionidae of the west coast of America. *Proceedings of the United States National Museum*, *51*, 575–579.

Deméré, T. A. (1994a). The family Odobenidae: a phylogenetic analysis of fossil and living taxa. *Proceedings of the San Diego Society of Natural History*, *29*, 99–123.

Deméré, T. A. (1994b). Two new species of fossil walruses (Pinnipedia: Odobenidae) from the Upper Pliocene San Diego Formation, California. *Proceedings of the San Diego Society of Natural History*, *29*, 77–98.

Deméré, T. A., and Berta, A. (2002). The Miocene pinniped *Desmatophoca oregonensis* Condon, 1906 (Mammalia: Carnivora) from the Astoria Formation, Oregon. *Smithsonian Contributions to Paleobiology*, *93*, 113–147. https://doi.org/10.5479/si.00810266.93

Deméré, T.A., Berta, A., and Adam, P. J. (2003). Pinnipedimorph evolutionary biogeography. *Bulletin of the American Museum of Natural History 279*, 32–76.

Deméré, T.A., and Berta, A. (2005). New skeletal material of *Thalassoleon* (Otariidae): Pinnipedia) from the late Miocene–early Pliocene (Hemphillian) of California. *Bulletin of the Florida Museum of Natural History*, *45*(4), 379–411.

Dorsey, R. J., Housen, B. A., Janecke, S. U., Fanning, C. M., & Spears, A. L. F. (2011). Stratigraphy record of basin development within the San Andreas fault system: Late Cenozoic Fish Cree-Vallecito basin, southern California. *Geological Society of America Bulletin*, *123*(5-6), 771–793.

Dubrovo, I. A. (1981). A new subfamily of fossil seals (Pinnipedia Kamtschatarctinae subfam. nov.). *Proceedings of the Academy of Sciences of the USSR*, *256*, 970–974.

Dumont, M. P., Baldauf, J. G., and Barron, J. A. (1986). *Thalassiosira praeoestrupii*-a new diatom species for recognizing the Miocene/Pliocene epoch boundary in coastal California. *Micropaleontology*, *32*(4), 372–377. https://doi.org/10.2307/1485728

Ehret, D. J., Macfadden, B. J., Jones, D. S., Devries, T. J., Foster, D. A., and Salas-Gismondi, R. (2012). Origin of the white shark *Carcharodon* (Lamniformes: Lamnidae) based on recalibration of the Upper Neogene Pisco Formation of Peru. *Palaeontology*, *55*(6), 1139–1153. https://doi.org/10.1111/j.1475-4983.2012.01201.x

Ekdale, E. G., and Deméré, T. A. (2022). Neurovascular evidence for a co-occurrence of teeth and baleen in an Oligocene mysticete and the transition to filter-feeding in baleen whales. *Zoological Journal of the Linnaean Society*, *194*(2), 395–415. https://doi.org/10.1093/zoolinnean/zlab017

Erdbrink, D. P., and van Bree, P. J. H. (1990). Further observations on fossil and subfossil odobenid material (Mammalia, Carnivora) from the North Sea. *Beaufortia*, *40*, 85–101.

Erxleben I. C. P. (1777). *Systema regni animalis per classes, ordines, genera, species, varietates, cum synonymia et histria animalium*. Weygand, Leipzig.

Eschmeyer, W.N., Herald, E. S., and Hamman, H. (1983). *A field guide to Pacific coast fishes of North America*. Houghton-Mifflin, Boston, Massachusetts.

Evans, H. E., and Lahunta, A. D. (2013). *Miller's anatomy of the dog*. Saunders-Elsevier, St. Louis, Missouri.

Fay, F. H. (1982). Ecology and biology of the Pacific Walrus, *Odobenus rosmarus divergens* Illiger. *North American Fauna*, *74*, 1–279. https://doi.org/10.3996/nafa.74.0001

Fordyce, R. E., Quilty, P. G., and Daniels, J. (2002). *Australodelphis mirus*, a bizarre new toothless ziphiid-like fossil dolphin (Cetacea: Delphinidae) from the Pliocene of Vestfold Hills, East Antarctica. *Antarctic Science*, *14*(1), 37–54. https://doi.org/10.1017/S0954102002000561

Gabb, W. M. (1866). Tertiary invertebrate fossils. *California Geological Survey*, *Paleontology*, *2*, 1–38.

Gatesy, J., Ekdale, E. G., Deméré, T. A., Lanzetti, Randall, J., Berta, A., El Adli, J. J., Springer, M. S., and McGowen, M. R. (2022). Anatomical, ontogenetic, and genomic homologies guide reconstructions of the teeth-to-baleen transition in mysticete whales. *Journal of Mammalian Evolution*, *29*, 891–930. https://doi.org/10.1007

Geraads, D. (1997). Carnivores du Pliocène terminal de Ahl al Oughlam (Casablanca, Maroc). *Geobios*, *30*(1), 127–164. https://doi.org/10.1016/S0016-6995(97)80263-X

Gill, T. N. (1865). Note on the family of myliobatoids, and on a new species of *Aetobatis. Annals of the Lyceum of Natural History of New York*, *8*(*art. 13*), 135–138.

Gill, T. (1866). Prodrome of a monograph of the pinnipedes. *Proceedings of the Essex Institute*, *5*, 1–13.

Gingras, M. K., Armitage, I. A., Pemberton, S. G., and Clifton, H. E. (2007). Pleistocene walrus herds in the Olympic Peninsula area: trace-fossil evidence of predation by hydraulic jetting. *Palaios*, *22* (5), 539–545. https://doi.org/10.2110/palo.2005.p05-120r

Girard, C. F. (1855). Characteristics of some cartilaginous fishes of the Pacific coast of North America. *Proceedings of the Academy of Natural Sciences of Philadelphia*, *7*, 196–197.

Gmelin, J. F. (1791). Vermes. In Gmelin J. F. (Ed.) *Caroli a Linnaei Systema Naturae per Regna Tria Naturae*. G. E. Beer, Leipzig.

Gould, A. A. (1841). *Report on the Invertebrata of Massachusetts, Comprising the Mollusca, Crustacea, Annelida, and Radiata. Published Agreeably to an Order of the Legislature, by the Commissioners on the Zoological and Botanical Survey of the State*. Folsom, Wells, and Thurston, Cambridge.

Gould, A. A. (1847). Descriptions of new shells, collected by the United States Exploring Expedition. *Proceedings of the Boston Society of Natural History*, *2*, 196-239.

Gradstein, F. M., Ogg, J. G., Schmitz, M., & Ogg, G. (2012). *The Geologic Time Scale 2012*. Oxford: Elsevier.

Gray, J. E. (1827). *A synopsis of the species of the class Mammalia, in The animal kingdom arranged in conformity with its organization, by the Baron Cuvier, with additional descriptions of all the species hitherto named, and of many not before noticed, by Edward Griffith, F.L.S., A.S., and others (E. Griffith, C. H. Smith, and E. Pidgeon, eds.), Vol. 1–5*. George B. Whittacker, London.

Gray, J. E. (1828). *Spicilegia Zoologica or original Figures and short systematic Descriptions of new and unfigured Animals (Vol. 1)*. Würtz Treüttel, London.

Gray, J. E. (1837). A synoptical catalogue of the species of certain tribes or genera of shells contained in the collection of the British Museum and the author's cabinet. *Magazine of Natural History, N.S.*, *1*, 370–376.

Gray, J. E. (1846). On the cetaceous animals. *The Zoology of the Voyage of HMS Erebus and Terror under the Command of Captain Sir James Clark Ross, RNF, RS, during the Years 1839 to 1843*, *1*, 13–53.

Gray, J.E. (1847). A list of the genera of recent Mollusca, their synonyma and types. *Proceedings of the Zoological Society of London*, *15*, 129–219.

Gray, J. E. (1859). On the sea bear of Foster, the Ursus marinus of Steller, Arctocephalus ursinus of authors. *Proceedings of the Zoological Society of London*, *27*, 102–103.

Grim, M. S., Chase, T. E., Evenden, G. I., Holmes, M. L., Normark, W. R., Wilde, P., Fox, C. G., Lief, C. J., and Seekins, B. A. (1992). Map showing bottom topography in the deep-sea basins of the Pacific Continental margin, Strait of Juan de Fuca to Cape Mendocino.

U.S. Geological Survey Miscellaneous Investigations Series Map, I-2091-C.

Hall, C. A. (2002). Nearshore marine paleoclimatic regions, increasing zoogeographic provinciality, molluscan extinctions, and paleoshorelines, California: Late Oligocene (27 Ma) to Late Pliocene (2.5 Ma). *Geological Society of America Special Paper*, *357*, 1–489. https://doi.org/10.1130/0-8137-2357-4.1

Haq, B. U., Hardenbol, J., and Vail, P. R. (1987). Chronology of fluctuating sea levels since the Triassic. *Science*, *235*(4793), 1156–1167. https://doi.org/10.1126/science.235.4793.1156

Harington, C. R. (1984). Quaternary marine and land mammals and their paleoenvironmental implications – some examples from northern North America. *Carnegie Museum of Natural History Special Publication*, *8*(2), 511–525. https://doi.org/10.1890/06-0624.1

Harington, C. R., and Beard, G. (1992). The Qualicum walrus: a late Pleistocene walrus (*Odobenus rosmarus*) from Vancouver Island, British Columbia, Canada. *Annales Zoologica Fennica*, *28*(3–4), 311–319.

Hasse, G. (1909). Les morses du Pliocene Poederlien à Anvers. *Bulletin de la Société de Géologie de Paleontologie et d'Hydrologie, Bruxelles, Mémoire*, *23*, 293–322.

Hermann, J. (1779). Beschreibung der Münchs-Robbe. *Beschäftigungen der Berlinischen Gesellschaft naturforschender Freunde*, *4*, 456–509

Horikawa, H. (1995). A primitive odobenine walrus of Early Pliocene age from Japan. *The Island Arc*, *3*(4), 309–328. https://doi.org/10.1111/j.1440-1738.1994.tb00118.x

Howell, A. B. (1929). Contribution to the comparative anatomy of the eared and earless seals (Genera *Zalophus* and *Phoca*). *Proceedings of the U. S. National Museum*, *73*(2736), 15:1–142. https://doi.org/10.5479/si.00963801.73-2736.1

Illiger, J. C. W. (1811). *Prodromus systematis mammalium et avium; additis terminis zoographicis utriusque classes, corumgue versione germanica.* C. Salfeld, Berlin.

Jacobs, D. K., Haney, T. A., and Louie, K. D. (2004). Genes, diversity, and geologic process on the Pacific coast. *Annual Review of Earth and Planetary Sciences*, *32*, 601–652. https://doi.org/10.1146/annurev.earth.32.092203.122436

Jones, T. L., Coltrain, J. B., Jacobs, D. K., Porcasi, J., Brewer, S. C., Buckner, J. C., Perrine, J. D., and Codding, B. F. (2021). Causes and consequences of the late Holocene extinction of the marine flightless duck (*Chendytes lawi*) in the northeastern Pacific. *Quaternary Science Reviews*, *260*, 106914. https://doi.org/10.1016/j.quascirev.2021.106914

Kastelein, R. A., Dubbeldam, J. L., and de Bakker, M. A. G. (1997). The anatomy of the walrus head (*Odobenus rosmarus*). Part 5: the tongue and its function in walrus ecology. *Aquatic Mammals*, *23* (1), 29–47.

Kastelein, R. A., Zweypfenning, R. C. V. J., Sprekreijse, H., Dubbeldam, J. L., and Born, E. W. (1993). The anatomy of the walrus head (*Odobenus rosmarus*). Part 3: the eyes and their function in walrus ecology. *Aquatic Mammals*, *19*(2), 61–92.

Keen, A. M. (1936). A new pelecypod genus of the family Cardiidae. *Transactions of the San Diego Society of Natural History*, *8*(17), 119–120.

Kellogg, R. (1921). A new pinniped from the Upper Pliocene of California. *Journal of Mammalogy*, *2*(4), 212–226. https://doi.org/10.2307/1373555

Kellogg, R. (1922). Pinnipeds from Miocene and Pleistocene deposits of California. *University of California Publications in Geological Sciences*, *13*, 23–132.

Kellogg, R. (1925). New pinnipeds from the Miocene diatomaceous earth near Lompoc, California. *Contributions to Paleontology from the Carnegie Institution of Washington*, *348*(2), 71–95.

Kellogg, R. (1927). Fossil pinnipeds from California. *Carnegie Institution of Washington Publication*, *348*(2), 27–37.

Kellogg, R. (1931). Pelagic mammals from the Temblor Formation of the Kern River region, California. *Proceedings of the California Academy of Sciences*, *19*(4), 217–397.

Kenyon, K. W. (1969). The sea otter in the eastern Pacific Ocean. *North American Fauna*, *68*, 1–352.

Kohno, N. (1992). A new Pliocene fur seal (Carnivora: Otariidae) from the Senhata Formation on the Boso Peninsula, Japan. *Natural History Research*, *2*(1), 15–28.

Kohno, N. (2006). A new Miocene odobenid (Mammalia: Carnivora) from Hokkaido, Japan, and its implications for odobenid phylogeny. *Journal of Vertebrate Paleontology*, *26*(2), 411–421. https://doi.org/10.1671/0272-4634(2006)26[411:ANMOMC]2.0.CO;2

Kohno, N., Narita, K., and Hakuichi, K. (1998). An early Pliocene odobenid (Mammalia: Carnivora) from the Joshita Formation, Nagano Prefecture, central Japan. *Research Reports of the Shinshushinmachi Fossil Museum*, *1*, 1–7.

Kohno, N., and Ray, C. E. (2008). Pliocene walruses from the Yorktown Formation of Virginia and North Carolina, and a systematic revision of the North Atlantic Pliocene walruses. *Virginia Museum of Natural History Special Publication*, *14*, 39–80.

Kohno, N., Barnes, L. G., and Hirota, K. (1995a). Miocene fossil pinnipeds of the genera *Prototaria* and *Neotherium* (Carnivora; Otariidae; Imagotariinae) in the North Pacific Ocean: evolution, relationships, and distribution. *The Island Arc*, *3*(4), 285–308. https://doi.org/10.1111/j.1440-1738.1994.tb00117.x

Kohno, N., Tomida, Y., Hasegawa, Y., and Furusawa, H. (1995b). Pliocene tusked odobenids (Mammalia: Carnivora) in the Western North Pacific, and their paleobiogeography. *Bulletin of the National Science Museum, Tokyo Series C (Geology & Paleontology)*, *21*(3–4), 111–131.

Kohno, N., and Yanagisawa, Y. (1997). The first record of the Pliocene Gilmore fur seal in the Western North Pacific Ocean. *Bulletin of the National Science Museum, Tokyo, Series C (Geology & Paleontology)*, *23*(3–4), 119–130.

Leach W. E. (1819). A list of invertebrate animals discovered by H. M. S. Isabella, in a voyage to the Arctic regions: corrected by W. E. Leach. Appendix II. In Ross, John (Ed.), *A voyage of discovery in His Majesty's ships Isabella and Alexander [in 1818] for the purpose of exploring Baffin's Bay and enquiring into the possibility of a north-west passage.* John Murray. London.

Leidy, J. (1859). Remarks on *Dromatherium sylvestre* and *Ontocetus emmonsi*. *Proceedings of the Academy of Natural Sciences of Philadelphia,* 1859, 162.

Lesson, R. P. (1828). Phone. In B. de Saint-Vincent (Ed.), *Dictionnarie classique d'historie naturelle, vol 13*. Rey et Gravier, Paris.

Linnaeus, C. (1758). *Systema Naturae per Regna Tria Naturae, Secundum Classes, Ordines, Genera, Species, cum Characteribus, Differentiis, Synonymis, Locis.* Laurentii Salvii, Holmiae.

Loomis, K. B. (1990). *Late Neogene depositional history and paleoenvironments of the west-central San Joaquin basin, California* [Unpublished doctoral dissertation] Stanford University.

Maddison, W. P., and Maddison, D. R. (2023). *Mesquite: a modular system for evolutionary analysis.* (Version 3.81). [computer software]. http://www.mesquiteproject.org.

Madrid, V. M., Stuart, R. M., and Verosub, K. L. (1986). Magnetostratigraphy of the late Neogene Purisima Formation, Santa Cruz County, California. *Earth and Planetary Science Letters*, *79*(3–4), 431–440. https://doi.org/10.1016/0012-821X(86)90198-6

Magallanes, I., Parham, J. F., Santos, G. P., and Velez-Juarbe, J. (2018). A new tuskless walrus from the Miocene of Orange County, California, with comments on the diversity and taxonomy of odobenids. *PeerJ*, *6*, e5708. https://doi.org/10.7717/peerj.5708

McLaughlin, W. N. F., Boatman, C. J., Davis, E. B., and Hopkins, S. S. B. (2022). Total dental occlusal area as a feeding constraint feature in extant walruses (*Odobenus rosmarus*), and implications for the evolution of molluscivory in Odobenidae. *Journal of Mammalian Evolution*, *29*, 571–583. https://doi.org/10.1007/s10914-022-09603-x

Merriam, C. H. (1897). A new fur-seal or sea-bear (*Arctocephalus townsendi*) from Guadalupe Island, off Lower California. *Proceedings of the Biological Society of Washington*, *11*, 175–178.

Middendorff, A.T. von. (1847). Vorläufige Anzeige bisher unbekannter Mollusken, als Vorarbeit zu einer Malacozoologia Rossica. *Bulletin de la Classe Physico-Mathématique de l'Académie Impériale des Sciences de Saint-Pétersbourg*, *6*, 113–122.

Miller, L. (1925). *Chendytes*, a diving goose from the California Pleistocene. *The Condor*, *27*, 145–147. https://doi.org/10.2307/1362992

Mitchell, E. D. (1961). A new walrus from the imperial Pliocene of Southern California: with notes on odobenid and otariid humeri. *Los Angeles County Museum Contributions in Science*, *44*, 1–28.

Mitchell, E.D. (1962). A walrus and a sea lion from the Pliocene Purisima Formation at Santa Cruz, California: with remarks on the type locality and age of the sea lion *Dusignathus santacruzensis* Kellogg. *Los Angeles County Museum Contributions in Science*, *56*, 1–24.

Mitchell, E. (1968). The Mio–Pliocene pinniped *Imagotaria*. *Journal of the Fisheries Board of Canada*, *25*, 1843–1900.

Miyazaki, S., Kimura, M., and Ishiguri, H. (1992). On a Pliocene walrus (*Odobenus* sp.) discovered in the Northern Pacific Ocean. *The Journal of the Geological Society of Japan*, *98*(8), 723–740.

Miyazaki, S., Horikawa, H., Kohno, K., Hirota, K., Kimura, M., Hasegawa, Y., Tomida, Y., Barnes, L.G., and Ray, C.E. (1995) Summary of the fossil record of pinnipeds of Japan, and comparisons with that from the eastern North Pacific. *The Island Arc*, 3 (4), 361–372.

Moerdijk, P. W., and Post, K. (2021). Early Pleistocene bivalve *Mya arenaria* Linnaeus, 1758, from the 'Kor en Bot' expedition in the Eastern Scheldt estuary: a dinner course of the walrus *Ontocetus emmonsi* Leidy, 1859? *Cainozoic Research*, *2*, 193–200.

Norris, R. D. (1986). Taphonomic gradients in shelf fossil assemblages: Pliocene Purisima Formation, California. *Palaios*, *1*(3), 256–270. https://doi.org/10.2307/3514689

Parham, J. F., Barron, J. A., and Velez-Juarbe, J. (2022). Middle and late Miocene marine mammal assemblages from the Monterey Formation of Orange County, California. In Aiello, I. W., Barron, J. A., & A. C. Ravelo (Eds.), *Understanding the Monterey Formation and Similar Biosiliceous Units across Space and Time* (pp. 229–240). Geological Society of America. https://doi.org/10.1130/2021.2556(10)

Peredo, C. M., Pyenson, N. D., Marshall, C. D., & Uhen, M. D. (2018). Tooth loss precedes the origin of baleen in whales. *Current Biology*, *28*, 3992–4000.

Perry, F. A. (1988). *Fossil invertebrates and geology of the marine cliffs at Capitola, California*. Santa Cruz City Museum Association, Santa Cruz.

Pimiento, C., Griffin, J. N., Clements, C. F., Silvestro, D., Varela S., Uhen, M. D., and Jaramillo, C. (2017). The Pliocene marine megafauna extinction and its impact on functional diversity. *Nature Ecology & Evolution*, *1*, 1100–1106. https://doi.org/10.1038/s41559-017-0223-6

Poust, A.W., and Boessenecker, R.W. (2017). Mandibles of the sea lion *Proterozetes ulysses* from the middle Pleistocene Port Orford Formation of Oregon. *Journal of Vertebrate Paleontology*, *37*(3), e1317637. https://doi.org/10.1080/02724634.2017.1317637

Powell, C. L., II. (1998). The Purisima Formation and related rocks (upper Miocene–Pliocene), greater San Francisco Bay area, central California-Review of literature and USGS collections (now housed at the Museum of Paleontology, University of California, Berkeley). *United States Geological Survey Open-File Report*, *98–594*, 1–101. https://doi.org/10.3133/ofr98594

Powell, C. L., II, Barron, J. A., Sarna-Wojcicki, A. M., Clark, J. C., Perry, F. A., Brabb, E. E., and Fleck, R. J. (2007). Age, stratigraphy, and correlation of the late Neogene Purisima Formation, central California coast ranges. *US Geological Survey Professional Paper,* 1740, 1–32. https://doi.org/10.3133/pp1740

Powell, C. L., II. (2008). Pliocene invertebrates from the Travertine Point outcrop of the Imperial Formation, Imperial County, California. *US Geological Survey Scientific Investigations Report*, *2008-5155*, 1–25.

Powell, C. L., II, Boessenecker, R. W., Smith, N. A., Fleck, R. J., Carlson, S. J., Allen, J. R., Long, D. J., Sarna-Wojcicki, A. M., and Guruswami-Naidu, R. B. (2019). Geology and Paleontology of the Late Miocene Wilson Grove Formation at Bloomfield Quarry, Sonoma County, California. *U.S. Geological Survey Scientific Investigations Report*, *2019*–5021, 1–77. https://doi.org/10.3133/sir20195021

Pyenson, N. D., and Lindberg, D. R. (2011). What happened to gray whales during the Pleistocene? The ecological impact of sea-level change on benthic feeding areas in the North Pacific Ocean. *PLoS ONE*, *6*, e21295. https://doi.org/10.1371/journal.pone.0021295

Racicot, R. A., Deméré, T. A., Beatty, B. L., and Boessenecker, R. W. (2014). Unique feeding morphology in a new prognathous extinct porpoise from the Pliocene of California. *Current Biology*, *24*(7), 774–779. https://doi.org/10.1016/j.cub.2014.02.031

Randall, J.W. (1839). Catalogue of the Crustacea brought by Thomas Nutall and J.K. Townsend, from the West Coast of North America and the Sandwich Islands, with descriptions of such species as are apparently new, among which are included several species of different localities, previously existing in the collection of the Academy. *Journal of the Academy of Natural Sciences at Philadelphia*, *8*, 106–147.

Ray, C. E. (1975). The relationships of *Hemicaulodon effodiens* Cope 1869 (Mammalia: Odobenidae). *Proceedings of the Biological Society of Washington*, *26*, 281–304.

Rémond de Corbineau, A. (1863). Description of two species of *Scutella*. *Proceedings of the California Academy of Natural Sciences*, *3*, 13–15.

Repenning, C. A., and Tedford, R. H. (1977). Otarioid seals of the Neogene. *US Geological Survey Professional Paper*, *992*, 1–87. https://doi.org/10.3133/pp992

Sawlan, M. G., and Smith, J. G. (1984). Petrologic characteristics, age and tectonic setting of Neogene volcanic rocks in northern Baja California Sur, Mexico. *Pacific Section SEPM Book*, *39*, 237–251.

Schneider, C. A., Rasband, W. S., & Eliceiri, K. W. (2012). NIH Image to ImageJ: 25 years of image analysis. *Nature Methods*, *9*(7), 671–675.

Schreber, J. C. D. von. (1776). Der zottige Seelöwe. In Schreber, J. C. D. (Ed.). *Die Saugethiere in Abbildungen nach der Natur, mit Beschreibungen*. Walthersche Kunst- und Buchhandlung, Leipzig.

Sivertsen, E. (1954). A survey of eared seals (family Otariidae) with remarks on the Antarctic seals collected by M/K "Norvegia" in 1928–1929. *Det Vorske Videnkaps-Akademii Oslo*, *36*, 1–76.

Smith, J. T., and Roy, K. (2006). Selectivity during background extinction: Plio–Pleistocene scallops in California. *Paleobiology*, *32*(3), 408–416. https://doi.org/10.1666/05078.1

Sowerby, J.D.C. (1815–1818). *The mineral conchology of Great Britain: or coloured figures and descriptions of those remains of testaceous animals or shells, which have been preserved at various times and depths in the earth*, *(2)* Benjamin Meredith, London.

Sowerby, J.D.C. (1825) *The mineral conchology of Great Britain: or coloured figures and descriptions of those remains of testaceous animals or shells, which have been preserved at various times and depths in the earth*, (*5*) Benjamin Meredith, London.

Stanley, S. M. (1986). Anatomy of a regional mass extinction: Plio–Pleistocene decimation of the Western Atlantic bivalve fauna. *Palaios*, *1*(1), 17–36. https://doi.org/10.2307/3514456

Stewart, J. D., and Perry, F. A. (2002). First paleomagnetic framework for *Isurus-Carcharodon* transition in the Pacific basin: the Purisima Formation, California. *Journal of Vertebrate Paleontology 22*(supplement to number 3), 111A. https://doi.org/10.1080/02724634.2003.10010538

Stimpson, W. (1860). Check lists of the shells of North America, 3. East coast: Arctic seas to Georgia. *Smithsonian Miscellaneous Collections*, *2*(128), 1–6.

Stirton RA. (1960). A marine carnivore from the Clallam Miocene Formation, Washington: its correlation with nonmarine faunas. *University of California Publications in Geological Sciences*, *36*, 345–368.

Swainson, W. (1822). *A Catalogue of the Rare and Valuable Shells which Formed the Celebrated Collection of the Late Mrs. Bligh: With an Appendix Containing Scientific Descriptions of Many New Species and Two Plates.* C. Dubois, London.

Tanaka, Y., and Ichishima, H. (2016). A new skull of the fossil porpoise *Numataphocoena yamashitai* (Cetacea: Phocoenidae) from the upper part of the Horokaoshirarika Formation (lower Pliocene), Numata Town, Hokkaido, Japan, and its phylogenetic position. *Palaeontologia Electronica*, *19*(3), 1–28. https://doi.org/10.26879/663

Tanaka, Y., and Kohno, N. (2015). A new late Miocene odobenid (Mammalia: Carnivora) from Hokkaido, Japan suggests rapid diversification of basal Miocene odobenids. *PLoS ONE*, *10*(10), e0131856. https://doi.org/10.1371/journal.pone.0131856

Tomida, Y. (1989). A new walrus (Carnivora, Odobenidae) from the Middle Pleistocene of the Boso Peninsula, Japan, and its implication on odobenid paleobiogeography. *Bulletin of the National Science Museum, Tokyo, Series C*, *15*(3), 109–119.

True, F. W. (1905). New name for *Pontoleon*. *Proceedings of the Biological Society of Washington*, *18*, 253.

Van Beneden, P. J. (1872). Les Baleines Fossiles d'Anvers. *Bulletin de l'Académie Royale des Sciences Belgique*, *34*, 6–20.

Van Beneden, P. J. (1877). Description des ossements fossiles des environs d'Anvers. *Annales du Musée Royal d'Histoire Naturelle de Belgique*, *1*, 1–88.

Velez-Juarbe, J., and Salinas-Marquez, F. M. (2018). A dwarf walrus from the Miocene of Baja California. *Royal Society Open Science*, *5*(8), 180423. https://doi.org/10.1098/rsos.180423

Velez-Juarbe J., Valenzuela-Toro, A. M. (2019). Oldest record of monk seals from the North Pacific and biogeographic implications.

Biology Letters, *15*(5), 20190108. https://doi.org/10.1098/rsbl.2019.0108

Vendrasco, M. J., Eernisse, D. J., Powell, C. L. II, and Fernandez, C. Z. (2012). Polyplacophora (Mollusca) from the San Diego Formation: a remarkable assemblage of fossil chitons from the Pliocene of Southern California. *Natural History Museum of Los Angeles County Contributions in Science*, *520*, 15–72.

Vermeij, G. (2012). The evolution of gigantism on temperate seashores. *Biological Journal of the Linnean Society*, *106*(4), 776–793. https://doi.org/10.1111/j.1095-8312.2012.01897.x

Viglino, M., Gaetán, C. M., Cuitiño, J. I., & Buono, M. R. (2020). First toothless platanistoid from the early Miocene of Patagonia: the golden age of diversification of the Odontoceti. *Journal of Mammalian Evolution*, *28*, 337–358.

Viglino, M., Gaetán, C. M., Cuitiño, J. I., and Buono, M. R. (2021). First toothless platanistoid from the early Miocene of Patagonia: the golden age of diversification of the Odontoceti. *Journal of Mammalian Evolution*, *28*, 337–358. https://doi.org/10.1007/s10914-020-09505-w

Wagner, H. M., Riney, B. O., Deméré, T. A., and Prothero, D. R.. (2001). Magnetic stratigraphy and land mammal biochronology of a nonmarine facies of the Pliocene San Diego Formation, San Diego County, California. *SEPM Pacific Section Book*, *91*, 359–368.

Werth, A. J. (2000). A kinematic study of suction feeding and associated behavior in the long-finned pilot whale, *Globicephala melas* (Traill). *Marine Mammal Science*, *16*(2), 299–314. https://doi.org/10.1111/j.1748-7692.2000.tb00926.x

Werth, A. J. (2006). Mandibular and dental variation and the evolution of suction feeding in Odontoceti. *Journal of Mammalogy*, *87*(3), 579–588. https://doi.org/10.1644/05-MAMM-A-279R1.1

Whitmore, F. C., & Kaltenbach, J. A. (2008). Neogene Cetacea of the Lee Creek Phosphate Mine, North Carolina. *Virginia Museum of Natural History Special Publication*, *14*, 181–269.

Wülker, G. (1910). Uber Japanische cephalopoden: Beitrage zur kenntnis der systematik und anatomie der dibranchiaten. *Abhandlungen der Mathematisch-Physikalischen Classe der Koniglich Bayerischen Akademie der Wissenschaften*, *3*, 1–77.

Handling Editor: Anthony Friscia.
Phylogenetics Editor: Pedro Godoy.